

Status of Thesis

Title of thesis | Modeling and Simulation of Cluster Formation Effects in Riser Section of
Fluid Catalytic Cracking Unit

I MESFIN BERHANU NEGASH

hereby allow my thesis to be placed at the Information Resource Center (IRC) of

Universiti Teknologi PETRONAS (UTP) with the following conditions:

1. The thesis becomes the property of UTP
 2. The IRC of UTP may make copies of the thesis for academic purposes only
 3. This thesis is classified as

Confidential

Non-Confidential

If this thesis is confidential, please state the reason:

The content of the thesis will remain confidential for _____ years.

Remarks on disclosure:

Endorsed by

Signature of Author

Signature of Supervisor

Permanent Address:

24998, Addis Ababa

Name of Supervisor

Ethiopia

Dr. Shuhaimi Mahadzir

Date: March, 2009

Date:

UNIVERSITI TEKNOLOGI PETRONAS

Approval by Supervisor(S)

The Undersigned certify that they have read, and recommend to the postgraduate studies program for acceptance, a thesis entitled "**Modeling and Simulation of Cluster Formation Effects in Riser Section of Fluid Catalytic Cracking Unit**" submitted by **Mesfin Berhanu** for the fulfillment of the requirements for the degree of Masters of Science in Chemical Engineering.

March, 2009

Date

Signature : _____

Main Supervisor : Dr. Shuhaimi Mahadzir _____

Date : _____

UNIVERSITI TEKNOLOGI PETRONAS

**Modeling and Simulation of Cluster Formation Effects in Riser Section of
Fluid Catalytic Cracking Unit**

By

Mesfin Berhanu

A THESIS

**SUBMITTED TO THE POSTGRADUATE STUDIES PROGRAMME
AS A REQUIREMENT FOR THE
DEGREE OF MASTERS OF SCIENCE IN CHEMICAL ENGINEERING
CHEMICAL ENGINEERING DEPARTMENT**

BANDAR SERI ISKANDAR,

PERAK

MARCH, 2009

Declaration

I hereby declare that the thesis is based on my original work except for quotations and citations which have been duly acknowledged. I also declare that it has not been previously or concurrently submitted for any degree at UTP or other institutions.

Signature: _____

Name : Mesfin Berhanu Negash

Date : March, 2009

Acknowledgements

First and foremost, I would like to give my sincere thanks to God, the almighty God, the source of my life and hope for giving me the strength and wisdom to complete the work.

I would like to express my sincere gratitude to my supervisor, Dr. Shuhaimi Mahadzir, for his guidance and dedication throughout this work. Many times, his patience and constant encouragement has steered me to the right direction. He always spared much time to help me. Again, I am most grateful to Prof. Duvvuri Subbarao for his support and help in this work. His help and ideas helped me a lot in completing my work on time.

I would like also express my gratitude to my best friends and my sincere thanks to postgraduate office.

To my beloved family, thanks for their understanding, support and care. They are always close to my heart.

Finally, I would like also to thank to all my friends who have been with me throughout my work and to all those who have helped me directly or indirectly, May God bless all of them.

Abstract

The riser reactor is a highly effective reactor for fast gas-solid reaction systems. In spite of extensive research in this area, the degree of understanding of these types of reactors is different. In this work, mathematical model for riser reactor is developed based on the conservation equations for non-isothermal riser reactor linked with hydrodynamics. The cracking reaction is described based on four lump kinetic models and the hydrodynamic is based on cluster based approaches. The advantage of this work is the model developed based on the concept of cluster formation. Resulting riser FCC models calculate flow and reaction parameters including conversion rates and product yields to determine performance. The resulting riser model is simulated using numerical method of Dormand-Prince, a member of Runge-Kutta family of ordinary differential equation (ODE) solvers, via MATLAB Environment. Simulation results of the base case riser model agree with plant data sufficiently well with majority of the data deviation lies between 1 and 5%. Simulation studies were also performed using the model to encompass the effect of inlet catalyst temperature, and catalyst-to-oil (CTO) ratio on reactor performance. The gasoline yield did not show direct relation with inlet catalyst temperature due to secondary reaction. Increasing CTO ratio increases conversion and other products. Further increase of CTO ratio beyond 10 did not increase the conversion and yield of gasoline due to increase in coking. These findings are useful to determine coking limit for CTO ratio and its cost. Finally, the effect of cluster formation on riser performance was investigated. Conversion was increased by 9% with the formation of cluster and an additional densification by 25% due to residence time of cluster increased. The reason for higher conversion may be explained by the formation of cluster which increases the residence time of catalyst inside the reactor. However, the formations of cluster had inverse effect on the production of gasoline, which drops by 5%, due to high temperature drop attained and higher residence time of catalyst. In summary, the objectives of this study, which are to develop mathematical model and build understanding on the parameters that influence the performance of riser reactor, have been achieved.

Abstrak

Reaktor jenis apung-naik (riser) adalah amat berkesan untuk tindakbalas pantas bagi sistem gas-pepejal. Walaupun banyak penyelidikan telah di lakukan didalam bidang ini, tahap kefahaman untuk reaktor jenis ini adalah berbeza-beza. Di dalam kerja penyelidikan ini, model matematik untuk reaktor jenis apung-naik telah dibina berdasarkan persamaan konservasi untuk system reaktor tak-isotermal dan dihubungkan dengan hidrodinamik. Tindakbalas pemecahan dirumus menggunakan model kinetik empat kandungan dan rumusan hidrodinamik dibina berdasarkan kaedah kumpulan (cluster-based). Model reaktor FCC mengambilkira parameter aliran dan tindakbalas termasuk kadar tindakbalas dan hasil produk. Model reaktor disimulasi menggunakan kaedah pengiraan berangka Dorman-Prince, iaitu sebahagian dari keluarga dalam kaedah Runge-Kutta bagi penyelesaian masalah “ordinary differential equation (ODE)”, melalui kod MATLAB. Keputusan simulasi untuk kes asas model reaktor jenis apung-naik menunjukkan bahawa data simulasi dan data dari loji adalah begitu baik dengan majority julat perbezaan hanya antara 1 dan 5%. Analisa simulasi juga dibuat untuk mengenalpasti kesan suhu masuk pemangkin dan juga kesan kadar mangkin-ke-minyak (CTO) ke atas prestasi reaktor. Hasil gasoline tidak menunjukkan kadar terus dengan suhu masuk pemangkin disebabkan tindakbalas sekunder. Peningkatan kadar CTO menunjukkan kenaikan hasil tidakbalas dan hasil produk lain. Peningkatan kadar CTO melampui 10 tidak menambahkan hasil tidakbalas dan hasil gasolin kerana peningkatan penghasilan “coke” pada masa yang sama. Kefahaman ini amat berguna untuk mengenalpasti limit “coking” untuk kadar CTO serta kos yang bekaitan. Akhir sekali, kesan pembentukan kumpulan (cluster) juga diselidiki. Hasil tindakbalas meningkat 9% dengan pembentukan kumpulan serta pemampatan isipadu kumpulan sehingga 25%. Sebab peningkatan hasil tindakbalas dapat diterangkan dengan peningkatan “residence time” pemangkin di dalam kumpulan yang terbentuk di dalam reactor. Bagaimanapun, pembentukan kumpulan membari kesan sonsang kepada penghasilan gasoline yang jatuh sebanyak 5% disebabkan oleh beza suhu (temperature drop) yang meningkat serta “residence time” yang tinggi. Secara keseluruhannya, objektif kajian ini, iaitu untuk membina model matematik bagi memahami jenis-jenis parameter yang memberi kesan kepada prestasi reaktor, telah pun di capai.

Table of Contents

	Page
Status of Thesis	ii
Certification of Approval	iii
Title Page	iv
Declaration.....	v
Acknowledgment	vi
Abstract.....	vii
Abstrak	viii
Table of Contents.....	ix
List of Tables	xii
List of Figures	xiii
Nomenclature	xvi
1. INTRODUCTION	1
1.1 General Background.....	1
1.2 Process Description of Riser Section.....	2
1.3 Theoretical Review	5
1.3.1 Catalyst Development	6
1.3.2 Catalyst Deactivation.....	7
1.3.3 Coke Formation	8
1.3.4 Catalytic Cracking Reaction	9

1.4 Problem Statement	10
1.5 Objectives of the Research	11
1.6 Scope	11
1.7 Thesis Outline	11
 2. LITERATURE REVIEW	13
2.1 Modeling Riser Section of FCC Unit.....	13
2.2 Kinetic Modeling	19
2.3 Effect of Coking.....	26
2.4 Hydrodynamics of Riser Section	27
 3. METHODOLOGY	33
3.1 Theory and Background	33
3.2 Riser Model Development.....	34
3.2.1 Riser Reactor Hydrodynamics.....	34
3.2.2 Cracking Reaction Kinetics in the Riser Section	36
3.3 Riser Model Equation	39
3.3.1 Hydrodynamic Model	39
3.3.2 Kinetic Model Development.....	43
3.3.2.1 Conservation of Mass	43
3.3.2.2 Conservation of Energy	47
3.4 Algorithm and Tools Used.....	47
 4. RESULTS AND DISCUSSION	51
4.1 Simulation of Base Case.....	53
4.2 Model Validation	57
4.3 Influence of Operating Parameter	64
4.4 Case Study: Effect of Cluster Formation on Riser Performance	69

5. CONCLUSIONS AND FUTURE WORKS	74
5.1 Conclusions	74
5.2 Future Works.....	76
REFERENCES	77
Appendix- A	83
Appendix -B	85
Appendix -C	90

List of Tables

	Pages
Table 2.1: Review of reaction kinetics schemes proposed for FCC reaction	25
Table 3.1: Dormand-Prince coefficients	50
Table 4.1: Base case operating conditions	51
Table 4.2: Riser geometry	51
Table 4.3: Catalyst properties	51
Table 4.4: Pre-exponential constant and activation energy	52
Table 4.5: Heat of reactions reported	52
Table 4.6: Molecular weight of lumped model	52
Table 4.7: Feed stock properties	52
Table 4.8: Industrial data reported by Derouin et al. [68]	59
Table 4.9: Industrial data reported by Ali et al. [69]	59
Table 4.10: Deviation of model predicted and plant data reported by Derioun et al. [68]	59
Table 4.11: Deviation of model predicted and plant data reported by Ali et al. [69]	59

List of Figures

	Pages
Figure 1.1: FCC process flow diagrams	4
Figure 1.2: Feed oil-cracked product comparison	5
Figure 2.1: Three-lump model	21
Figure 2.2: Ten-lump model	22
Figure 2.3: Six-lump model	22
Figure 2.4: Four-lump model	23
Figure 2.5: Five-lump model	24
Figure 2.6: Seven-lump model	24
Figure 2.7: (a) and (b) Cluster structure in a circulating fluidized bed	31
Figure 3.1: Temperature plot at the feed vaporization section of riser	36
Figure 3.2: Momentum balance on riser section	42
Figure 3.3: Mass balances around the riser	44
Figure 3.4: Algorithm to compute model equation	49
Figure 4.1: Conversion of gas oil vs. riser height	54
Figure 4.2: Gasoline, Gas and Coke yield vs. riser height.	55
Figure 4.3: Temperature drop vs. riser height.	55
Figure 4.4: Velocity of catalyst (v_c) and gas (v_g) phase vs. riser height	56
Figure 4.5: Solid holdup vs. riser height	56

Figure 4.6: Catalyst activity vs. riser height	57
Figure 4.7: Pressure drop vs. riser height.	57
Figure 4.8 (a): Validation with conversion data provided by Derioun et al. [68].	60
Figure 4.8 (b): Validation with gasoline data provided by Derioun et al. [68].	60
Figure 4.9: Validation of data provided by Ali et al. [69] with (a) conversion, (b) Gasoline yield, (c) gas yield and (d) coke yield of the model result.	61
Figure 4.10 (a): Validation with conversion data provided by Gupta et al. [3].	62
Figure 4.10 (b): Validation with gasoline data provided by Gupta et al. [3].	62
Figure 4.10 (c): Validation with gas data provided by Gupta et al. [3].	63
Figure 4.10 (d): Validation with coke data provided by Gupta et al. [3].	63
Figure 4.11 (a): Effect of CTO on conversion at different cluster diameter.	66
Figure 4.11 (b): Effect of CTO on gasoline yield at different cluster diameter.	67
Figure 4.11 (c): Effect of CTO on gas yield at different cluster diameter.	67
Figure 4.11(d): Effect of CTO on coke yield at different cluster diameter.	68
Figure 4.12: Effect of temperature on conversion and gasoline yield.	68
Figure 4.13: Conversion vs. riser height	70
Figure 4.14: Gasoline yield vs. riser height	71
Figure 4.15: Gas yield vs. riser height	71
Figure 4.16: Coke yield vs. riser height	72

Figure 4.17: Temperature vs. riser height 72

Figure 4.18: Catalyst activity vs. riser height 73

Figure 4.19: Solid hold up vs. riser height 73

Nomenclature

ΔH_{vap}	Heat of vaporization of gas oil (kJ/kg)
A_0	Pre-exponential constant (m^3/kgs)
A_c	Projected area of cluster (m^2)
C_a	Concentration of gas oil lump (kmol/m^3)
C_b	Concentration of gasoline lump (kmol/m^3)
C_c	Concentration of gas lump (kmol/m^3)
C_d	Concentration of coke lump (kmol/m^3)
C_D	Drag coefficient
COC	Coke on catalyst (kg coke/kg catalyst)
Cp_c	Heat capacity of catalyst (kJ/kg k)
Cp_g	Heat capacity of gas phase feed (kJ/kg K)
Cp_l	Heat capacity of liquid phase feed (kJ/kg K)
Cp_s	Heat capacity of steam (kJ/kg k)
d_c	Cluster diameter (m)
dt	Differential time (s)
dv	Differential volume of riser reactor (m^3)
dz	Differential riser height (m)
E	Activation energy (kJ/kmol)
E_c	Activation energy of catalyst (kJ/kmol)

f_i	Molar flow rate of each species or component (kmol/s)
F_c	Feed flow rate of catalyst (kg/s)
F_{cw}	Friction force between cluster and riser wall (N)
F_g	Feed flow rate of gas oil (kg/s)
F_{gw}	Friction force between gas and riser wall (N)
F_s	Feed steam flow rate (kg/s)
g	Gravitation constant (m/s^2)
G_c	Solid flux ($\text{kg}/\text{m}^2\text{s}$)
ΔH_{ab}	Heat of reaction for cracking of lump gas oil to gasoline (kJ/kg)
ΔH_{ac}	Heat of reaction for cracking of lump gas oil to gas (kJ/kg)
ΔH_{ad}	Heat of reaction for cracking of lump gas oil to coke (kJ/kg)
ΔH_{bc}	Heat of reaction for cracking of lump gasoline to gas (kJ/kg)
ΔH_{bd}	Heat of reaction for cracking of lump gasoline to coke (kJ/kg)
K	Reaction rate constant (m^3/kgs)
K_{ab}	Reaction constant from gas oil to gasoline (m^3/kgs)
K_{ac}	Reaction constant from gas oil to gas (m^3/kgs)
K_{ad}	Reaction constant from gas oil to coke (m^3/kgs)
K_{bd}	Reaction constant from gasoline to coke (m^3/kgs)
K_{bc}	Reaction constant from gasoline to gas (m^3/kgs)
K_d	Deactivation constant

K_{d0}	Pre-deactivation constant
L	Length of the riser (m)
m_c	Mass of cluster (kg)
M	Lump molecular weight (kg/kmol)
n	Mole of each species or component (mole)
P	Pressure drop (kpa)
Q	Volumetric flow rate (m^3/s)
q	Exponential power of deactivation model
Q_g	Volumetric gas flow rate (m^3/s)
Q_p	Particle flow rate (m^3/s)
r	Reaction rate ($\text{kmol}/\text{m}^3\text{s}$)
r_a	Reaction rate of gas oil lump (kmol/s)
r_b	Reaction rate of gasoline lump (kmol/s)
r_c	Reaction rate of gas lump (kmol/s)
r_d	Reaction rate of coke lump (kmol/s)
R	Universal gas constant (kJ/kgmolK)
Re_c	Reynolds number of cluster
r_i	Rate of reaction for each component (kmol/s)
T	Temperature inside riser (K)
T_b	Feed boiling temperature (K)

T_c	Feed temperature of catalyst (K)
T_F	Feed gas oil inlet temperature (K)
T_{mix}	Final temperature of the mixture after vaporization (K)
T_s	Feed temperature of steam (K)
u_c	Velocity of cluster (m/s)
u_g	Velocity of gas phase (m/s)
u_0	Superficial gas velocity (m/s)

Subscript

a	Gas oil
b	Gasoline
c	Gas
d	Coke
cw	Cluster -wall
F	Feed
g	Gas
gw	Gas-wall
i	Lump
vap	Vaporization

Greek Letter:

ε_c	Volume fraction of cluster
ε_g	Volume fraction of gas
μ_g	Viscosity of gas phase (kg/ms)
Ω	Cross sectional area of riser (m ²)
\emptyset	Deactivation function
ρ_c	Density of cluster (kg/m ³)
ρ_g	Density of gas (kg/m ³)

CHAPTER 1

INTRODUCTION

1.1 General Background

The fluid catalytic cracking (FCC) process represents a major application of the riser reactor technology in oil refinery. In FCC process, heavy petroleum fractions such as gas oil are converted into gasoline, other light products and by-products. FCC has become the major upgrading process because of its simple but efficient operations and its relatively inexpensive operational cost.

FCC technology was initiated by the effort of research engineers at the Standard Oil Development Company, now Exxon, in the early 1940's [1]. Their aim was to develop a pneumatic conveying system for the catalytic cracking of kerosene. Collaborative efforts of various companies resulted in the first commercial FCC unit to go into production in 1942. This initial model had a capacity of 2,000 m³/d or 13,000 barrels of feed per day. Within a few years, 30 FCC units of this type had been built with production capacities reaching up to 16,000 m³/d or 100,000 barrels of feed per day. The next breakthrough in FCC technology came in 1962 when Mobil developed zeolite catalyst, which provided its superiority over the silica-alumina catalyst through higher rates of cracking as well as improved gasoline yields [2]. With the development of this new type of catalyst, it has become possible to upgrade the FCC design with feed oil being sprayed into the fast up flowing lean-phase stream of regenerated catalyst [3], [4]. This arrangement shortens the contact time and allows flow conditions that are closer to plug flow conditions.

Current operational FCC units process over 2.4 million tons of feed per day or 16 million barrels of feed per day [5]. This constitutes more than a quarter of world crude production. Considering that the conversion of low value material into highly desired products with a value addition of \$60/m³, it is easy to realize the incredible impact this process has on the world economy.

In spite of significant improvements in the FCC process involving both design and catalyst over the last fifty years, this technology continues to evolve. Wei and Kuo [6] have shown that it is possible to lump a number of species together and still reasonably describe the overall reaction behavior of the system. Thus, the use of lumped kinetic schemes presents a useful tool to describe the main features of the reactions. FCC riser reactor performance is measured in terms of gasoil conversion and product yields. According to Gupta [3], current values for conversion in conventional FCC riser units have reached up to 67% with approximately 43% gasoline yields. Many schemes have been suggested for the cracking reaction in the riser reactor. Especially due to the reaction process change the direction abruptly with operating condition, any investigation in this area is bound to have highly beneficial economic outcomes. Enhancements in gasoline yield and gas oil conversion will also have a valuable environmental advantage due to decreased output of side products.

1.2 Process Description of Riser Section

A typical FCC unit is composed of two main parts, which are the riser reactor and the regenerator. The main focus of this study will be riser section of reactor. The feed for the riser comes from the heavy atmospheric gas oil (HGO) cut from the atmospheric distillation section of the crude unit and from the vacuum gas oil (VGO) cut from the vacuum distillation section. Combined HGO and VGO are called Gas Oil. In the riser reactor feed oil vaporization and endothermic cracking reactions occur. Vaporized petroleum feed is cracked in the reactor upon contact with catalyst particles at approximately 500°C. The cracked products are collected at the exit of the reactor. Catalyst particles provide heat and reaction sites for the vaporization and cracking reactions in the riser. Gradually the catalyst particles are deactivated by coke deposition. The cracking reaction is followed by the separation of feed stock products from spent catalyst particles, which occurs in the separator. In the regenerator, the exothermic burning of coke deposits off the catalyst particles provides energy in the form of heat to the recycled catalyst particles. Regenerated hot catalyst is sent back to the reactor and cracking of new feed continues.

The flow through the riser is two-phase reacting flow. Hot catalyst particles enter the bottom of the riser in a suspension of carrier gas. Additional lift gas is needed at the catalyst inlet zone for dispersion. The hot catalyst particles travel up the riser and encounter the feed oil droplet in the feed injection zone. The feed oil droplets are injected from the outer circumference of the riser and undergo vaporization and cracking reactions in the presence of the catalyst particles. The degree of feed atomization of gas oil determines the vaporization and reaction processes. The good feed atomization developed small droplets which have high heat transfer potential during mixing with catalyst improves the conversion and yield. The cracked products and the catalyst particles exit at the top of the riser.

The riser reactor is a modern transport fluidized bed reactor where the catalyst and feed mix on the way to separation section of the old reactor now called separator. Usually, risers are designed to have a length to diameter (L/D) ratio of at least 20. Vaporized feed enters the riser at a velocity around 4.5-12 m/s and exits multiples of inlet values due to volumetric expansion. Gas velocities of over 28 m/s are usually seen as upper limits of operation since wear becomes critical. In general, gas residence time in the order of 2 to 4 seconds whereas catalyst particles spend longer time in the reactor. Risers outlet temperature are typically in the range of 450-550°C. Catalyst-to-oil ratio, which is defined as the mass ratio of catalyst to feed, is usually in the range of 4-11 [1].

A typical example of a modern FCC riser unit [7] is shown in Figure 1.1. The heavy oil feed is mixed with steam at the riser entrance for better dispersion. The catalyst particle have to be fluidized by roughly 3-5% steam in the entrance of the riser since the catalyst particles are moving opposite to the direction of gravity. The presence of steam in the riser makes the process diluted. The inlet of the riser is equipped with numerous atomizing feed nozzles that distribute the feed radial across the riser column in the form of small droplets. This allows for good oil to catalyst contact.

The riser reactor is designed as straight column without any curved sections. At the riser exit, a special closed cyclone system removes catalyst particles quickly from the

gaseous mixture. The solid particles then enter the stripper, where it flow downward, counter current to steam that is injected at the bottom. The steam strips hydrocarbons that are adsorbed onto the catalyst avoiding their combustion in the regenerator, which in turn avoids unnecessary deactivation of catalyst and waste of valuable product. The catalyst particles then enter the regenerator, which is essentially a combustor that removes coke deposition on spent catalyst upon contact with air. The coke oxidizes to carbon monoxide and carbon dioxide, leaving behind water. Other products include nitrogen oxide and sulfur, which exit the system as flue gasses [8].

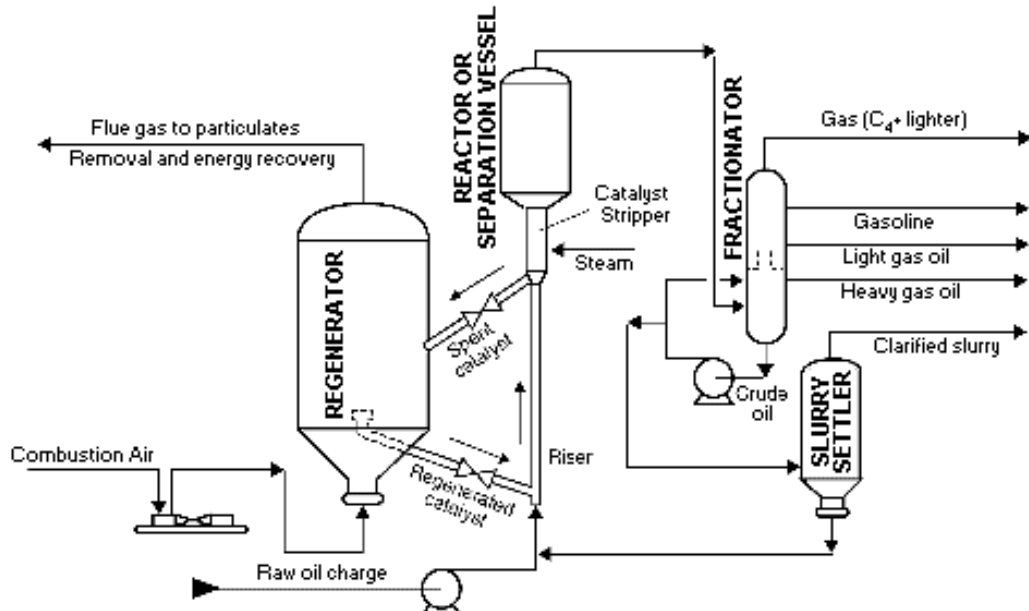


Figure 1.1: FCC process flow diagram [7]

At the exit of the riser, the products are normally defined by their molecular weight. The concentration of the petroleum products may be plotted as a function of their molecular weight to give an idea of the degree to which conversion of the feed oil takes place. A typical yield curve [9] for cracked product at the exit is compared to the heavy feed oil composition at the inlet in Figure 1.2. This yield curve may be shifted to adapt the riser products output for certain products, such as gasoline, diesel fuel or olefins. The riser performance therefore may be determined by what quantities of the desired products are exiting the riser section.

Product yields are highly sensitive to operating conditions in the riser reactor. Small changes in these conditions can have a large effect on the product yields, magnified by the enormous amounts produced daily by these units. Investigation of the effect of various operating conditions whose changes are relatively easy to implement will provide a guideline for the operations of the units that allows greater selectivity of the products. The ability to predict numerically the effects of operating conditions on the performance provides significant advantage over costly testing facilities and trial-and-error operations. This will help the industry to improve the process and increase the profitability of the process.

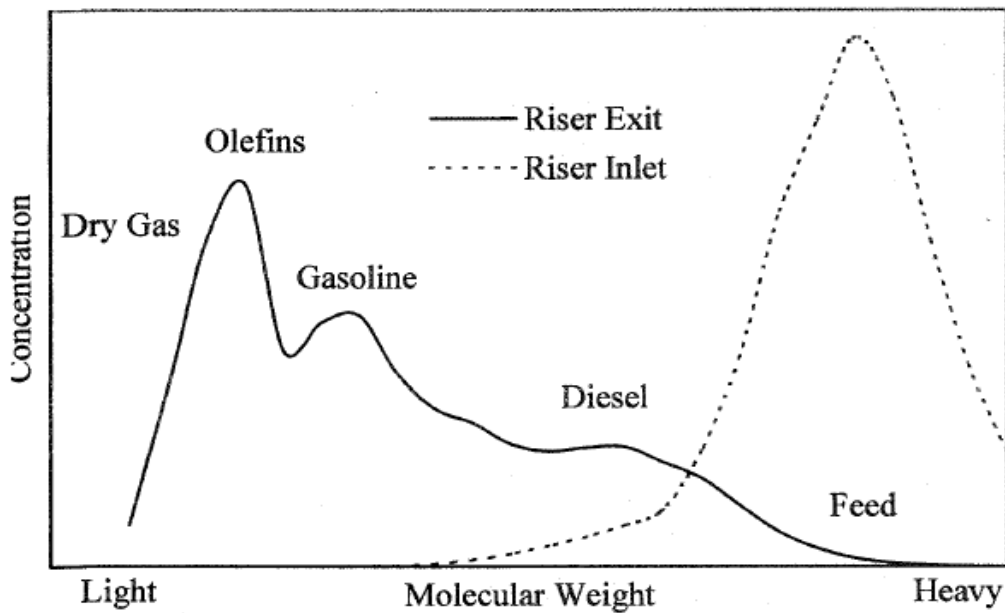


Figure 1.2: Feed oil cracked product comparison [9]

1.3 Theoretical Review

This review covers on the following important theoretical aspects of fluid catalytic cracking riser section such as catalyst development, catalyst deactivation, coke formation and catalytic reaction of riser reactor unit.

1.3.1 Catalyst Development

A catalyst is a substance that normally accelerates the rate of approach to chemical equilibrium. Commercial cracking catalysts fall into one of the three following categories such as acid treated natural alumina silicates, amorphous synthetic silica-alumina and crystalline synthetic silica-alumina catalyst called zeolite or molecular sieves. Each of this catalyst was used during a certain era and is presented chronologically.

Aluminum chloride was the first catalyst discovered that can catalytically crack heavy oils to lighter hydrocarbons [2]. However, the process was not feasible due to high catalyst recovery cost and the process was soon discontinued. Acid leached natural clay catalyst was widely employed by the industry during the early 1940's [8]. This catalyst was highly temperature sensitive. Thus, the regeneration temperature was limited and resulted in low burning rate and rapid decline in the catalyst activity. These catalysts suffered also from low activity and selectivity. In addition, they had poor fluidization characteristics. Taking into consideration the ever increasing demand for aviation fuels during this period, research for more active and selective catalyst had begun. In a few years, synthetic silica-alumina catalyst rapidly dominated the catalytic cracking industry. The synthetic silica-alumina catalyst went through several stages of development starting with low activity catalyst containing 10-13% alumina, then to the more active and stable high alumina content 25% alumina, and ending with the introduction of crystalline synthetic silica-alumina catalyst.

The zeolite catalyst is a crystalline alumina silicate which is found either in naturally occurring minerals or synthesized. The zeolite catalyst has regular crystalline structure and uniform pore size. The synthetic silica-alumina improved fluidization characteristics over the natural clays and provided more activity and selectivity. A major breakthrough in catalyst design came in the mid 1960's, when zeolite was first introduced. The use of zeolite catalyst has several advantages. The catalyst provides higher activity than conventional catalyst, permits short residence time and improved throughput rates. Improved catalyst activity further prompted the adoption of the riser

type FCC unit. Zeolite catalyst also shows significant increase in conversion per pass without over cracking. These results from high selectivity to gasoline compared to coke and dry gases. The zeolite catalyst also has better thermal and hydrothermal stability. In addition it exhibits better resistance to attritional poisons such as metals and nitrogen. In comparison to other catalyst, the zeolite catalyst is also relatively low cost to manufacturing.

Different types of zeolite catalysts are classified according to their compositions catalyst containing y-zeolite in a catalytically inert matrix, catalysts containing y-zeolite in a catalytically active matrix, and catalyst containing rare earth y-zeolite and an octane boosting additives such as the ZSM-5 zeolite [10].

The uses of catalyst additives are greatly enhancing the flexibility of the FCC unit. Additives avoid the cumbersome task of having to change the complete inventory of catalyst to comply with a temperature change in the unit operating objectives. They can easily be taken in and out of the use and their effect is fairly quick. They are also economical because they do not require an external option to purify the feed charge from some metal poisons. Catalyst additives have been developed during the last 30 years and there are still more additives expected to be developed. These additives are necessarily inert to the primary cracking reactions. The concentration of additives except for active control is estimated below 5% and in common practice less than 1%. Additives are more often expensive than the main catalyst. Thus, a high concentration will be economically prohibitive as well. Some of the roles of additives are octane enhancing, heavy oil retardant, fluidization, passivating agents and for increase selectivity [11].

1.3.2 Catalyst Deactivation

The loss of activity experienced by catalyst used in catalytic reactions is primarily due to the following mechanisms such as solid state transformations, poisoning and coking. The first classification of catalyst deactivation mechanisms include those that are related to physical and structural changes suffered by the catalyst. For example,

changes in the pore size distribution, sintering of the catalyst because of high temperatures and impurities [2]. On the other hand, deactivation of the catalyst by poisoning is the result of an irreversible process caused by impurities introduced with feed. For instance, the effects of metal contaminants especially metal contaminants such as Ni and V over the activity decay of cracking catalyst and related topics have been the subject of a number of studies. Finally, the catalyst deactivation by coking accounts for the loss of catalyst activity due to coke deposition over the catalyst activity sites. Usually, most of the coke deposited over the surface of the catalyst is a product of the reaction itself. Some very heavy hydrocarbon molecules may be introduced with the feedstock and remain adsorbed on the catalyst surface.

1.3.3 Coke Formation

There is no clear understanding of the mechanism by which coke is formed. However, it has been suggested that olefin oligomerization and aromatics alkylation, followed by cyclization, aromatization and condensation process are the main reactions towards the formation of coke. The presence of highly unsaturated hydrocarbons of high molecular weights adsorbed on the catalyst surface and their facility to protonation, as well as the relatively high stability of the resulting carbonium ion, indicates that aromatic feeds should have a high tendency to coke formation [11].

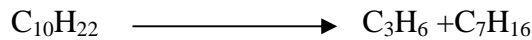
Coke, consisting of a poly-aromatic condensed ring structure similar to the structure of graphite, has a molecular weight in the range of 940 to 1040. Chemical and physical characterizations of the coke deposited over the surface of a catalyst confirmed the presence of carbon, hydrogen, oxygen, sulphur and nitrogen [2]. Ni, Cu and V among others are the principal contaminants of metal contaminated feed stocks. These metal contaminants have a strong deactivation effect over the catalyst. Moreover, such a deactivation, partial or total, by means of an irreversible destruction of the zeolite crystallite not only introduces a reduction in the catalyst activity and selectivity, but also negatively influences the cracking process producing more hydrogen and coke. A number of theoretical studies were done and concluded that formation of coke on the catalyst is an unavoidable situation in catalytic cracking of

hydrocarbons. As coke formation increases, the H/C ratio of coke decreases due to hydrogen transfer to other products. Eventually coke becomes non volatile and blocks the pores and active sites of the catalyst. The source of coke in riser reactor has been suggested to originate from Catalytic coke, Contaminant coke, Feed residue coke and Catalyst-to-oil coke [12].

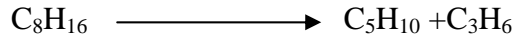
1.3.4 Catalytic Cracking Reactions

Catalytic cracking reactions comprise primary and secondary reactions. Primary reactions are cracking reaction starting with a carbon-carbon bond rupture. These reactions are represented by the following equations [9]:

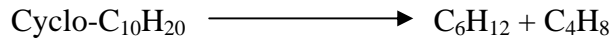
- i. Large paraffins cracked to smaller paraffins and olefin, e.g.



- ii. Olefins cracked to smaller olefins, e.g.



- iii. Cyclo-parafins cracked to olefins and smaller ring compound, e.g.

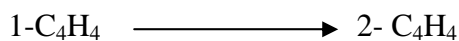


- iv. Aromatic side-chain scission, e.g.

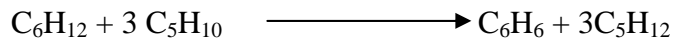


In addition to the primary cracking reactions, secondary reactions are very important from the point of view of the gasoline octane number. The secondary reaction includes a large number of reaction steps such as isomerization, hydrogen transfer, alkyl-group transfer, dehydrogenation and condensation reactions as shown below [12]:

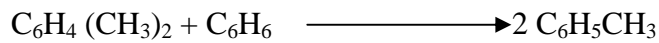
- i. Isomerization (Normal olefin to iso-olefins), e.g.



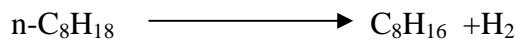
ii. Hydrogen transfer (cyclo aromatization), e.g.



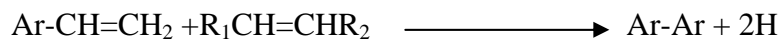
iii. Alkyl-group transfer, e.g.



iv. Dehydrogenation, e.g.



v. Condensation, e.g.



1.4 Problem Statement

A lot of research that have been conducted on modeling of riser section focused on kinetics, hydrodynamics, feed atomization and performance investigations. All these works were based on different assumptions and lead to different conclusions. In fluidization systems, a high quantity of particles forms agglomerates or clusters defined as region characterized by higher particle concentration in relative to the average solid concentration in the riser column. These groups of particles move as a single body with little internal relative movement. Such clusters can strongly affect operational characteristics such as increase particle holdup, increase pressure drop, reduce wall heat transfer and increase axial mixing. The existences of cluster formation on circulating fluidized bed have significant impact on hydrodynamics which leads to significant impact on riser performance. So In this work the modeling and simulation to investigate the effect of cluster formation on riser performance is covered. The importance of modeling the process is to determine the performance, the insufficient number of investigations in the literature, and the economic incentives are

the main guiding factors in formulating the objectives and the scope of this research work.

1.5 Objective of the Research

The main objective of the present work is to investigate the effect of cluster formation on the performance of riser section of fluid catalytic cracking unit. To accomplish this objective the following tasks are included:

- i. Development of model that links both the kinetics of the reaction and hydrodynamics of the riser reactor and determination of conversion and yield of product distribution through the riser reactor height.
- ii. Analyses the effect of operating parameters like Inlet catalyst temperature and catalyst-to-oil ratio on the performance of the unit using the model developed in this study.

1.6 Scope

This study will address only the riser section of fluid catalytic cracking unit. The riser section is modeled in one dimensional pseudo steady state. In this work, detail analyses of cluster duration time and occurrence frequency, particle to cluster interaction, and cluster to cluster collision parameters leads to kinetic energy dissipation is not included. However, the effect of cluster formation on the riser performance is investigated. The tool used for programming is MATLAB version 7 on PC Windows XP, RAM 1GB, Pentium IV and processor speed 2 GHZ.

1.7 Thesis Outline

The thesis is divided into five chapters: Chapter 1-Introduction, Chapter 2-Literature Review, Chapter 3-Methodology, Chapter 4-Results and Discussions and Chapter 5-Conclusions and Future Works.

Chapter 1 briefly introduces FCC reactor and its developmental stage in chronological order. The riser reactor process description is given along with the theoretical review

of riser section of FCC. Problem statement, objectives of the research, scope of work and outline of the thesis are also included.

Chapter 2 covers literature reviews on cluster formations, kinetics and hydrodynamics of FCC riser section. This previous work is a good basis for understanding the basic principle of the process. The impetus for determination of cluster characteristics and their importance to operational features of circulating fluidized bed and the concept of clusters incorporated in modeling riser section of FCC reactor behavior is reviewed.

Chapter 3 is methodology which covers the development of model to describe the hydrodynamics and reaction kinetics of FCC riser section. The reaction kinetics is modeled using four-lump cracking kinetic model and the hydrodynamics is based on cluster based approach. Catalyst deactivation is formulated based on coke deposition on the catalyst surface. The kinetic model is integrated with riser hydrodynamic models. The integrated model makes possible to determine conversion and product yield at each increment along the riser reactor column. Furthermore, the integrated model allows the performance of the riser reactor to be investigated under different case. The tools and algorithm used to solve the model are also described.

Chapter 4 presents results and discussions of the model. The base case simulation is performed to study the performance of riser reactor and the results obtained are validated with plant data obtained from the literature. Parametric study is focused on the effect of the inlet catalyst temperature and catalyst-to-oil ratio on riser performance. Using developed model, a case study is also presented by taking industrial operating FCC riser section to investigate effect of cluster formations on riser performance.

Finally, Conclusions and recommendations for future works are summarized in Chapter 5. Detail derivations of the model and reference data plots are included in the Appendix.

CHAPTER 2

LITERATURE REVIEW

This chapter presents literature review on kinetics and hydrodynamics of typical riser section of FCC. The previous works are good basis for understanding the basic principles of the process. It also provides abundant information for developing new models that allow more rigorous evaluations of the impact of cluster formation on the performance of riser section.

2.1 Modeling Riser Section of FCC Unit

Research works on riser section of FCC unit vary according to the type of problem. The analysis of this work focused on previous modeling and simulation works on riser section of FCC reactor. Ali [12] proposed a three lump model for FCC reactions. The three lumps are feed, gasoline range product and coke. The model is based on the assumptions that the reactor is a perfectly mixed continuous stirred tank reactor, the catalyst hold up remains constant, the reaction rates are first order, and gasoline does not crack into coke. The model utilizes the ideal gas law to simplify the equations. The model in its final form consists of six coupled, non-linear, ordinary differential equations which were solved numerically. The advantage of this model is that it follows the theoretical approach by using the conservation principle to describe the system. This model has not been compared to any commercial unit data.

Elnashaie and ElHennawi [13] employed the reaction network proposed earlier by Weekman and Nace [14]. The developed model overcame many limitations of the previous models. For instance, the model uses a reaction network that relates the different steps of the cracking reactions to each other and to the reactor model. The use of reaction network that lumps hundreds of components into three lumps for the purpose of investigating the bifurcation behavior and gasoline yield is sound. However there still exists the problem of lumping coke and the light hydrocarbon gases

into one lump. The model has been used to investigate the multiplicity phenomenon in FCC units. The results of this investigation suggested that the multiplicity region covers a wide range of operating conditions. The drawback of this work was that the model has not been checked against the performance of a commercial FCC unit.

Elshishini and Elnashaie [15] extended their earlier model [13] by investigating the effect of varying feed composition on the performance of the FCC unit. In this model, the change in volumetric gas flow rates between the inlet and outlet of the reactor was accounted, the partial cracking of gasoline and gas oil to lighter hydrocarbons were modified, the recycling of heavy cyclic oil and light cyclic oil were considered and the ratio of coke to coke plus light gases was determined. The model showed satisfactory results when compared to two industrial FCC units with respect to gasoline yield, reactor temperatures, amount of unconverted gas oil, amount of coke formed, and the overall heat of cracking. Later an extension [16] of the steady state model developed earlier [15] were investigated. The authors investigated the sensitivity of the model prediction to the model dimensionality. They showed that reliability of the results depend to a great extent on the model dimensions and recommended that any further reduction in the model dimensionality should be treated with great caution.

Farag and Tsai [17] used a number of empirical relations to predict the conversion level and the product yield. The model was based on the correlations developed between gasoil conversion and some of the system parameters. In this model, it was found that for the same conversion, the gasoline yield increases with the increase of combined feed ratio. This type of empirical model is widely used in industry because of its simplicity. However, it cannot be used for hydrodynamic and parametric studies.

Lopez-Isunza and Ruiz-Martinez [18] model was developed to describe the dynamic behavior of a riser type FCC unit. The authors used the reaction network developed by Weekman and Nace [14] to describe the cracking reactions. The model was used to find the optimum operating conditions which give the maximum gasoline yield. One

important conclusion described by the authors was the fact that the riser dynamics are much faster than those of the regenerator. Thus, the riser energy and mass balances were expressed in terms of quasi-steady state equations which reduce the mathematical complexity and facilitate the solution of the model.

Zheng [19] developed model for the riser reactors based on a cracking reaction network proposed by Weekman [20] and Lee et al. [21]. This network was similar to the five-lumped kinetic scheme suggested by Corella and Frances [22]. The fundamental difference between this network and others networks suggested was that it was assumed that the feed cracking reactions were first order. Several assumptions were incorporated such as gas-solid slip ratio of unity and flow in the riser was plug flow mode. In addition the dynamics of the riser were assumed to be very fast compared to the regenerator thus quasi steady state equations were developed. The model predictions were compared to a commercial unit for three different steady states. The drawback of this model was the fact that the assumption of solid-gas slip ratio of unity means the model development doesn't consider the existence of the cluster formation.

Theologos et al. [23] model was developed to investigate the effects of feed stock atomization on FCC riser reactor selectivity. The developed model was based on the assumptions of three lump model cracking reaction kinetics, three dimensional, plug flow reactor, two phase flow, mass and heat transfer considered and steady state. The results of this investigation indicate that the higher the degree of atomization, the faster the vaporization, and the faster the initiation of cracking reactions. In this work effect of feed stock atomization was quantified using droplet size. As the initial droplet size was reduced, the conversion rates and gasoline selectivity increase.

Sharma et al. [24] studied parametric effect of particle size and gas velocity on cluster characteristics in fast fluidized beds. This work was presented results of an experimental study of cluster characteristics using digital electronic capacitance probe measurements. The experimental work focused on cluster characteristics, parametric effect of particle

size and superficial gas velocity on cluster characteristics. The experimental results of this work compared with commercial results. This work formed the basis for further study on clusters.

Gupta et al. [3, 4] studied the effect of feed atomization on the performance of fluid catalytic cracking reactor. The authors found that the size of droplet formed during atomization have effect on the riser performance during cracking reaction. The result of the model has been found to be in good agreement with data of commercial FCC unit.

Kikkinides et al. [25] developed correlation of reactor performance with catalyst structural changes during coke formation in FCC processes. Their work showed that during the early stage of FCC reaction, the catalyst with the larger surface area and pore volume showed higher conversion and yield while, at the same time, has a lower fraction of poisoned sites in the porous network.

Pareek et al. [26] focused on modeling of non-isothermal FCC riser. Several assumptions were incorporated to develop the model including non-isothermal, plug flow reactor, four and ten lump kinetics of the reaction and volumetric expansion. Total temperature drop of 40°C, which was predicted through the total height of riser, was quite significant. The rate of reaction would have been highly overestimated if the temperature drop was not taken in to account. The model was also focused to show that the over simplification of modeling riser reactor under isothermal conditions and constant heat of reaction.

Benyahia et al. [27] model were developed for numerical analysis of a reacting gas and solid flow in the riser section of an industrial fluid catalytic cracking unit. The results of this work indicated that the cracking reaction of heavy oil increased in the gas axial velocity along the riser height, which has a significant impact on the gas-solid flow hydrodynamics. Nevertheless, this work was limited to hydrodynamics of solid-gas in riser reactor.

Leon-Becerril et al. [28] studied the effect of pressure gradient in industrial FCC risers. The following assumptions were included one dimensional, plug flow reactor, adiabatic, instantaneous vaporization, mass and heat balance and five lump models. The result of this investigation showed that the addition of a simplified momentum balance to the model, assuming that the only contribution to the axial pressure drop is the hydrostatic head of solids, improved the prediction of feedstock conversion and yield to products. The model was however limited to show the importance of pressure drop in developing mode for riser.

Nayak et al. [29] developed model for vaporization and cracking of liquid oil injected in a gas-solid riser. The model developed considered the following assumptions: adiabatic system, four lump kinetics, heat transfer and mass transfer. The simulated result indicated that the influence of droplet diameter on riser performance was sensitive to the value of oil properties, the kinetics used and the operating conditions. The drawback of the model was that the volumetric expansion was not considered and limited to feed vaporization section only.

Arandes et al. [30] published multiplicity of steady states in FCC units. The conclusion from this work shows the number of steady state in FCC unit was fixed and independent of operating condition at least within the typical operating condition. Four lump, instantaneous vaporization and pseudo steady state were the assumptions considered.

Sertic-Bionda et al. [31] developed model for kinetics of gas oil catalytic cracking. The result of this work indicated that the kinetics can be represented sufficiently using lump model.

Fernandes et al. [32] developed dynamic modeling of an industrial double regenerator reactor (R2R) FCC unit. The model showed the importance of double regenerator FCC unit for heavy feed oil. Most of this works focused on control part of FCC unit. Six-lump

model, instantaneous vaporization, pseudo steady state, adiabatic and plug flow were assumed in the model.

Lu et al. [33] developed model for numerical simulation to study the flow behaviour of particles and clusters in riser using two granular temperatures. A gas-solid multi-fluid model with two granular temperatures of the dispersed particles and the clusters in risers was developed to predict hydrodynamics of dispersed particles and clusters flow in circulating fluidized bed. Additional equations for the dispersed particles in the dilute phase and clusters in the dense phase were introduced. The phase interactions between dilute phase and dense phase were considered by drag forces. Distributions of volume fractions and velocities of gas, dispersed particles and clusters were obtained. Effects of the clusters on the hydrodynamics were illustrated. The contribution of this work was that it indicated the effect of cluster formation on the performance of circulating fluidized bed. The work was compared with experimental result from Manyele et al. [34]. The computed particle volume fractions and mass fluxes with the proposed model were in agreement with the measured data.

Cabezas-Gomez et al. [35] identified and characterized clusters in the riser of a circulating fluidized bed from numerical simulation results. The result of this work demonstrated that the use of a cluster identification and characterization methodology allows qualitative and quantitative analyses of some hydrodynamics phenomena of the gas-solid riser flows. The drawback of this work is a qualitative rather than quantitative analysis is performed mainly owing to the unavailability of operational data.

Guenther et al. [36] were studied cluster dynamics in a circulating fluidized bed. The size and number of cluster at variable radial and axial positions in a circulating fluidized bed were investigated.

Theologies and Markatos [37] detailed three-dimensional two-phase modeling study of the flow patterns and heat transfer in riser reactor concluded that the overall performance

of the riser was predicted using one dimensional mass, energy and species balances. Moreover, the presence of high efficiency feed injection system in modern units justifies the assumptions of plug flow in the riser. The feed phase change and molar expansion as the reactions proceed in the intermediate and the final zone result in typical 3-4 fold increase in the gas superficial velocity along the riser. The advantage of this work was change due to volumetric expansion is considered which would contribute to the discrepancy between the model prediction and the plant data.

Bowman et al. [9] developed a new spray vaporization model that includes multi-component droplet effects by defining new droplet transport property and develop a new catalytic cracking kinetic model that relates the reaction rate constants to the physical properties of the catalyst using computational soft ware CFD. The new model enhances the computation of droplet vaporization rates by describing the actual vaporization process in a more physically realistic manner.

2.2 Kinetic Modeling

Kinetic models are the heart of the complete process models. Reactions kinetic contribute strongly to the development and the optimization of a process technology. For FCC reactor modeling, the establishment of a kinetic model for catalytic cracking reaction is even a key step as the feedstock contains a large number of components. Generally, predicting oil product composition is a much more difficult work than predicting the heat balance. Several thousand compounds are involved in reaction. A complete description of the system in terms of individual compound is impractical for complex feedstock typically processed in modern FCC. Therefore, it is necessary to find a procedure that makes the work manageable. One of the best approaches to model the reactions of the mixtures containing many components is to group molecules that react at similar rates together into compound classes or kinetic lumps. The lumps are then treated as pseudo-components in the model [38].

Fluid catalytic cracking feed stocks are characterized by a wide range of boiling points, usually from 250 to 550°C, depend on the feed origin. This wide range of feedstock boiling points is the result of the large number of hydrocarbon species presents. Therefore, a lumping strategy comprising a small number of pseudo species group in a large number of chemical species can be used to represent the complex of kinetics of the system.

Several lumping models were developed for the kinetic representation of the catalytic cracking reactions. Perhaps, the most popular model, given its simplicity and reliability, is the three-lump model proposed by Weekman [20]. To overcome some of the deficiencies for the three-lump model, other models proposed in the literature included four-lump model, five-lump model, six-lump model, seven-lump model and ten-lump model. However, as the number of lumps considered by the model increases, additional complexities are introduced during the experimental stage and during the parameter estimation stage. It has been pointed out that models based on ten or more lumps involve at least 20 parameters that cannot be calculated with precision [14]. Therefore, the model to be selected for the representation of the catalytic cracking of gas oil should be carefully considered. Moreover, the advantages and disadvantages of the models, as well as the degree of precision achieved for the parameter estimates with the experimental information available, should also be carefully weighed.

Weekman and Nace [14] developed a three-lump model consisting of feedstock, gasoline (C_5-C_{12} fraction) and light gases (C_1-C_4 fraction) plus coke lump as shown in Figure 2.1. A three lump model has been successfully implemented for the representation of the gasoline selectivity in many studies ranging from fixed bed laboratory reactors to industrial fluid catalytic cracking units. A three lump model is a well possessed semi-mechanistic model for the representation of the cracking of hydrocarbons. However, the main drawback of the model is the lumping of the light gases and coke fractions formed during reactions. This feature of the model is not relevant for the simulation of the FCC

riser given that the temperature of operation in the regenerator is decided by the amount of coke formed in the reactor. For this reason, the use of a three lump model should be complemented with an additional model to represent the coke produced by reaction. Moreover, it has been indicated that the rate constants calculated with a three lump model is a function of the gas oil composition. Therefore, it can be concluded that a good model for the representation of the coke formation is additionally required to be used with a three-lump model. Furthermore, extrapolations using rate constants from a three lump model to other types of feedstock with dissimilar composition are not strongly recommended.

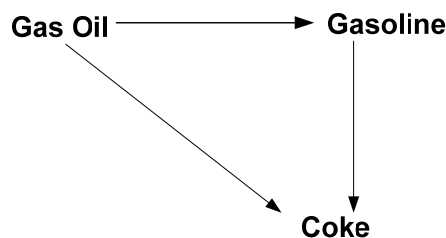


Figure 2.1: Three-lump model

Jacob et al. [38] suggested a network consisting of ten lumps as shown in Figure 2.2. This model is based upon the molecular structure and restricted to lumps that could be measured. It was more detailed than three lump models for describing the cracking reactions. The major advantage of such a model is that the conversion of gas oil to different products can be determined easily. However, the model offers complicated mathematics and it also lumps the coke and light gases as one component as the three-lump model. The rate constants in this model were invariant with respect to the original crude source of the lumps. The lumping scheme considers the feed is lumped into paraffins (Ph, P1), naphthenes (Nh, N1), aromatic rings (Ah, A1) and aromatic groups in both the heavy (CAh) and light fractions (CA1) of the charge stock. The products are divided into two lumps. One is gasoline range (G10) and the other is coke and light gases (C10).

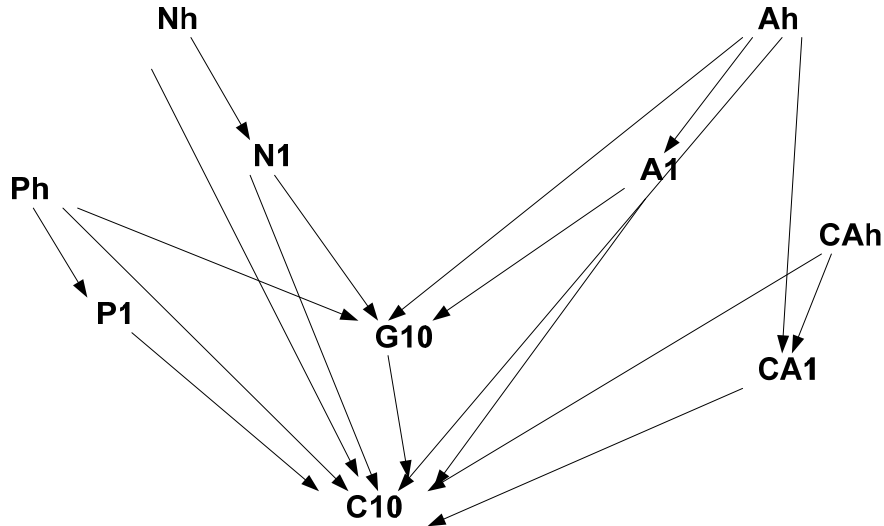


Figure 2.2: Ten-lump model

Takatsuka et al. [39] observed that the catalytic cracking of residual oil or gas oil is strongly influenced by the nature and prior treatment of the feedstock. The authors included the feed stock Vacuum Gas Oil (VGO) in the cracking kinetics to give a six-lump model as shown in Figure 2.3. The lumps are VGO(Vacuum gas oil), GLN(Gasoline), LPG(Liquid petroleum gas), FG(Fuel gas), LCO(Light cycle oil) and CK(Coke).

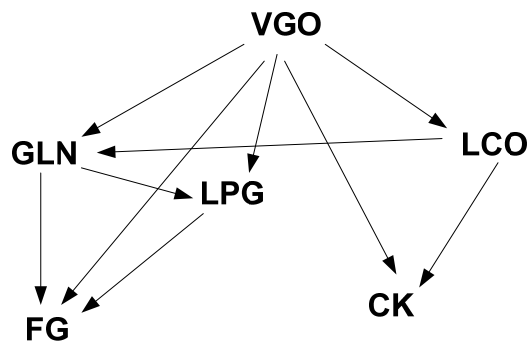


Figure 2.3: Six-lump model

The four lump models for the evaluation of the kinetics of catalytic cracking can be considered as an extension of the three-lump model. The four lump models further expand the three lump models by separating the light gases from the coke into two different lumps. This feature of the model is very relevant for the simulation of the FCC riser given that the temperature of operation in the regenerator will be decided by the amount of coke formed in the reactor. Moreover, as it is expected from cracking more metal contaminated feed stocks, a higher coke yield will have a large impact on catalyst activity. The different reaction schemes [40] proposed for the four lump models are included in Figure 2.4. As indicated by the proposed reaction mechanism, the gas oil lump may crack into gasoline, light gases and coke lump. Moreover, the gasoline lump is considered to contribute to the production of light gases (over cracking) and coke formation. However, it is expected that the extent of the last two reactions will be decided by the operating conditions and in some cases their contribution to the kinetic representation of the system may be neglected. Moreover, it can be speculated that the error introduced by considering or discarding the contribution of the light gases lump to coke formation is normally insignificant given the accuracy of the model predictions [21].

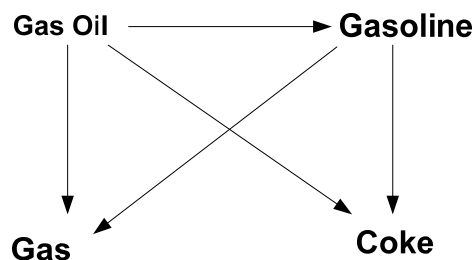


Figure 2.4: Four-lump model

Corella and Frances [21] introduced a five-lump model as shown in Figure 2.5. The five groups are Feed stock (vacuum gas oil), Gas oil, Gasoline, Light gases and coke. These lumps are interconnected with seven different kinetic cracking constants.

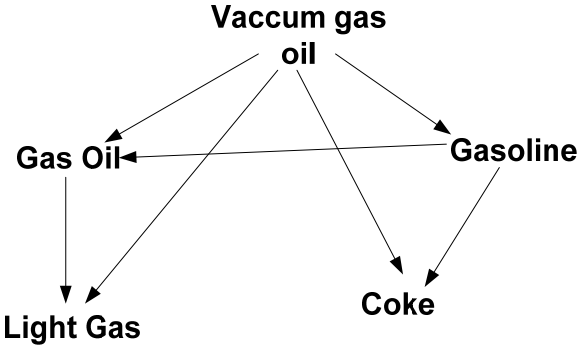


Figure 2.5: Five-lump model

Most recently, Al-Khattaf and De Lasa [41] suggested a seven-lump scheme as shown in Figure 2.6. The seven lumps are Gas oil, Olefins, Napthenes, Paraffins, Aromatic, Methane and Coke. From this we summarized the comparison between the various schemes suggested about kinetics lump model in Table 2.1.

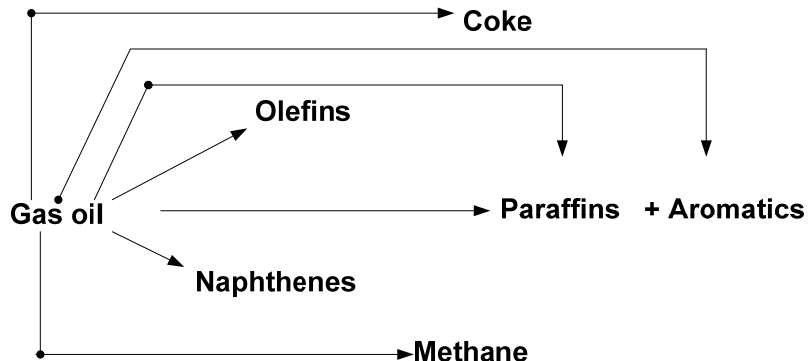


Figure 2.6: Seven-lump model

Table 2.1: Review of reaction kinetics model proposed for FCC

TYPE OF LUMP	AUTHORS	LUMPS	KINETIC CONSTANTS	ADVANTAGES	LIMITATIONS
Three-lump	Weekman & Nace [14]	1- Gas oil 2- Gasoline 3- Light gases & coke	3 reaction constants	<ul style="list-style-type: none"> • simple mathematically • can determine gas oil conversion and gasoline yield 	<ul style="list-style-type: none"> • it lumps coke and light gases into one component
Ten-lump	Jacob et al. [38]	1,2- Paraffins 3,4- Naphthenes 5,6- Aromatic rings 7,8- Aromatic groups 9- Gasoline 10- Gases & coke	17 reaction constants	<ul style="list-style-type: none"> • gas oil conversion can be estimated and the production rate of some particular products can be calculated 	<ul style="list-style-type: none"> • complicated mathematically • experimentally tedious • lumping of gases and coke as one component
Six-lump	Takatsuka et al. [39]	1- Gas oil 2- LPG 3- Light gases 4- Gasoline 5- LCO 6- Coke	6 reaction constants	<ul style="list-style-type: none"> • separates gases from coke 	<ul style="list-style-type: none"> • applicable for the case studied
Four-lump	Dave et al. [40]	1- Gas oil 2- Gasoline 3- Coke 4- Light gases	5 reaction constants	<ul style="list-style-type: none"> • simple mathematically • separates gases from coke • agreement between theory and experiment 	<ul style="list-style-type: none"> • does not predict olefins yields
Five-lump	Corella & Frances [22]	1- Feed stock 2- Gas oil 3- Gasoline 4- Coke 5- Light gases	7 reaction constants	<ul style="list-style-type: none"> • gases and coke are as two lumps 	<ul style="list-style-type: none"> • more applicable for hydro cracking units (suggests that feedstock cracks to gas oil)
Seven-lump	Al-Khattaf & dcLasa [41]	1- Gas Oil 2- Olefins 3- Naphthenes 4- Paraffins 5- Aromatics 6- Methane 7- Coke	7 reaction constants	<ul style="list-style-type: none"> • Olefins in separate lump • Coke in separate lump 	-

However the three lump kinetic model is simple and fairly rigorous to evaluate cracking reactions. The three lump and ten lump models combine coke and light gas as one lump. Therefore, a reliable prediction of the mass of coke produced by cracking reactions and the amount of coke remaining after catalyst regeneration can't be determined easily, which is considered as an extremely important factor for the control and operation of FCC riser. An extension to other lump model is not considered in this work due to the availability of experimental data and the increased computational efforts. The four-lump model is detailed enough to describe the cracking reactions and it is applied to this work.

2.3 The Effect of Coking

In addition to the kinetic lump model, the strong adsorption of coke over the active sites of the catalyst translates in a reduction of catalyst activity. This is evidence by a drop in total conversion, which significantly affect the riser performance. Hence it is important to consider the effect of coking in the kinetic lump model. To represent the effects of the coke deposition on the catalyst activity two approaches have been used. One is based on measurements of time-on-stream (TOS) and the second approach is based on the mass of coke on catalyst (COC) [42].

The time-on-stream decay model was the first approaches to catalyst deactivation. This approach assumes that the coking rate is independent of reactant composition, extent of conversion, and hydrocarbon space velocity. Based on TOS models, many deactivation models could be derived by assuming the rate of catalyst decay as a function of the number of active sites. Thus, the rate of catalyst activity decay can be expressed as a function of the fraction of remaining active sites. The simplest one would be that a linear relationship between the catalyst activity and time-on-stream. However, many of them can be represented as a differential equation of different orders.

The use of a kinetic model including the catalyst activity decay as a function of the coke on catalyst can be considered as a more phenomenological based model compared to the TOS approach. The COC form of the activity decay function has been successfully used

for the representation of data of many researchers [3], [21], [26]. Moreover, it is interesting to observe that model on COC are similar to model TOS except for COC model contains the coke-on-catalyst concentration as the independent variable while the TOS model includes the time-on-stream as the independent variable. Therefore, comparing the COC decay function and the TOS decay function, it can be concluded that the equations involving the time-on-stream are much simpler using the catalyst residence time as main variable. On the other hand, the coke-on-catalyst method requires an additional rate equation for assessing coke formation and important for determining amount of coke formation and also for regenerator model. This work used coke-on-catalyst deactivation model.

2.4 Hydrodynamics of Riser Section

Flow of fluidized solid in risers has been the subject of several investigations during the last few decades. Here, the vaporized feed carries the solid fine particles through the length of the riser section. The riser is divided in to three sections comprising the inlet, the middle and the top section.

In the inlet section, liquid feed is brought into contact with the hot regenerated solid catalyst. The inlet zone is considered to be the most complex part since high turbulence, high temperature gradients, high concentration gradients, and flow heterogeneity occurs.

There are two distinct models followed in designing feed inlet systems. One incorporates prior catalyst lift and acceleration, while the other involves the introduction of the catalyst at its maximum free flowing density [43]. The former approach has the advantages of pre-treating the catalyst to lower the effect of metals decreasing the oil partial pressure and simpler distribution of feed over the catalyst. In addition, the lift gas moves the feed out of the high temperature mixing zone fairly quickly, hence, decreases the probability of thermal cracking. This in turn increases the gasoline yield and decreases the diameter of the feed inlet zone. The shortcoming of gas lift is that the gas

rates above incipient fluidization velocity cause the formation of bubbles. Feed transfer to the bubbles results in thermal cracking. In contrast to gas lift, introducing the catalyst at its maximum free-falling density totally eliminates the chances for thermal cracking. However, catalyst flowing at high density necessitates the presence of a high penetration feed inlet system. It is essential to provide a continuous liquid stream flowing in a flat pattern from a number of nozzles to have the desired action. The feed coats the catalyst particles and vaporizes due to intimate contact. Increasing vapor formation lowers the density of the system and consequently, increases the velocity of the flowing system.

The majority of cracking reactions take place in the second section at the middle of the riser. The function of this zone is to maintain good contact between the catalysts and oil to avoid back mixing. The temperature and concentration profile exhibit intermediate homogeneity in this section between the inlet feed and the final section. The problem of back mixing can be minimized by using straight risers operating at the maximum allowable velocity. This velocity is determined to avoid erosion. The velocity limitation also determines the height of the riser, and its value has increased with improvements in riser design and the use of better internal refractory insulation [12].

The top final section of the riser is the most crucial part. It is desirable to achieve the last 5 to 10 percent of feed conversion in this section. But, it is also of great importance to avoid over cracking of the valuable gasoline product. There are many schemes proposed to prevent over cracking of gasoline, among these is the folded riser design. This design is characterized by down flow in the final riser section. This down flow minimizes the opportunity for gasoline over cracking and practically eliminates slip. A complete down flow system is considered to be the future cracker. Another means of limiting further cracking is by using cyclones. Closed cyclones, presently under investigation, minimize over cracking and maintain good separation characteristics. The explanation of these flow behaviors is important for the industrial application of the risers [1].

One key feature of the hydrodynamic behavior in FCC riser section is the existence of clusters. Clusters are region characterized by high particle concentration in relation to the average solids concentration in the riser column. These are regions of particle aggregations in a gas-solid two-phase flow. These groups of particles move as a single body with little internal relative movement. When clusters form in a riser, it will affect the gas-solid flow behaviors in the reactor. Various experimental efforts have been made [44], [45] in the past to study the formation of clusters and their properties in the circulating fluidized bed, such as the size, velocity and solid volume fraction. Recently, numerical methods have been widely used to study about cluster characteristics and flow systems.

The study of clusters has received a great deal of attention during the last decade resulting in a large number of numerical works on fluidized beds. Gidaspow[44], Wilhelm and Kwauk[45] were among the first to produce experimental evidence of particle clusters in fluidized beds. Kaye and Boardman [46] performed later an interesting study of cluster formation in dilute suspensions. Jayaweera et al. [47] proposed that clusters comprised of 2-6 spheres fall faster than a single sphere. They found that, in a viscous fluid, 2-6 particles organized themselves in stable cluster configurations falling faster than isolated particles. The rate of fall was found to increase as the averages inter particle distance decreased, in the range of ten to five times particle diameter. When the number of particles surpassed six times particle diameter, the clusters split and formed stable sub-groups of clusters.

According to Horio and Clift [48], agglomerates are groups of particles joined together by the action of inter-particle forces, and clusters are groups of particles joined together as a result of hydrodynamic effects. However, in several articles in the literature the term “agglomerate” is used to refer to clusters. In previous work, the axial solid velocity of isolated particles was found to be significantly higher than for particles moving in clusters during their period of formation [49], [50], [51] and [52]. Fluctuations in the

solid velocity are related to the fluctuations in the solid concentration as accelerations of the solid phase correspond to the bypass of clusters or denser solid phase. Horio and Kuroki [53] visually measured the cluster size in a circulating fluidized bed riser using capacitance-probe measurements as shown in Figure 2.7 (a) and (b). Yerushalmi et al. [54] measured large slip velocities in fast fluidized beds, which later were attributed to the formation of clusters. An experimental investigation showed that the local solid velocities of up-flowing clusters increased linearly with their size. Thus the amplitude of the velocity fluctuations seems to depend on the cluster size. Xu and Kato [55] reported correlations for estimating the cluster size as a function of the suspension density, particle density and particle size. Sharma et al. [24] analyzed effects of particle size and superficial velocity on cluster duration time, occurrence frequency and concentration in a riser. Zhang et al. [56] concluded that the formation of clusters is affected by a range of variables related to operational conditions, particle characteristics and properties, and bed properties and geometry.

Agrawal et al. [57] predicted cluster flow using a fine grid resolution method. The author found that cluster interactions plays a major role to hydrodynamics of gas-particle flows in risers. The authors suggested that the phase interaction between the particle and the cluster need to be considered in modeling flows of risers. Mostoufi and Chaouki [58] also observed clusters in bubbling and turbulent fluidized beds and estimated the cluster size relation to effective solids velocity. However, mechanisms of cluster formation remain unclear. Better understanding cluster hydrodynamics in riser will benefit reliable design of a circulating fluidized bed. While the occurrence of particle clusters is now well accepted, little is known about the importance to be consider in modeling and effect on the performance of FCC riser.

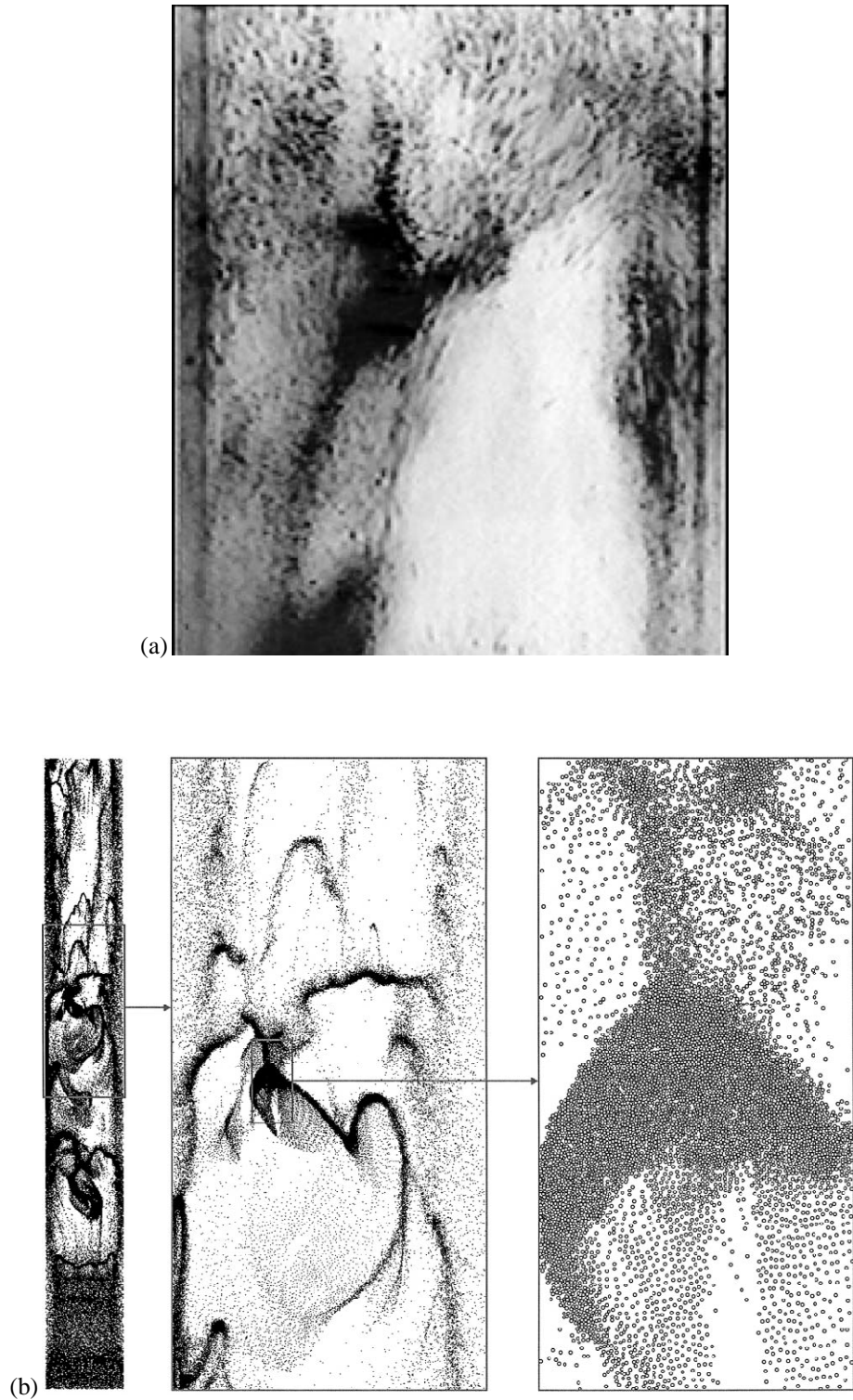


Figure 2.7: (a) and (b) Cluster structure in FCC riser reactor [53]

Shida and Kawai [59] showed that dissipation of kinetic energy through particle-to-particle collision causes clusters to form even without fluid effects. Tanaka et al. [60] stated that the influence of the collision parameters plays an important role in the formation of clusters in diluted vertical risers. McNamara and Young [61] studied numerically the clustering behavior as a function of inelastic collisions.

In summary, previous efforts on modeling riser section were focused on kinetics, hydrodynamics, feed atomization and performance investigations. All these works were based on different assumptions and lead to different conclusions. Recent studies showed that the existence of cluster formation on circulating fluidized bed have significantly influence on the riser performance. This work will cover the modeling and simulation to investigate the effect of cluster formation on riser performance.

CHAPTER 3

METHODOLOGY

In this chapter a brief description of the principles of developing a mathematical model for riser section of FCC is presented. A detail discussion on the general features of the riser unit and the proposed model equations are demonstrated.

3.1 Theory and Background

Developing mathematical models for an industrial unit require a great deal of understanding and knowledge of the physical and chemical phenomena occurring within the unit. These phenomena include the mechanism and rates of mass and heat transfer, the hydrodynamics descriptions, reaction kinetics and thermodynamics.

Ideally, for model development, all the mentioned processes are determined separately and then combined into the model. However, in real situations this is quite difficult due to the complexity of the process to describe mathematically. Therefore, most models are not totally based on detailed mathematical formulations and incorporate simplifying empirical formulas. The presence of these formulas limits the models generality. In addition any model includes a certain number of simplifying assumptions that should be chosen so as not to affect the reliability and the predictive nature of the model. The key factor which controls the number of simplifying assumptions imposed on the model is governed by the required model accuracy.

Model building constitutes a number of steps. The first step in mathematical modeling is to identify the unit configuration, its environment and the modes of interaction between the unit components. The subsequent step is the identification of the relevant state variables which describe the unit and the process taking place within the unit boundaries. This is followed by the determination of the basic principles governing the rate of the process in terms of the state variables and identification of the input variables acting on the system. The model equations are then formulated based on the mass, energy and momentum balances. The introduction of the necessary justifiable assumptions is very

important in simplifying the model equations. After the model equations have been generated, an appropriate algorithm for the solution of the model equations is then developed. The final step is the validation of the model simulation results against the literature data to ensure the reliability of the model. This step may result in imposing more simplifying assumptions or relaxing some of them. The above mentioned steps are interactive and the result of each step should lead to re-evaluation of the results of all previous steps.

In this work the riser model is developed by applying the law of conservation of mass, energy and momentum to differential volume elements within the flowing solid and liquid. Cluster based approach for hydrodynamics and four-lump model for cracking reaction kinetics is applied.

3.2 Riser Model Development

Fresh gas oil is brought into contact with the hot regenerated catalyst at the entrance of the riser which leads to the instantaneous vaporization of the gas oil. The large volume change associated with the vaporization process rapidly raises the velocity, while lowering the density of the flowing mixture as the vapors lift the catalyst particles upwards. Modeling of the riser reactor requires understanding of both the hydrodynamic aspects and the reactions kinetic that occur in the riser.

3.2.1 Riser Reactor Hydrodynamics

The hydrodynamic study of riser reactors revealed that the radial solid fraction profile in the riser is flat and uniform which results in a large reduction of gas and solid back mixing. The riser hydrodynamic is modeled as a plug flow reactor with a one-dimensional model that only considered axial variations of the variable and conservation of mass, momentum and heat. Therefore it can be inferred from gas-solid flow pattern, the riser is plug flow reactor with two phase flow in the axial direction. The gas phase was modeled as a continuum phase and thus the continuity equation is used to obtain the solid flux. From the previous discussion, the riser was separated into three major zones

which are the inlet, intermediate and final zones. The inlet zone was considered to be the most complex part of the riser. This is attributed to the presence of high turbulence, high temperature and concentration gradients, and flow heterogeneity. In modern riser, however, nozzles studies have shown that continuous liquid streams flowing through a number of nozzles coat the catalyst particles providing the intimate contact between the feed and the catalyst pellets. This contact rapidly vaporized the feed. According to plant data, it takes about 0.1 second to fully vaporize the feed [29]. This time represents about 3% of the residence time in the riser. Therefore it's justifiable to assume instantaneous vaporization of the feed. The vaporized feed pneumatically conveys the solid particles from the bottom to the top of the riser.

A vaporization step occurs at the feed injection point of the riser where the feed is put into direct contact with hot catalyst that comes recycled from regenerator. Vaporization step is modeled here as a mixer without any reaction. It has been proved industrially that instantaneous vaporization is a correct assumption at the inlet. Hence, an energy balance equation is developed to describe the heat exchange between the hot regenerated catalyst and the gas oil feed at the entrance of the riser reactor. The determination of the mixing helps to determine the initial temperature of the cracking reaction at the inlet of the reactor. The energy balance equation [7] is:

$$F_c C p_c (T_c - T_{mix}) = -F_s C p_s (T_s - T_{mix}) + F_g [C p_l (T_b - T_F) + \Delta H_{vap} + C p_g (T_{mix} - T_b)] \quad (3.1)$$

In equation (3.1), T_b - is boiling temperature of gas oil, T_s - is steam temperature, T_{mix} - is the temperature of mixture and T_F - is the temperature of gas oil feed. The temperature plot at the feed vaporization section is shown in Figure 3.1.

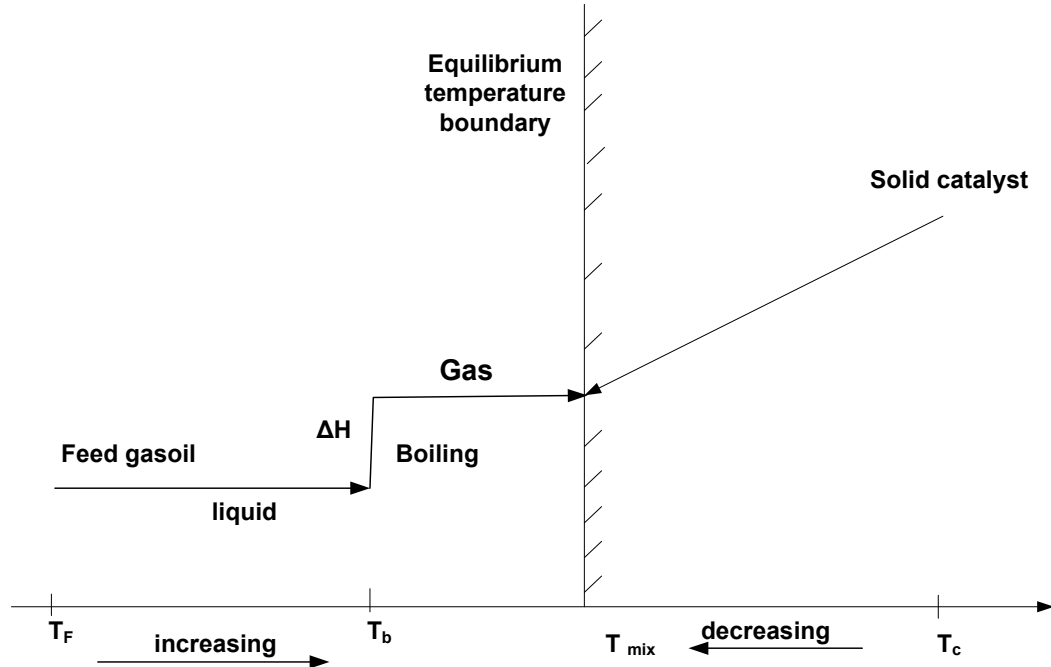


Figure 3.1: Temperature plot at the feed vaporization section of riser

3.2.2 Riser Cracking Reaction Kinetics

All cracking reactions are assumed in riser section of FCC. A four-lump kinetic model is used to describe the cracking reactions in the riser section of this study. An extension to five- and ten-lump scheme is not considered in this paper due to the incomplete experimental data and the increased computational efforts required.

The four-lump model is described with a deactivation model depending on the catalyst coke content. The lumps considered are gas oil, gasoline, light gas and coke. The reactions between lumps have been presented in the Figure 2.4. Similarly to other authors [3], [21] and [31] gas conversion to coke is not considered since the kinetic constants for these reactions are negligible in comparison to the other reactions. The general reaction rate expression [21] is given by:

$$r = -\phi K C^\gamma (M/\rho_g)^\omega \quad (3.2)$$

In equation (3.2), r - reaction rate, \emptyset - deactivation constant, K - reaction constant, C - concentration, M - molecular weight and ρ_g - density of gas oil. Except for the second order gas oil cracking reactions $\gamma = 2$ and $\omega = 1$, all reactions are first order which is $\gamma = 1$ and $\omega = 0$.

The reaction kinetic constant K is related to temperature by Arrhenius law.

$$K = A_0 \exp(-E/RT) \quad (3.3)$$

In equation (3.3), A_0 - the pre-exponential constant and E - activation energy data are obtained from literature of experimental work.

In this work the catalyst deactivation was based on coke deposition or COC decay model. Hence the deactivation is related to coke content through the following rate equation:

$$\frac{d\emptyset}{dCOC} = -K_d \emptyset^q \quad (3.4)$$

The parameters in COC decay model are \emptyset - deactivation function and COC- the coke on catalyst. The exponential $q=1$ has been the most widely used for low and medium coke content. The above equation has the advantage of involving one fitting parameter K_d . The integration of the differential equation (3.4) gives:

$$\emptyset = \exp(-K_d * COC) \quad (3.5)$$

Where the catalyst deactivation coefficient K_d is related to temperature by the following equation:

$$K_d = K_{d0} \exp\left(-E_c/RT\right) \quad (3.6)$$

The following assumptions are used to develop the model for riser section of FCC unit:

- i. Instantaneous vaporization of the gas oil feed by the hot catalyst. It is a justifiable assumption because it takes about 0.1 second to fully vaporize the gas oil [29].
- ii. A detailed three-dimensional two-phase modeling study of the flow pattern and heat transfer in FCC riser reactors was presented by Theologos and Markots [23]. They concluded that the overall performance of the riser can be predicted using one dimensional model equation.
- iii. Plug flow behavior is assumed for the riser model.
- iv. The change due to molar expansion is accounted for in this work.
- v. All cracking reactions are considered to take place in the riser. This assumption is reasonable since the zeolite catalyst and the multi-function catalyst additives highly activate the cracking reaction rate. Furthermore, the coke formation sharply decreases the catalyst activity towards the exit of the riser.
- vi. The riser has a high combined stream velocity and a very short residence time. Thus, it can be assumed that the dynamic terms due to vapor phase concentrations, coke formation and riser temperatures are negligible in comparison with the corresponding terms of the coke burning and temperature in the regenerator. Therefore, the model equations are considered at steady state.
- vii. Steam used to disperse the feed at the entrance of the riser is considered.

3. 3 Riser Model Equations

Based on the above discussion and assumption developed, the riser model equations which are the hydrodynamic and the cracking reaction kinetic model are presented.

3.3.1 Hydrodynamic Model

The proposed riser model considers a system comprising the cluster phase and the gas phase. Cluster phase are agglomerates of loosely held particles [48]. The cluster phase and gas phase hold up vary along the riser height. Solid particles spend more time in the riser than hydrocarbon vapor due to slip velocity between the two phases. The slip velocity observed in the riser is higher than the terminal settling velocity of a single particle. The reason for the higher slip velocities is attributed to particle moving in cluster. Particle in the form of clusters move due to drag force exerted on them by gas phase. In cluster model, an equation of motion is solved for each individual cluster during the free flight phase from force balance as shown in equation (3.7). Net force on cluster is equal to the difference between drag force on cluster and the gravitational force.

$$m_c \frac{du_c}{dt} = \frac{1}{2} C_D A_c \rho_g (u_g - u_c)^2 - m_c g \quad (3.7)$$

The right-hand side of the sum of the forces acting on the cluster is the drag force between the gas and solid phase and the second one is force due to gravity.

For simplicity, the calculations of cluster volume and surface area can be based on equivalent spherical diameter. This allows the mass and projected area of the cluster to be represented. Substituting mass of cluster and projected area in equation (3.7) gives:

$$\frac{du_c}{dt} = \frac{3}{4} \left(\frac{C_D}{d_c} \right) \left(\frac{\rho_g}{\rho_c} \right) (u_g - u_c)^2 - g \quad (3.8)$$

Using equation (3.7) and (3.8) we obtain:

$$\frac{-d\varepsilon_c}{dz} = \frac{A\rho_c}{F_c u_0} \varepsilon_c^2 (1 - \varepsilon_c) \left(\frac{3}{4} \left(\frac{C_D}{d_c} \right) \left(\frac{\rho_g}{\rho_c} \right) \left(\frac{u_0}{1 - \varepsilon_c} - \frac{F_c}{A\rho_c} \right)^2 - g \right) \quad (3.9)$$

In equation (3.9), ε_c - the solid volume fraction, C_D - drag coefficient, d_c - cluster diameter. The detailed derivation of equation (3.9) is shown in appendix A.1. When the drag coefficient is calculated, Stoke's law applies for low particle Reynolds number while is given by equation (3.10) below:

$$Re_c = \frac{\rho_g (u_g - u_c) \varepsilon_g d_c}{\mu_g} \quad (3.10)$$

If $Re_c > 1000$ then C_D becomes:

$$C_D = 0.44 \quad (3.11)$$

Various empirical correlations have been incorporated for drag coefficient calculations in the intermediate range. These corrections have been observed to cause relatively minor changes in results. The correlation by Issangya [62] has been used for $Re_c < 1000$.

If $Re_c < 1000$ then C_D becomes:

$$C_D = \frac{24}{Re_c} (1 + 0.15 Re_c^{0.687}) \quad (3.12)$$

Superficial velocity is the volumetric flow of material per unit cross sectional area of the reactor. In the riser section of the reactor for the hydrodynamic case two phase flow of gas and solid exists. The superficial velocity will be the superficial gas velocity and superficial solid velocity. Superficial gas velocity is the volume flows of gas per unit cross sectional area of the riser reactor. The equation for superficial velocity is given by:

$$u_o = \frac{Q}{\Omega} \quad (3.13)$$

The fraction of pipe cross-sectional area available for the flow of gas is usually assumed to be equal to the volume fraction occupied by gas, which is void fraction ε_g . The fraction of pipe area available for the flow of solids is therefore $(1 - \varepsilon_g)$ or ε_c and then the actual gas velocity for both the gas and cluster velocities will be:

$$u_g = \frac{Q}{\Omega \varepsilon_g} \quad (3.14)$$

and

$$u_c = \frac{Q}{(1 - \varepsilon_g)\Omega} \quad (3.15)$$

In equation (3.14) and (3.15), u_g, u_c - gas and particle velocity, Q - volumetric flow rate and Ω - cross sectional area.

Then, gas phase volume fraction is obtained using the relation:

$$\varepsilon_g + \varepsilon_c = 1 \quad (3.16)$$

Thus a superficial gas velocity is related to actual velocity by the equation:

$$u_g = \frac{u_o}{\varepsilon_g} \quad (3.17)$$

Consider a length of transport pipe into which are feed particles at mass flow rates of F_c . The continuity equations for particles flow rate is:

$$F_c = \Omega u_c (1 - \varepsilon_g) \rho_c \quad (3.18)$$

and for solid flux is :

$$G_c = u_c (1 - \varepsilon_g) \rho_c \quad (3.19)$$

In order to obtain an expression for pressure drop along a section of transport line, the momentum equation is used for a section of pipe on solid particle. The free body diagram of momentum balance on riser reactor is shown in Figure 3.2.

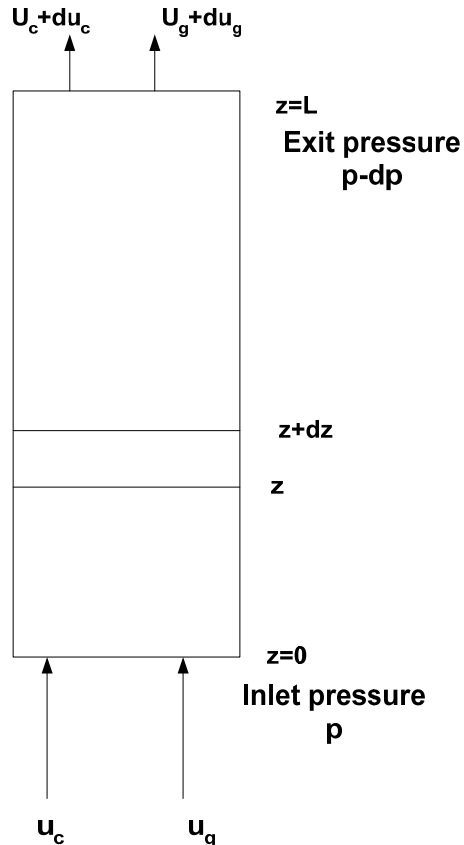


Figure 3.2: Momentum balance on riser section

From Figure 3.2, the velocity of the solid particle and gas increases and at the same time there is pressure drop. To determine pressure drop, consider a section of pipe of cross-sectional area- Ω , differential length- δz and carrying a suspension of volume fraction($1 - \varepsilon_g$). The momentum balance equation is:

$$-\delta P = \rho_c(1 - \varepsilon_g)u_c\delta u_c + F_{gw}\delta z + F_{cw}\delta z + (1 - \varepsilon_g)\rho_c\delta z g \quad (3.20)$$

(1)

(2)

(3)

(4)

In equation (3.20), where F_{gw} and F_{cw} are the gas-to-wall friction force and solids-to-wall friction force per unit volume of pipe, respectively.

Equation (3.20) can apply to the flow of any gas-particle mixture in a pipe. Assumption has been made as the particles are transported in dilute phase. Equation (3.20) indicates that the pressure drop along a straight length of pipe carrying solids in dilute phase transport is made up of a number of terms: (1) pressure drop due to particle acceleration, (2) pressure drop due to gas-to-wall friction, (3) pressure drop related to solid-to-wall friction and (4) pressure drop due to the static head of the solid.

Some of these terms may be neglected depending on circumstances. If the solids are already accelerated in the line, then the first terms should be omitted from the model of the pressure drop. The main difficulties are in knowing what the solids-to-wall friction is and whether the gas-to-wall friction can be assumed independent of the presence of the solids. In this study solid-to-wall and gas-to-wall friction is assumed as being not significant. The detail derivation of the model is found in the Appendix A.2.

Finally, equation (3.20) is simplified to final model equation:

$$-\frac{dP}{dz} = \rho_c(1 - \varepsilon_g)g + \rho_c(1 - \varepsilon_g)u_c \frac{du_c}{dz} \quad (3.21)$$

3.3.2 Kinetic Model Development

3.3.2.1 Conservation of Mass

The riser model equation using the four lump schemes is derived. The mass balance equation is derived by taking an increment with cross sectional area Ω and a very small differential width dz . As shown in Figure 3.3, gas oil and regenerated catalyst at the inlet lead to product formation and at the outlet spent catalyst and product are separated, spent catalyst is sent to regenerator to remove the coke in the catalyst and to become regenerated catalyst.

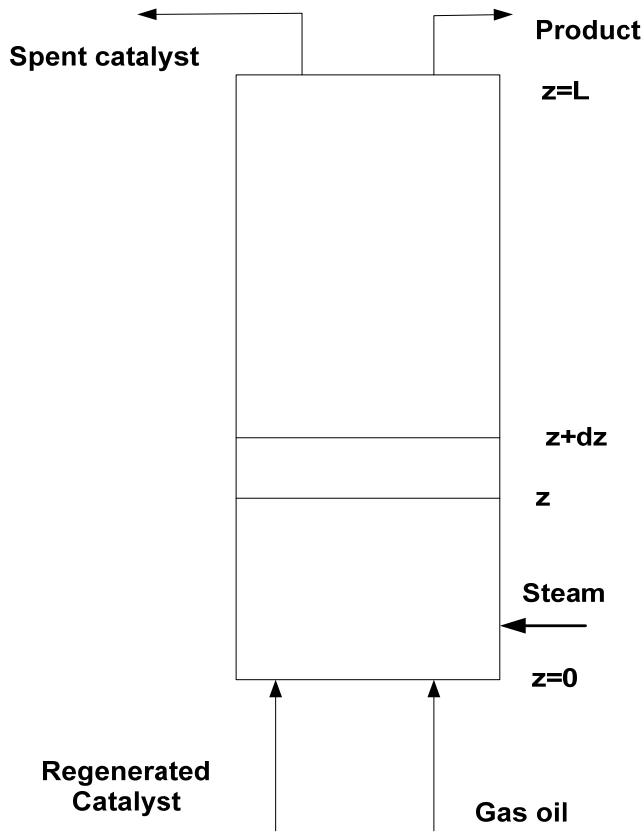


Figure 3.3: Mass balances around the riser of FCC

A mass balance over a differential element dv of the reactor:

$$\frac{df}{dv} + \frac{1}{dv} \frac{dn}{dt} = (1 - \varepsilon_g) \sum \phi r \quad (3.22)$$

In equation (3.22), where f - represents molar flow of the compound in the differential volume dv , ε_g - the void fraction, $\sum \phi r$ - the rates of reactions involving compound expressed per volume of catalyst.

The gas oil mass balance equation is derived by taking an increment with cross sectional area Ω and a very small width dz , the conservation principle when applied to this increment results in:

$$\Omega dz (1 - \varepsilon_g) \frac{dC_a}{dt} = Q C_a[j] - Q C_a[j + 1] + \Omega dz (1 - \varepsilon_g) (-r_a) \quad (3.23)$$

Rearranging equation (3.23):

$$\frac{dC_a}{dt} = -\frac{Q}{\Omega(1-\varepsilon_g)} \frac{\partial C_a}{\partial z} + (-r_a) \quad (3.24)$$

Taking the limit at ∂z approaches zero, equation (3.24) becomes:

$$\frac{dC_a}{dt} = -\frac{Q}{\Omega(1-\varepsilon_g)} \frac{\partial C_a}{\partial z} + (-r_a) \quad (3.25)$$

Substitute for gas oil reaction term ($-r_a$) into (3.25)

$$-r_a = -\emptyset \rho_c \left(\frac{M_a}{\rho_g} \right) (K_{ab} + K_{ac} + K_{ad}) C_a^2 \quad (3.26)$$

$$\frac{dC_a}{dt} = -\frac{Q}{\Omega(1-\varepsilon_g)} \frac{\partial C_a}{\partial z} - \emptyset \rho_c \left(\frac{M_a}{\rho_g} \right) (K_{ab} + K_{ac} + K_{ad}) C_a^2 \quad (3.27)$$

By using superficial velocity u_0 , equation 3.27 becomes:

$$\frac{dC_a}{dt} = -\frac{u_0}{(1-\varepsilon_g)} \frac{\partial C_a}{\partial z} - \emptyset \rho_c \left(\frac{M_a}{\rho_g} \right) (K_{ab} + K_{ac} + K_{ad}) C_a^2 \quad (3.28)$$

Applying the same procedure to the gasoline, gas, and coke balances results in the following equations. The detailed derivations are presented in Appendix B.

- The gasoline mass balance equation is,

$$\frac{dC_b}{dt} = -\frac{u_0}{(1-\varepsilon_g)} \frac{\partial C_b}{\partial z} - \emptyset \rho_c [(K_{bd} + K_{bc}) C_b - \left(\frac{M_a}{\rho_g} \right) K_{ab} C_a^2] \quad (3.29)$$

- The light gases mass balance equation is,

$$\frac{dC_c}{dt} = -\frac{u_0}{(1-\varepsilon_g)} \frac{\partial C_c}{\partial z} + \emptyset \rho_c \left(\left(\frac{M_a}{\rho_g} \right) K_{ac} C_a^2 + K_{bc} C_b \right) \quad (3.30)$$

- The coke mass balance equation is,

$$\frac{dC_a}{dt} = -\frac{u_0}{(1-\varepsilon_g)} \frac{\partial C_a}{\partial z} + \emptyset \rho_c \left(\left(\frac{M_a}{\rho_g} \right) K_{ad} C_a^2 + K_{bd} C_b \right) \quad (3.31)$$

The riser bed is act as a fast moving bed with a high combined stream velocity and a shorter residence time of a few second. The riser dynamics have been shown to be much faster than those of the regenerator [12]. Therefore, the riser energy and mass balance equations can be expressed in the form of a quasi steady state mode. Thus it can be assumed that the dynamic terms of vapor phase composition, coke formation and riser temperature are negligible in comparison with the corresponding terms of the coke burning and temperature of the emulsion phase in the regenerator. The mass and energy balance based on these assumptions are given by the following set of equations:

- Gas oil:

$$\frac{dC_a}{dz} + \frac{\rho_c(1-\varepsilon_g)}{u_0} \emptyset \left[\left(\frac{M_a}{\rho_g} \right) (K_{ab} + K_{ac} + K_{ad}) \right] C_a^2 = 0 \quad (3.32)$$

- Gasoline:

$$\frac{dC_b}{dz} + \frac{\rho_c(1-\varepsilon_g)}{u_0} \emptyset \left[(K_{bd} + K_{bc}) C_b - \left(\frac{M_a}{\rho_g} \right) K_{ab} C_a^2 \right] = 0 \quad (3.33)$$

- Light gases:

$$\frac{dC_c}{dz} - \frac{\rho_c(1 - \varepsilon_g)}{u_0} \emptyset \left(\left(\frac{M_a}{\rho_g} \right) K_{ac} C_a^2 + K_{bc} C_b \right) = 0 \quad (3.34)$$

- Coke:

$$\frac{dC_d}{dz} - \frac{\rho_c(1 - \varepsilon_g)}{u_0} \emptyset \left(\left(\frac{M_a}{\rho_g} \right) K_{ad} C_a^2 + K_{bd} C_b \right) = 0 \quad (3.35)$$

3.3.2.2 Conservation of Energy

The riser reactor is assumed as a plug flow reactor. With this assumption the catalytic cracking reaction in the riser section of a reactor can be described by:

$$(F_g Cp_g + F_c Cp_c + F_s Cp_s) \left(\frac{dT}{dz} \right) = -\Omega \emptyset (1 - \varepsilon_g) M_a \sum (\Delta H_i) (-r_i) \quad (3.36)$$

From equation (3.36), the rate of heat consumed for endothermic reaction is expressed by:

$$\sum (\Delta H_i) (-r_i) = \left(\frac{M_a}{\rho_g} \right) \rho_c (\Delta H_{ab} K_{ab} + \Delta H_{ac} K_{ac} + \Delta H_{ad} K_{ad}) C_a^2 + (\Delta H_{bc} K_{bc} + \Delta H_{bd} K_{bd}) C_b \quad (3.37)$$

3.4 Algorithm and Tools used

The riser is conceptually considered to consist of a number of ‘N’ equal sized differential volumes along the axis as shown in Figure 3.3. Numbering of compartments is from the bottom to top. In the entry zone, each compartment consists of three phases. The phases are solid phase (catalyst particle), gas phase (vaporized feed and dispersion steam) and liquid phase (liquid feed gas oil). Once the feed is completely vaporized, remain only two

phase namely solid phase and gas phase. Within a differential volume, each phase is assumed to be well mixed. Hence the conditions and properties at the differential volume outlet are the same as those inside the differential volume. Model equations are written inside the differential volume for each lump in terms of material and energy balance considering hydrodynamics, reaction kinetics while accounting for gas phase properties and catalyst activity. The input parameters at the inlet conditions of the riser are known, which are used as an initial value for the systems of differential equation. The steady state riser ordinary differential equations (ODE) are solved using MATLAB code. All the output variables are integrated with respect to the height of the riser. Output variables contain the product distributions, solid volume fractions, pressures and temperatures of the riser exit gas stream. The output values of the differential volume riser are updated with volumetric expansion. In general outlet conditions for the first differential volume serve as inlet conditions for the next differential volume. Computations are performed for each differential volume starting from the riser inlet to outlet. The computational algorithm is as shown in Figure 3.4.

The main tools used are MATLAB and Microsoft Excel. The MATLAB provides the platform to develop code to solve systems of differential equation using numerical method and the Microsoft Excel also provides convenient spreadsheet platform to handle the data and analysis of the results. In numerical analysis the Dormand-Prince method, a member of the Runge-Kutta family of ODE solvers, is selected for solving ordinary differential equation. The Dormand-Prince method uses six function evaluations to calculate fourth and fifth order accurate solutions. The difference between these solutions is then taken to be the error of the fourth order solution. This error estimate is very convenient for adaptive step size integration algorithms.

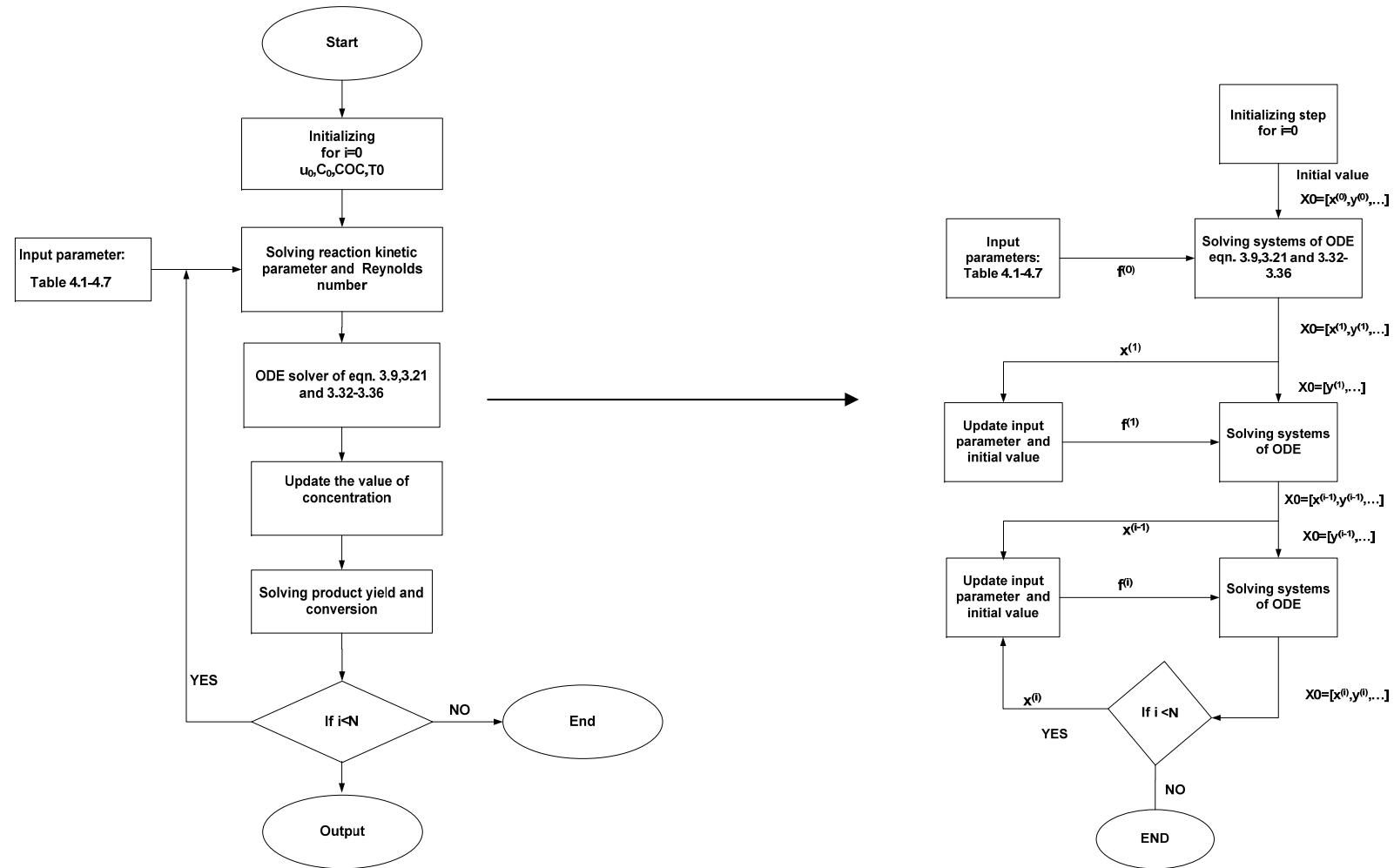


Figure 3.4: Algorithm to compute model equation

The Dorman-Prince method has seven stages, but it uses only six function evaluations per step because it has the first same as last property. The last stage is evaluated at the same point as the first stage of the next step. Dorman-Prince method [63] chooses the coefficient of their method to minimize the error of the fifth-order solution as shown in Table 3.1. For this reason, the Dorman-Prince method is more suitable when the higher order solution is used to continue the integration, a practice known as local extrapolation. The reason for using the coefficient of Dorman-Prince is that since the structure of the coefficients includes an error vector, the implementation is able to ascertain whether adaptive step sizes can be computed.

Table 3.1: Dorman-Prince coefficients

A	B matrix						
0							
1/5	1/5						
3/10	3/40	9/40					
4/5	44/45	-56/15	32/9				
8/9	19372/6561	-25360/2187	64448/6561	-212/729			
1	9017/3168	-355/33	46732/5247	49/176	-5103/18656		
1	35/384	0	500/1113	125/192	-2187/6784	11/84	
E1	5179/57600	0	7571/16695	393/640	-92097/339200	187/2100	1/40
E2	35/384	0	500/1113	125/192	-2187/6784	11/84	0

In Table 3.1, A and B matrix is used to solve the fourth and the fifth order Runge-kutta solution. The row of E1 coefficients gives the fourth-order accurate solution, and the second row E2 has order five. The difference between these solutions is then taken to be the error of the fourth order solution.

CHAPTER 4

RESULTS AND DISCUSSION

In this chapter the model results and the effect of change of key parameters are presented. The plant data from literature is used to validate the model. The base case operating conditions and the geometry of riser are listed in Table 4.1 and 4.2 [32], [64], [65]. The physical properties of the catalyst used are obtained from Fernandes et al. [32] and listed in Table 4.3. The kinetic parameters for the cracking reactions for the four lump kinetic scheme and heat of reactions were obtained from Han et al. [66] and presented in Table 4.4 and 4.5. The molecular weight of lumps obtained from Nyak et al. [29] presented in Table 4.6 and feed stock properties from Gupta et al. [67] presented in Table 4.7.

Table 4.1: Base case operating conditions [32] and [64]

Base Case Operating Condition	
Fresh feed flow rate (kg/s)	60.82
Fresh feed temperature (K)	502
Steam flow rate entering the riser (kg/s)	3.58
Steam temperature (K)	592.25
Catalyst-to-oil ratio, CTO (kg/kg)	6.9
Superficial gas velocity	8

Table 4.2: Riser geometry [65]

Riser geometry	
Riser height (m)	32
Diameter (m)	1.6

Table 4.3: Catalyst properties [32]

Zeolite catalyst properties	
Average particle diameter (m)	7.4×10^{-5}
Density (kg/m ³)	1450
Specific heat (J/(kgK))	1197.5
Porosity	0.5

Table 4.4: Pre-exponential constant and activation energy [66]

Reaction	Pre-exponential constant(1/s)	Activation Energy(kJ/kgmole)
K_{ab}	1457.50	57359
K_{ac}	127.59	52754
K_{ad}	1.98	31820
K_{bc}	256.81	65733
K_{bd}	6.29×10^{-4}	66570
Deactivation coefficient	$K_{d0}=1.1 \times 10^{-5}$	$E_c=49000$

Table 4.5: Heat of reactions [66]

Heat of reaction	Value (kJ/kg)
ΔH_{ab}	195
ΔH_{ac}	670
ΔH_{ad}	745
ΔH_{bc}	530
ΔH_{bd}	690
ΔH_{vap}	270

Table 4.6: Molecular weight of lump model [29]

Lumps	Molecular weight (kg/kmole)
Gas oil	350
Gasoline	100
Light gas	40
Coke	16
Steam	18

Table 4.7: Feed stock properties [67]

Feed stock properties	
°API	21.8
Watson characterization factor , K_w	11.8
Specific heat capacity of liquid feed (kJ/kgk)	2.1
Boiling temperature of liquid feed (K)	532
Density of liquid feed (kg/m3)	870
Evaporation temperature (K)	530
Specific heat of vapor feed (kJ/kgk)	3.2
Density of vapor feed (kg/m ³)	8.40
Gas phase viscosity (kg/ms)	1.3×10^{-5}

4.1 Simulation of Base Case

Before using the model to understand effect of cluster formation on riser performance, the simulations of base case were carried out using computation along the riser height. For the simulation, the data from literature as shown in Table 4.1-4.7 were used. The model is used to simulate the performance of FCC riser reactor. The performance of FCC riser reactor is expressed using conversion and the product yields. The simulated results of the base case are shown in the Figure 4.1- 4.7. The conversion of gas oil as shown in Figure 4.1 increased and attained 64% gas oil conversion. The yield of gasoline is 48%, yield of gas is 18% and yield of coke formation is 6% at the outlet as shown in Figure 4.2. It can be seen from the result that steepest rise occurred at the inlet section of the riser because of the highest temperature and lowest catalyst coke content encountered at the riser inlet.

It has been proved industrially that instantaneous vaporization is a correct assumption for feed vaporization section. Feed vaporization section is modeled as a mixer without any reaction. The gas temperature initially rises at the feed vaporization section due to rapid heat transfer from the solid particles. During cracking, the temperature decrease along the riser height with temperature drop of 32K due to endothermic nature of cracking reaction as shown in Figure 4.3. Cracking reactions rapidly increase the volumetric expansion and therefore cause significant increase in the gas and catalyst velocity as shown in Figure 4.4. The velocity profiles clearly show that there is slip factor, ratio of gas to particle velocity, between the two phases that decrease along the riser. This slip factor between the two phases is largely due to the formation of clusters of catalyst particles. The volumetric expansion makes the solid void fraction or solid hold up decrease from 0.054 to 0.014 along the riser height as shown in Figure 4.5, while the gas void fraction increase as expected. Gas usually flows along a less resistant path, following the region of low solids density. Gases can be easily distributed in comparison with solids. Therefore, the major concern has been solids distributions. Velocity of gas control non-homogeneity of solid hold up along the riser columns. The effect of gas velocity is much

more evident in the distribution of solid particle because the gas phase has to carry the suspension upward against gravity.

It was assumed that the coke formed due to cracking reaction gets deposited on the catalyst, as shown in Figure 4.2 the coke formation on catalyst increases along the riser height and obtained 6.5%. Therefore, a reliable prediction of the mass of coke produced by cracking reactions is possible using a four lump model. This feature of the model is very relevant for the simulation of the FCC riser given that the temperature of operation in the regenerator will be given by the amount of coke formed in the reactor. The deactivation function shows the activity of catalyst measured in terms of coke formation. In addition to the kinetics lump model, the strong adsorption of coke over the active sites of the catalyst translates in a reduction of catalyst activity as shown in Figure 4.6. This is evidence by a drop in catalyst activity from 1 to 0.14, which significantly affect the riser performance. Figure 4.7 shows the pressure drop decrease along the riser with a total drop of 16 KPa. The results of the base case discussed above are consistent for the prevailing understanding of riser performance. The computation model was then evaluated with by comparing model predictions with the published plant data.

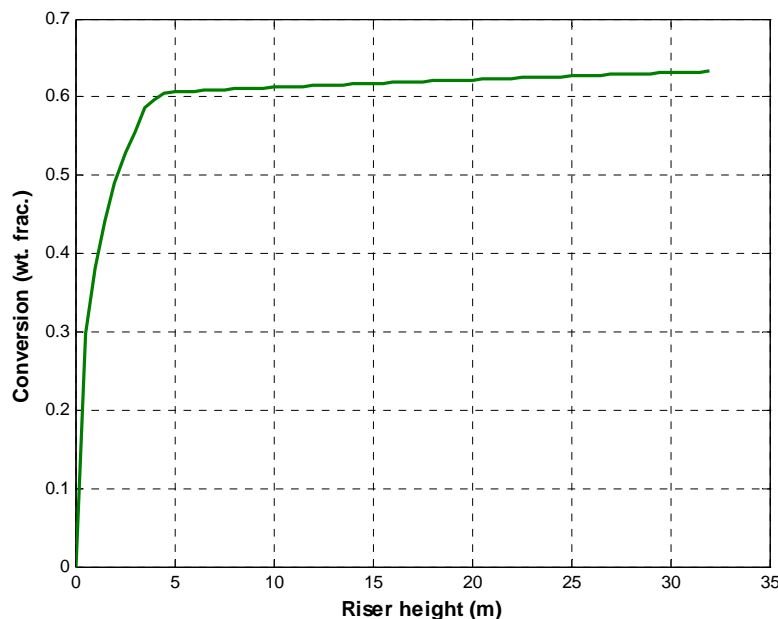


Figure 4.1: Conversion of gasoil vs. riser height.

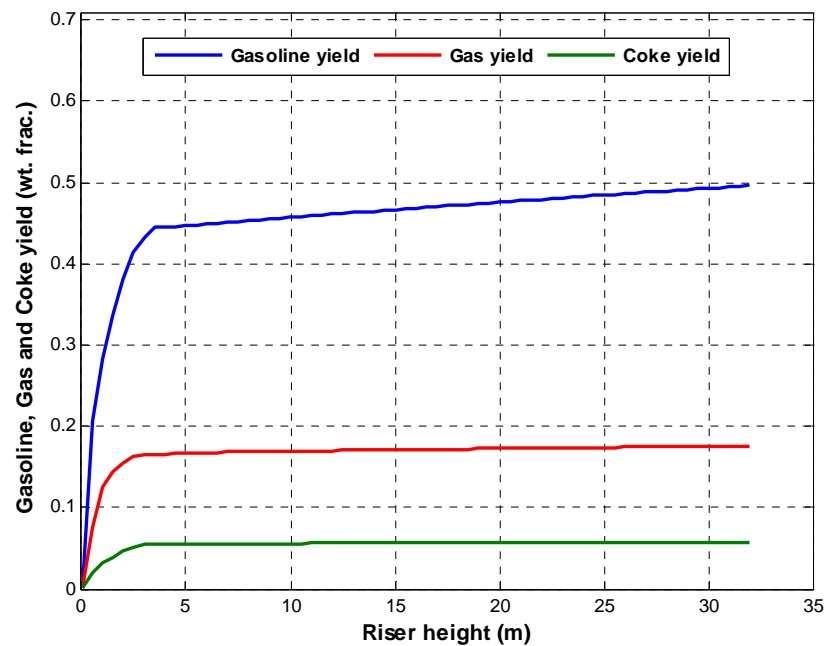


Figure 4.2: Gasoline, Gas and Coke yield vs. riser height.

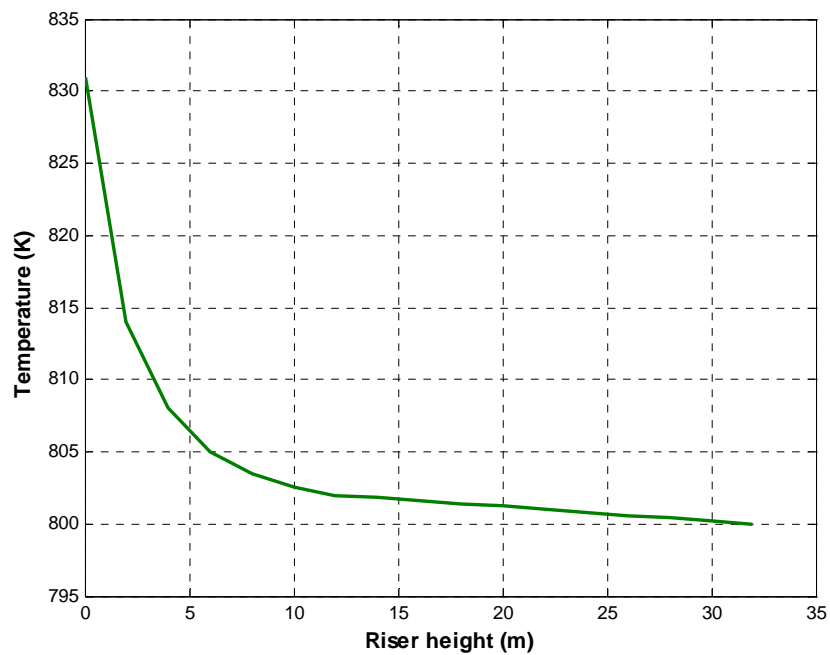


Figure 4.3: Temperature drop vs. riser height.

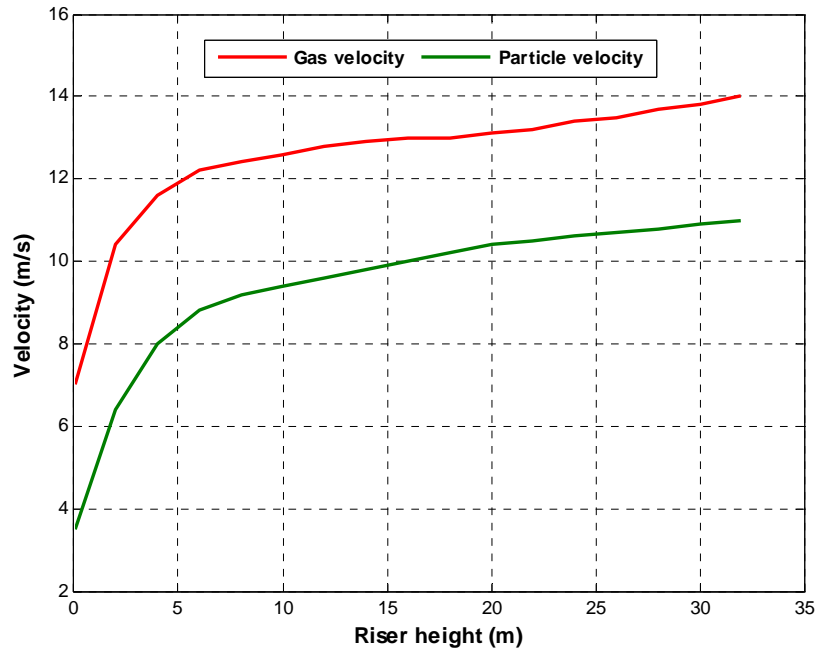


Figure 4.4: Velocity of catalyst (v_c) and gas (v_g) phase vs. riser height.

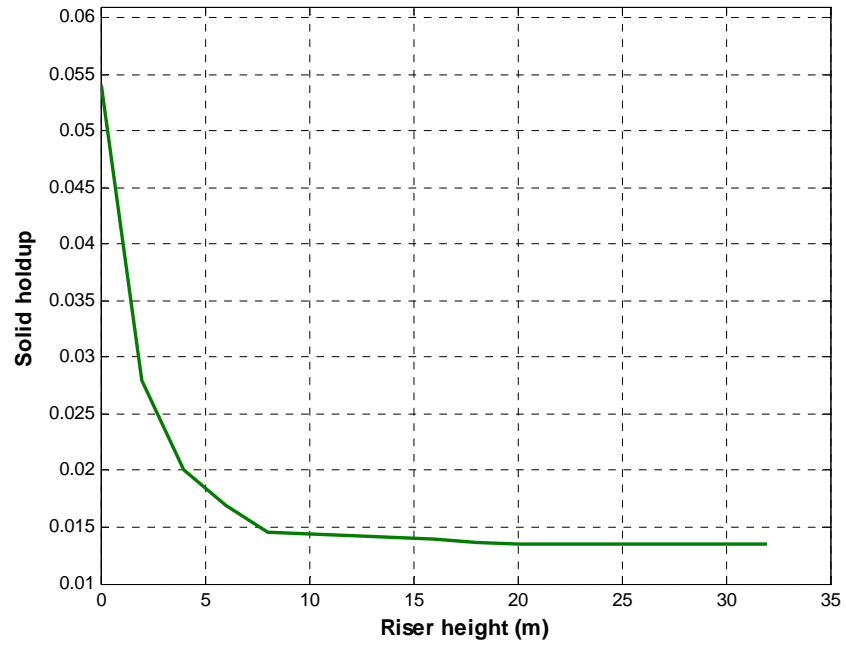


Figure 4.5: Solid holdup vs. riser height.

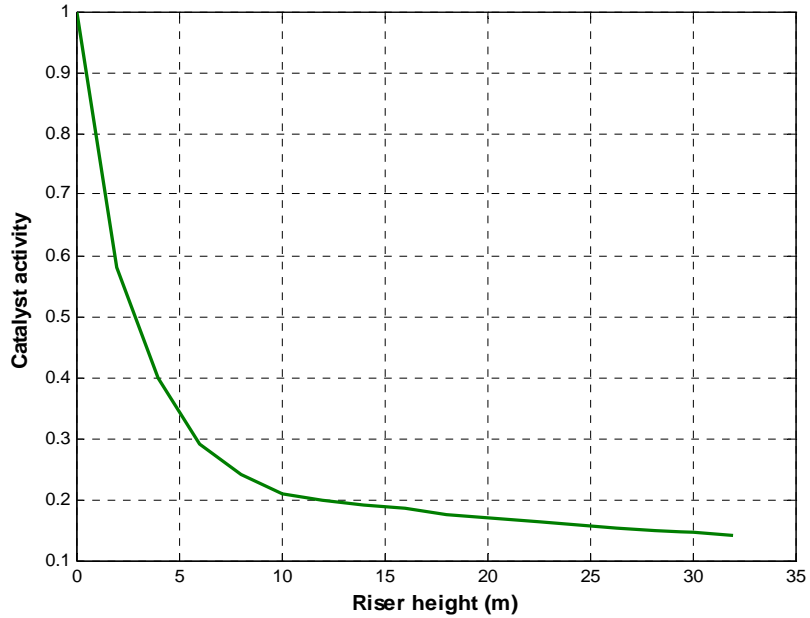


Figure 4.6: Catalyst activity vs. riser height.

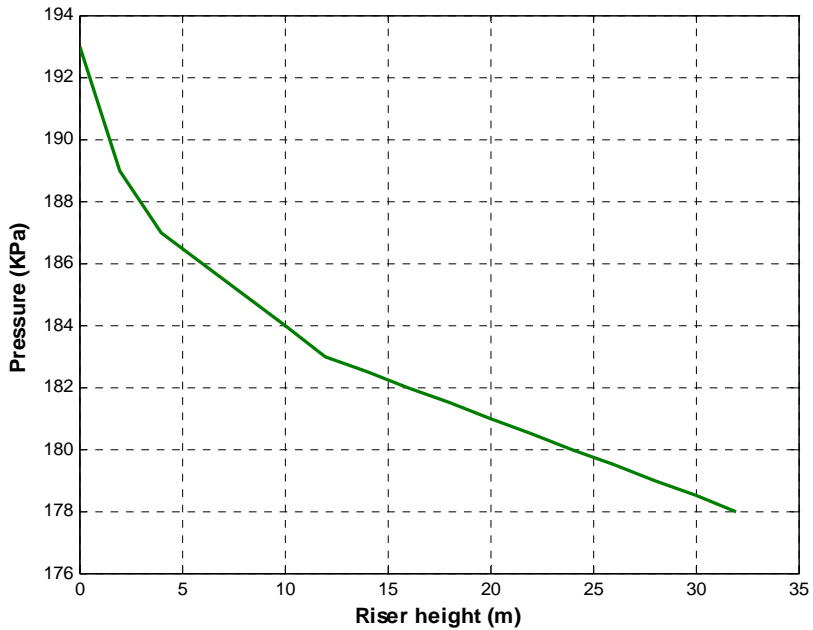


Figure 4.7: Pressure drop vs. riser height.

4.2 Model Validation

The comparison of model prediction of industrial riser reactors with plant data is not straight forward. The model requires detail information about the design and operating

condition of the industrial reactor. Adequate and complete information is seldom available from the published data. It is therefore necessary to make suitable assumption to enable simulation. In the present work, the developed model was used to validate the plant data reported by Derouin et al. [68] and Ali et al. [69].

Derouin et al. [68] reported the gas oil conversion and gasoline yield in industrial riser. They reported the data at four points along the riser height. Equipment and operating conditions considered in the simulation of case reported by Derouin et al. are listed in Table 4.8. The comparison of the plant data and the model predicted result are shown in Figure 4.8(a) and (b). From Table 4.10, it can be seen that the deviation of model predicted results shows reasonable good agreement with majority of the data deviation lies between 1 and 5%. It can conclude from the deviation of model and actual plant data that most of the cracking reaction takes places within the inlet range of the riser because of overestimation of the model result at the inlet. Thus the riser inlet range plays a major role in the performance of the riser.

Simulations were also carried out for another case of riser for which data is reported by Ali et al. [69]. Equipment and operating conditions considered in the simulation of case reported by Ali et al. are also listed in Table 4.9. The model predictions for conversion and axial yield profiles of gasoline, gas and coke are presented along with the actual plant data at the riser outlet are plotted in Figure 4.9. The deviation of model predicted from plant data is shown in Table 4.11 and the agreement is reasonable. From this result we can conclude that the model has good prediction at the outlet.

One of the distinguished features of the developed FCC model is that it combines both the hydrodynamics and reaction kinetics. In fact, the model represents what is happening actually in the FCC riser unit. The open literature models proposed for riser reactor lack the advantage of the model developed in this study. The comparison between the model and industrial plant data indicates that the model predicts the plant data reasonably well. It gives close values for output of the riser such as conversion and products yield. This shows that the model assumptions made in this study were reasonable.

Table 4.8: Industrial data reported by Derouin et al. [68]

Variable	Value
Riser diameter	1 m
CTO	5.53
Catalyst inlet temperature	960 k
Riser height	32m
Feed flow rate	85 kg/s
Feed inlet temperature	650 K

Table 4.9: Industrial data reported by Ali et al. [69]

Variable	Value
Riser diameter	0.8 m
CTO	7.2
Catalyst inlet temperature	960 k
Riser height	33 m
Feed flow rate	20 kg/s
Feed inlet temperature	494 k

Table 4.10: Deviation of model predicted and plant data reported by Derouin et al. [68]

Type	Plant data	Model predicted	Deviation (%)
Conversion	0.48	0.58	10%
	0.60	0.62	4%
	0.65	0.63	2%
	0.7	0.65	5%
Gasoline	0.31	0.44	13%
	0.42	0.47	5%
	0.47	0.48	1%
	0.48	0.49	1%

Table 4.11: Deviation of model predicted and plant data reported by Ali et al. [69]

Type	Plant data	Model predicted	Deviation (%)
Conversion	0.62	0.64	2%
Gasoline	0.6	0.49	11%
Gas	0.22	0.18	4%
Coke	0.075	0.062	1.3%

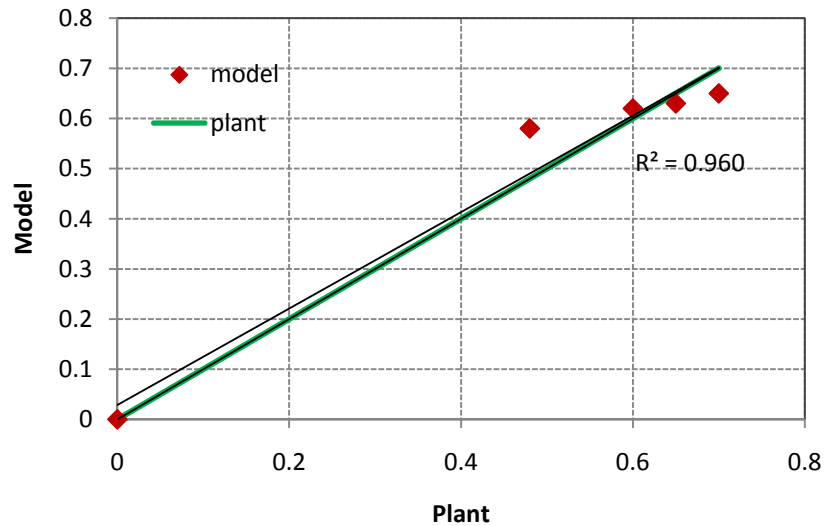


Figure 4.8 (a): Validation with conversion data provided by Derioun et al. [68].

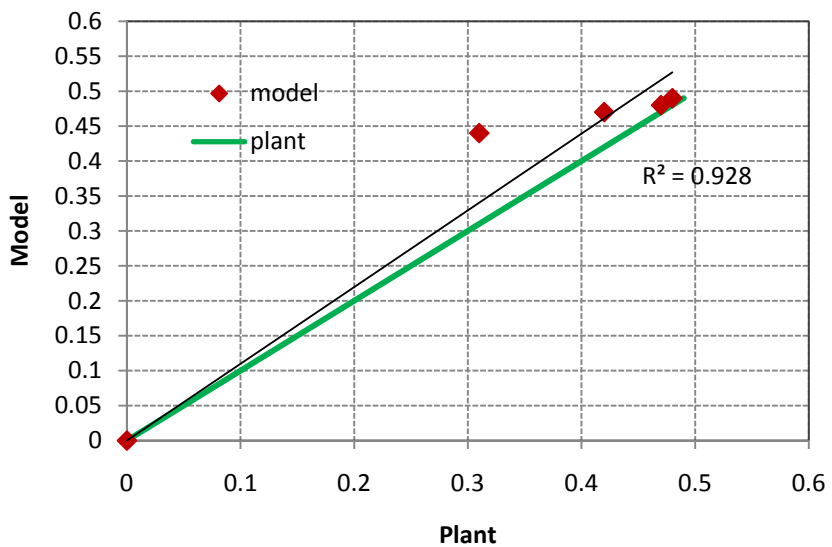
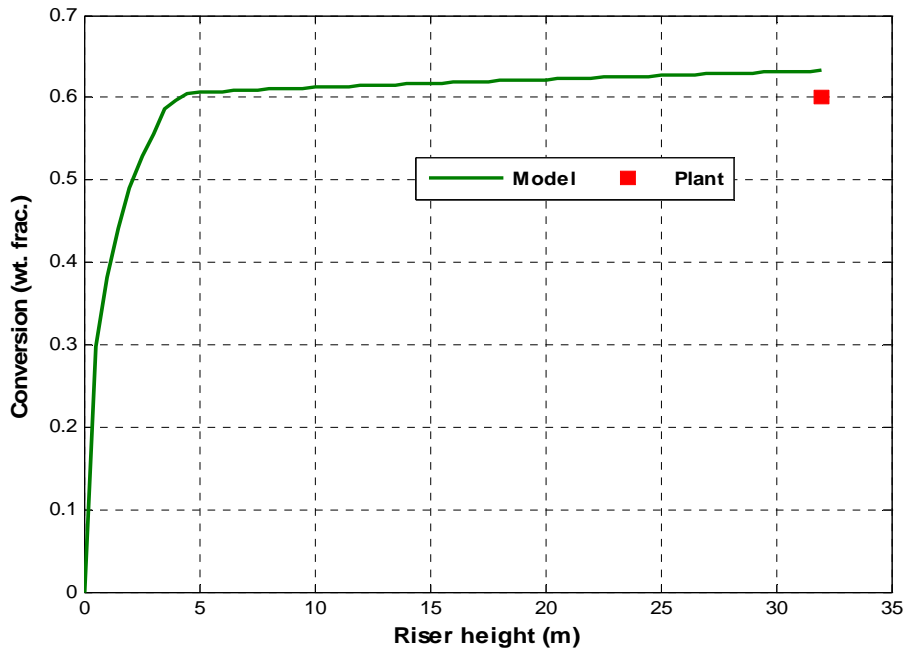
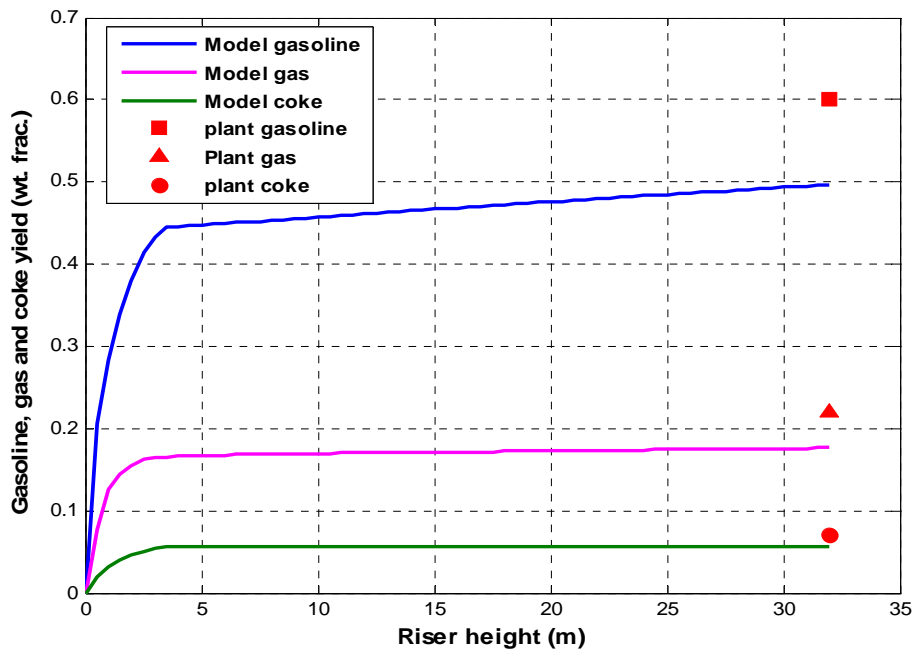


Figure 4.8 (b): Validation with gasoline data provided by Derioun et al. [68].



(a)



(b)

Figure 4.9: Validation of data provided by Ali et al. [69] with (a) conversion and (b) gasoline, gas, and coke yield of the model result.

Comparison of this work with other simulation results developed by Gupta et al. [3] also considered as a case to validate the model result of this work. As shown in figure 4.10, comparison of results predicted by this work and those reported by Gupta et al. [3] is shown using graphical method known as parity plot. This work agree to the literature data with the average correlation coefficient of $R^2=0.98$.

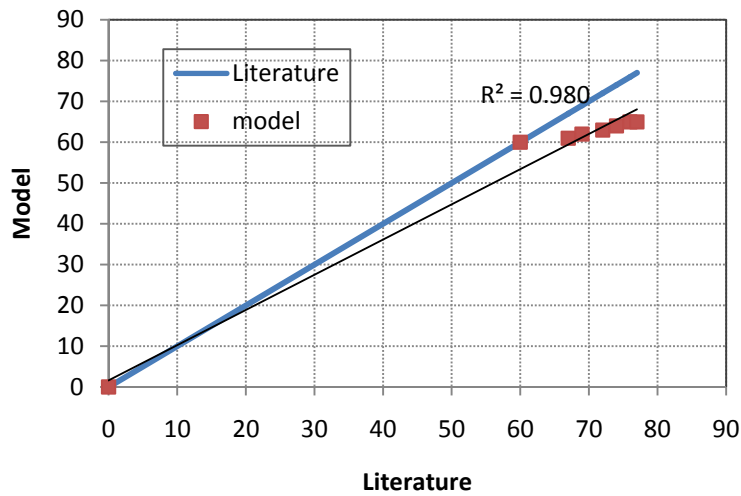


Figure 4.10 (a): Validation with conversion data provided by Gupta et al. [3].

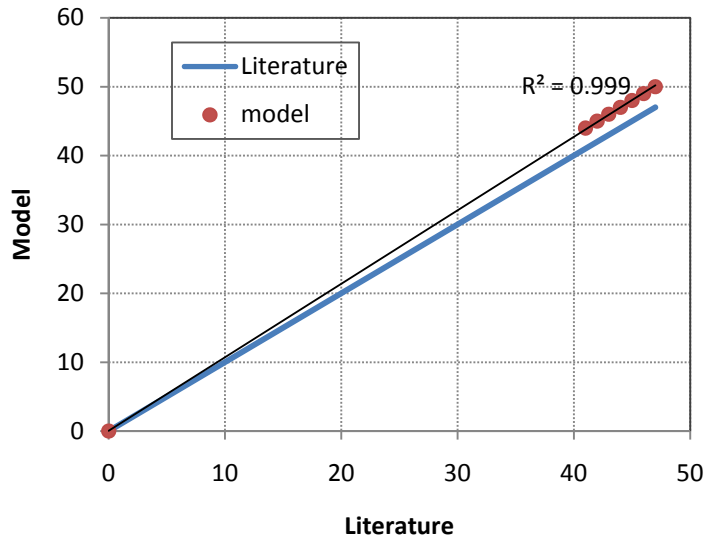


Figure 4.10 (b): Validation with gasoline data provided by Gupta et al. [3].

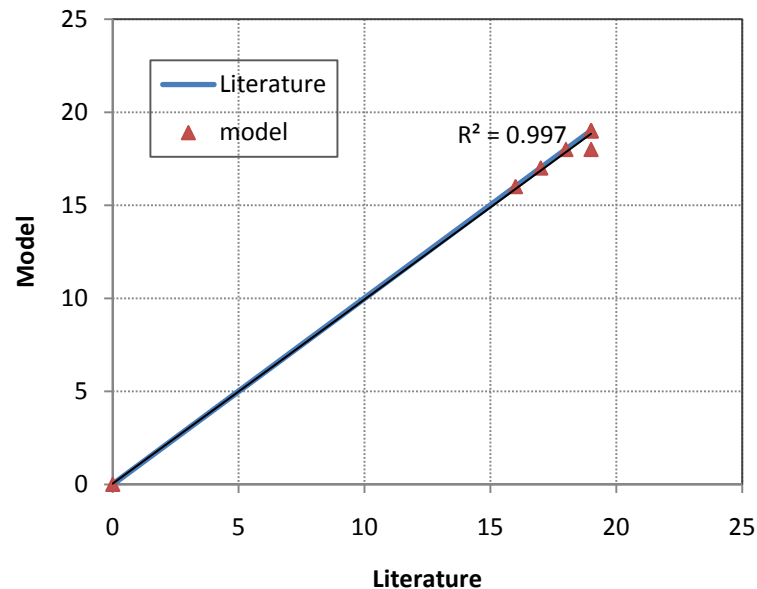


Figure 4.10 (c): Validation with gas data provided by Gupta et al. [3].

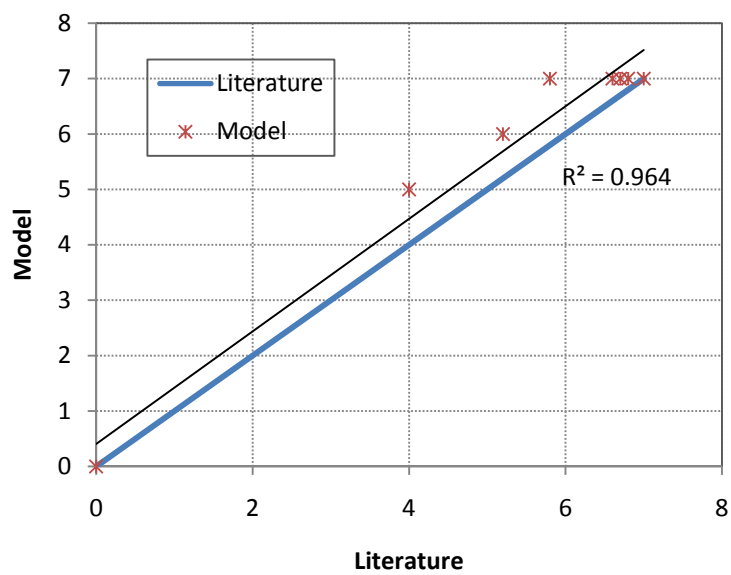


Figure 4.10 (d): Validation with coke data provided by Gupta et al. [3].

4.3 Influence of Operating Parameters

In this study we focused on the effect of parameter, catalyst-to-oil ratio and catalyst inlet temperature, in the performance of riser reactor. The catalyst to oil ratio is changed by either increasing the catalyst flow rate or flow rate of gas oil in the riser. The oil feed flow rate to the unit is kept constant here. For instance, the rate of oil is one kilogram per hour while the rate of catalyst changed depending on the CTO. The CTO ratio can be represented mathematically as:

$$CTO = \frac{F_c}{F_g} \quad (4.1)$$

In this work, the CTO ratio is changed in the range of 5 to 12. The comparison for each variable in the unit is conducted at three different cluster sizes in order to quantify cluster formation. Influences of the CTO ratio on the conversion of feed gas oil keeping other parameter same as base case is shown in Figure 4.11(a). It can be observed that as the CTO ratio increases, the conversion increases monotonically up to certain ranges as there is more catalyst available. This is because of the increases in CTO ratio increase the temperature of the process and favors the endothermic reaction forward. The amount of operating temperature in the reactor depends on CTO ratio. For the stated operating conditions if the clusters size same as particle size, increasing the reactor CTO from 5 to 12 results in 63% conversion, which corresponds to an increase by 10%. If we assumed that the cluster size is 100 times particle size, results in 72% conversion, which corresponds to an increase by 13%. As we can see from Figure 4.11(a), conversion during cluster formation is higher this is due to increase in cluster size increase the residence time of the catalyst which facilitate the conversion. The further increase in CTO ratio beyond 10 didn't result in significant increase in conversion. This may be due to formation of coke higher.

According to Figure 4.11(b), the gasoline yield is found to increase when CTO ratio is increased from 5 to 10. The further increase in CTO ratio beyond 10 didn't result in significant increase in gasoline yield. The difference in yield between CTO ratio of 5 to

10 and CTO ratio above 10 is 2%. For example, if the clusters size same as particle size, the gasoline yield at CTO of 10 is 48.7 % while it is 49.7%, in which the CTO of 12. This is insignificant especially if intended for a commercial unit however the cost of catalyst. This may be due to over cracking of gasoline. Consequently, operating at higher CTO ratio is desirable if the objective is to improve the intermediate products. For the stated operating conditions if the clusters size same as particle size, increasing the reactor CTO from 5 to 12 results in 56% gasoline yield. If we assumed that the cluster size is 100 times particle size, results in 51% gasoline yield. Which indicated that the cluster formation don't facilitate the gasoline yield. The increase in gases yields with increasing CTO ratio can be explained by the effect of more conversion at higher temperature as shown in the Figure 4.11 (c). The optimum gases yield results when operating at high CTO ratio. The coke yield is also increase with CTO ratio because coke is one of the products from conversion. This behavior is expected since more gas and gasoline converted to coke at higher temperature at increasing CTO ratio as shown in Figure 4.11(d).

The Influence of the catalyst inlet temperature on conversion and gasoline yield while keeping all parameters invariant as base case parameters is shown in Figure 4.12. It can be seen that as catalyst inlet temperature is increased from 800K to 920K, there is significant rise in conversion. However, further increase in catalyst inlet temperature hardly resulted in increase in the predicted gasoline yield. The gasoline yield may not show a direct relationship to temperature. It can also be seen from Figure 4.12 that the predicted gasoline yield exhibits a maximum with respect to catalyst inlet temperature. For example from Figure 4.12, the gasoline yield at temperature of 860K is 55.2 % while it is 41.3% at the temperature of 920K. In fact, the yield of gasoline is highest at temperature of 860. The difference in yield between 860k and 920K is 13.9%. This is due to gasoline leads to secondary reaction or over cracking of gasoline at high temperature which is significant especially if intended for a commercial unit.

In general, The FCC process operates at very dilute flow conditions with solid volume fraction as low as 3%. The catalyst to oil ratio is a very important parameter in this

process since the smallest increase in catalyst hold up can lead to higher conversion. The increase in conversion has to be carefully balanced against added cost of using increased amounts of highly valuable catalyst. From Figure 4.11 (a), the effect of doubling the catalyst concentration in the FCC reactor is that the conversion is estimated to be increased by 10%. Beyond the CTO ratio of 12, the incremental increase in conversion may not be justifiable considering the cost of added catalyst.

It should be also noted that, a limitation of the riser reactor is the choking limit for the CTO ratio, since there exist a maximum amount of catalysts that can be pushed upward by the gas against gravity, so for the design of riser the maximum value of CTO ratio is found such that, the gas velocity in operating conditions must be higher than choke velocity. Before deciding on a CTO ratio, it is important to consider the effect of increased CTO ratio and its cost.

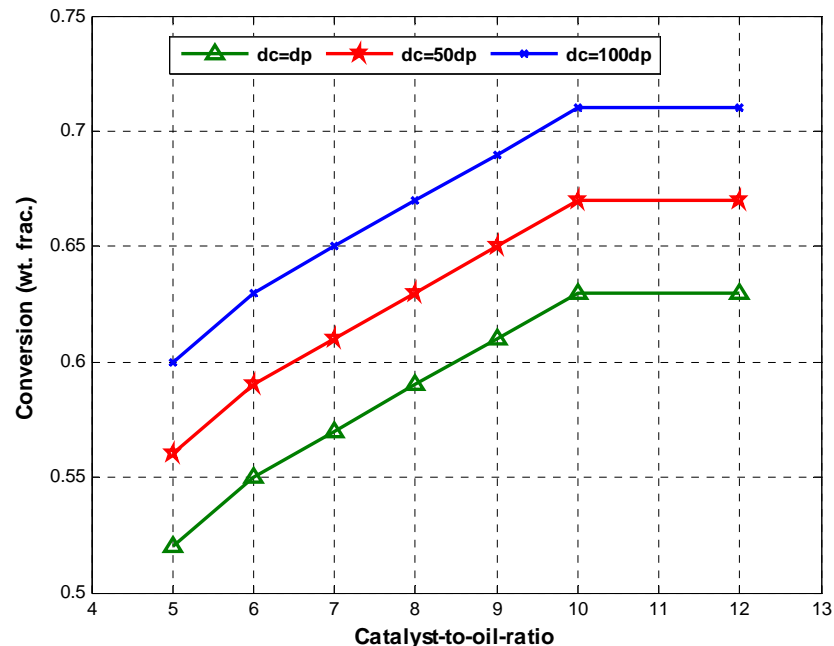


Figure 4.11 (a): Effect of CTO on conversion at different cluster size.

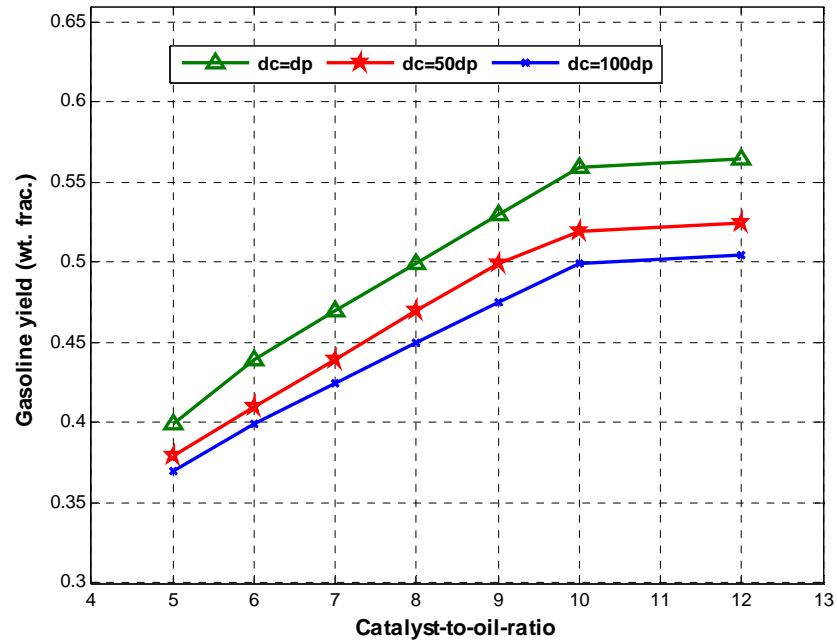


Figure 4.11(b): Effect of CTO on gasoline yield at different cluster size.

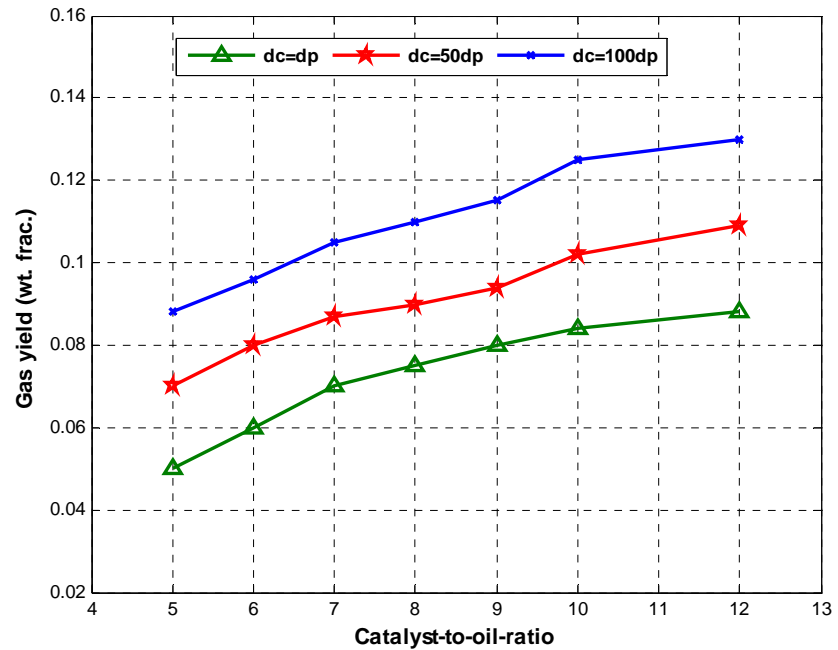


Figure 4.11(c): Effect of CTO on gas yield at different cluster size.

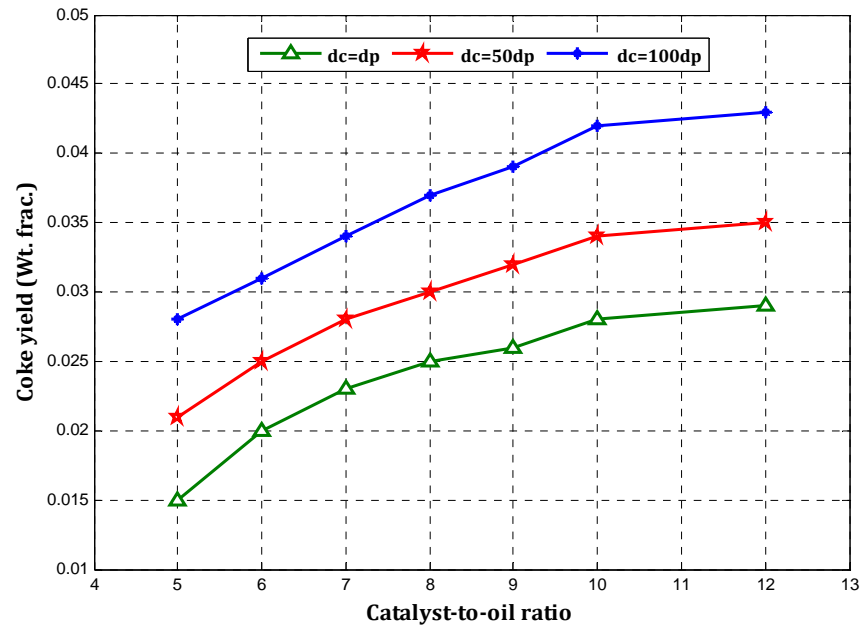


Figure 4.11(d): Effect of CTO on coke yield at different cluster size

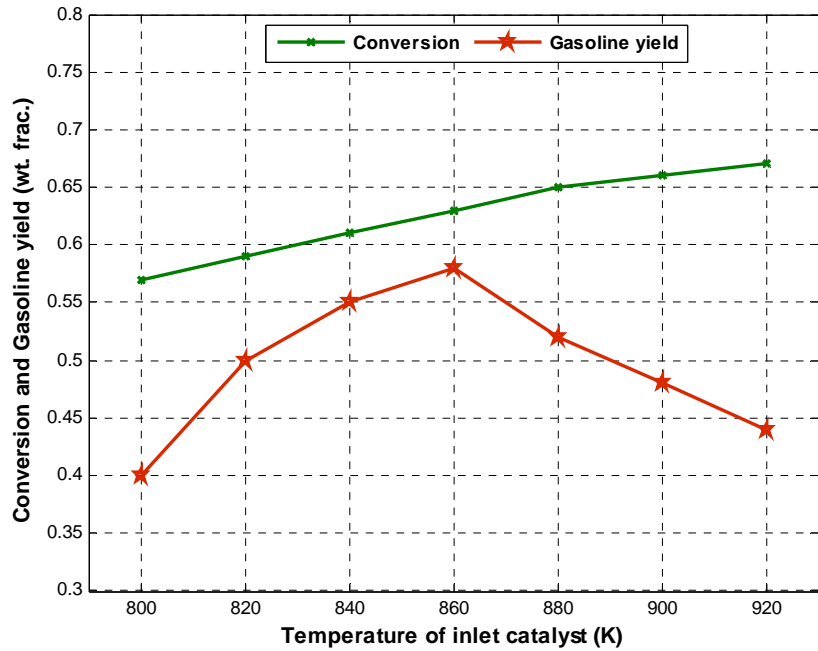


Figure 4.12: Effect of temperature on conversion and gasoline yield.

4.4 Case Study: Effect of Cluster Formation on Riser Performance

Riser geometry and operating conditions listed in Table 4.1- 4.7 are used to carry out case study to investigate the effect of cluster formation on the performance of FCC riser reactor. Three different cluster diameter ratios are used to quantify cluster formation. The results presented were obtained by considering the existence of clusters with a diameter 50 and 100 times bigger than single particle diameter.

The effects of cluster formation on the riser performance are shown in Figure 4.13- 4.19. Axial profile of gas oil conversion, yield of gasoline, gas and coke computed for three different cluster diameters are shown in Figure 4.13- 4.16, respectively. The result of riser reactor performance, in terms of higher over all conversion, lower gasoline yield, higher gas yield and higher coke make, is predicted for higher cluster diameter size. This may be explained in the following way. From Figure 4.13, the formation of cluster favors the conversion. If it is assumed that there is a cluster size which is 100 times the size of catalyst particle ($dc=100dp$) then the conversion of gasoil increased to 74%, this conversion corresponds to an increase by 9% compared to system without cluster formation. This is because of formation of cluster increase the residence time of the catalyst inside the riser. Nonetheless the higher the residence time due to cluster formation will also produce higher quantity of coke as shown in Figure 4.16. For cluster size which is 100 times the size of catalyst particle ($dc=100dp$), coke formation was 7.6% compared to 7% without cluster formation.

From Figure 4.14, we can observe that the formation of cluster have positive effect on gasoline yield at the inlet of the riser section of FCC. In the middle section of riser, the formation of cluster has negative impact on gasoline yield because of high temperature drop attained in the riser and higher residence time of the catalyst. If it is assumed that there is a cluster size which is 100 times the size of catalyst particle ($dc=100dp$) then the gasoline yield decreased from 53% to 48%. The effect of cluster formation on axial temperature profile is shown in Figure 4.17. If it is assumed that there is a cluster size which is 100 times the size of catalyst particle ($dc=100dp$) then the temperature drop was

55K, which is higher as compared to without cluster formation. Cluster formation lead to high catalyst temperature drop in the riser due to higher residence time of the catalyst. Thus for FCC risers, formation of cluster favored higher catalyst temperature to vaporized feed in the riser. This condition promotes secondary cracking of gasoline to coke. Secondly, higher residence time of catalyst leads to formation of coke. Higher coke generation, predicted for cluster formation, leads to fast catalyst deactivation and hence lower gasoline yields. If it is assumed that there is a cluster size which is 100 times the size of catalyst particle ($dc=100dp$) then the catalyst activity decrease from 0.19 to 0.1 as shown in Figure 4.18.

It is evident that increasing cluster formation causes more non-homogeneity in solids hold up along the riser column, indicated by steeper solids hold up profile near the inlet riser unit. At the stated operating condition, increasing cluster diameter size from dp to $100dp$ in the riser is estimated to cause an average additional densification of 25% as shown in Figure 4.19, higher densification increases solid-hold up in the fully developed flow region from 0.03 to 0.04. This is because of lower drag forces exerted on clusters.

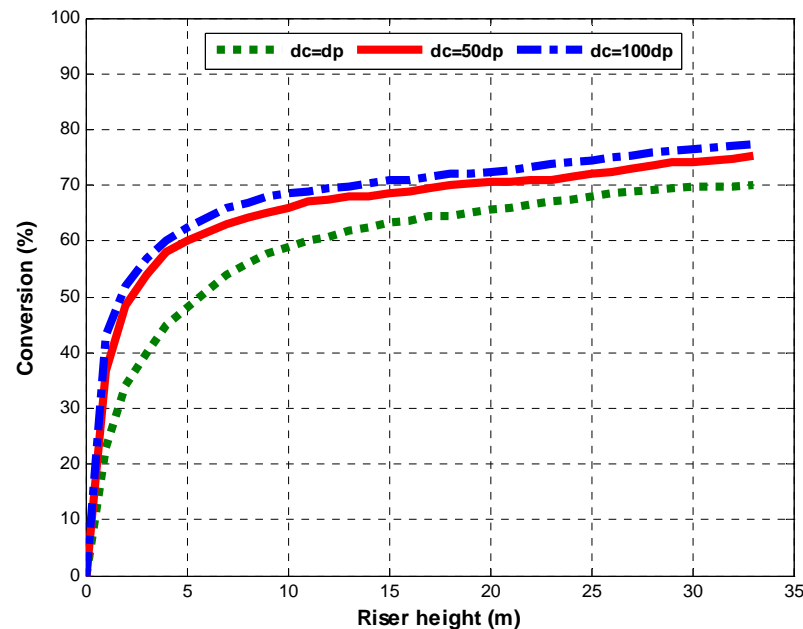


Figure 4.13: Conversion vs. riser height

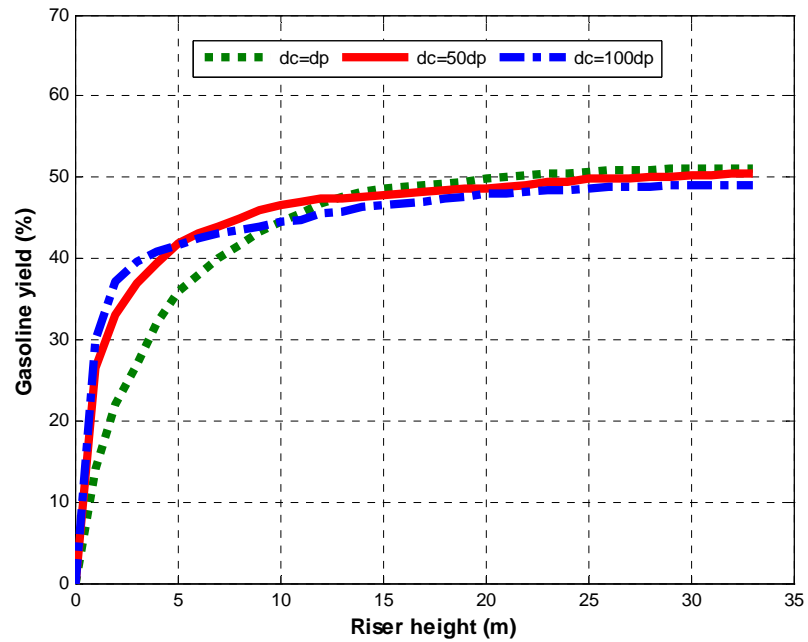


Figure 4.14: Gasoline yield vs. riser height

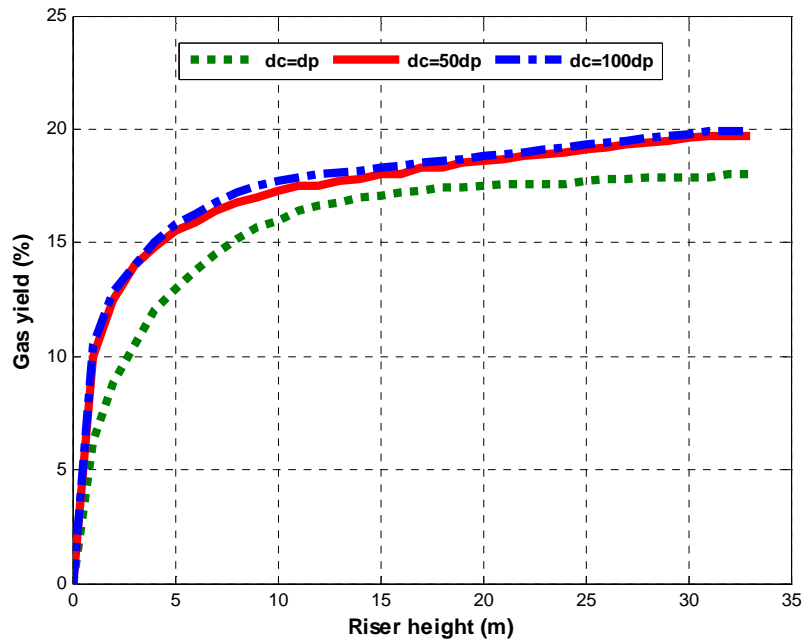


Figure 4.15: Gas yield vs. riser height

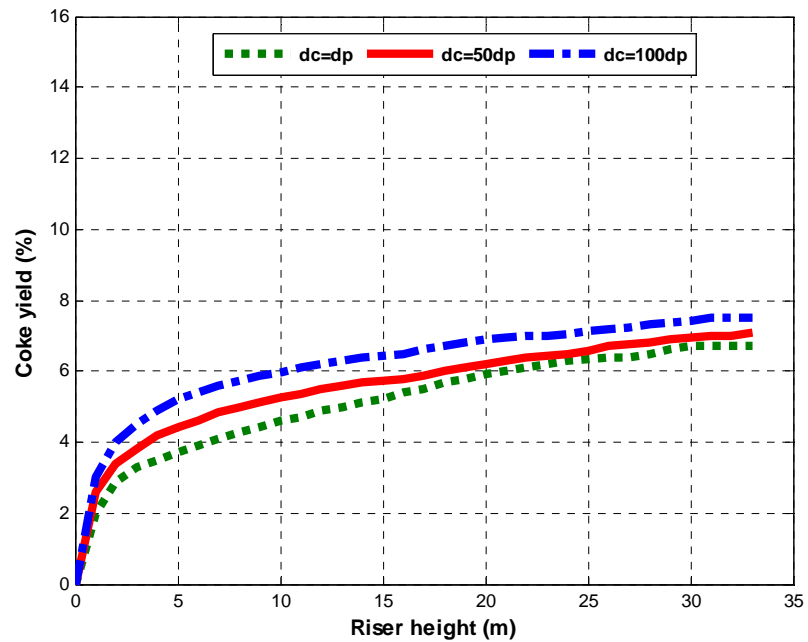


Figure 4.16: Coke yield vs. riser height.

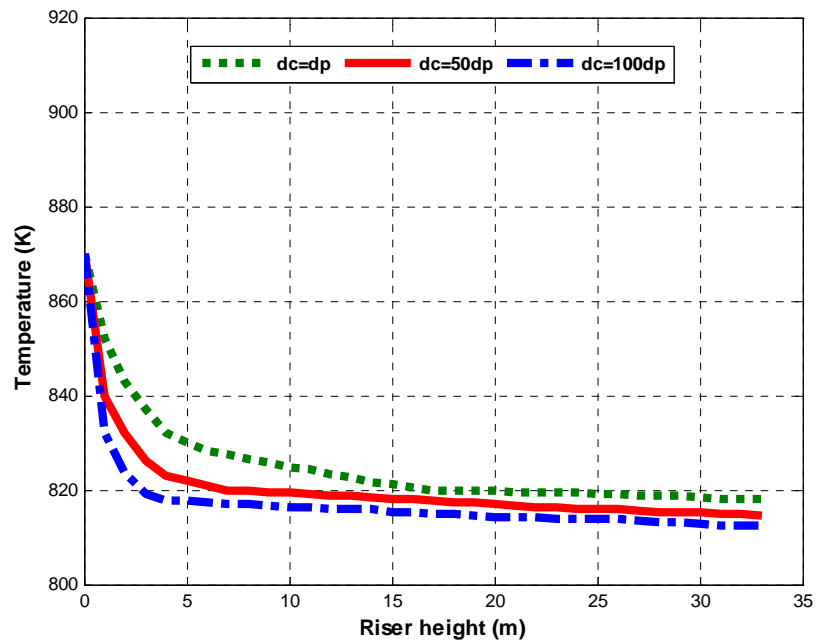


Figure 4.17: Temperature vs. riser height.

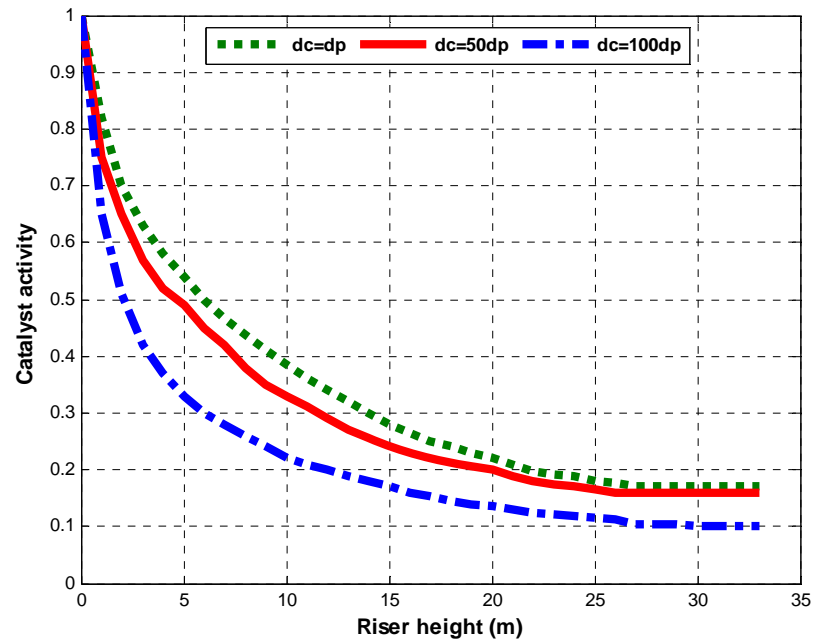


Figure 4.18: Catalyst activity vs. riser height.

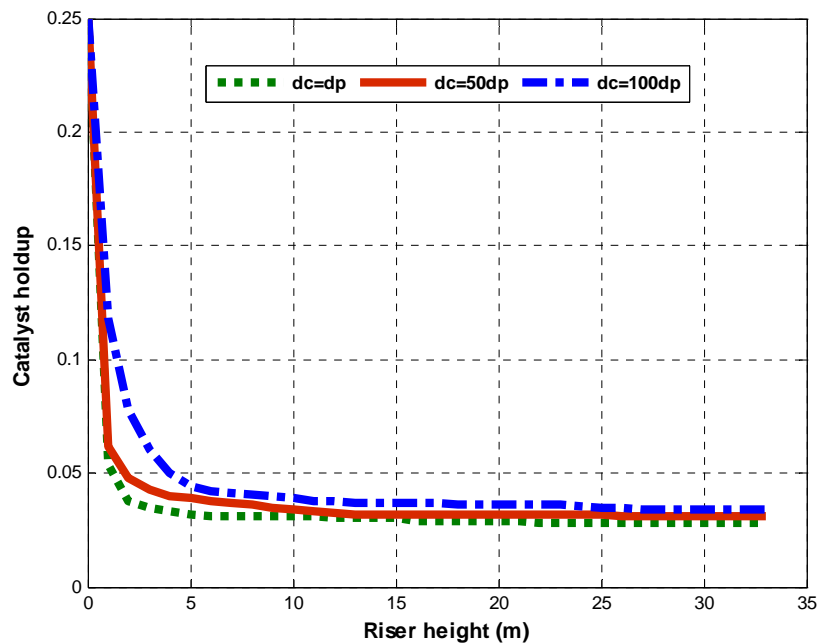


Figure 4.19: Solid hold up vs. riser height.

CHAPTER 5

CONCLUSIONS AND FUTURE WORKS

5.1 Conclusions

The main objective of this study was to develop predictive models, the hydrodynamics was based on cluster based approach and the kinetics was modelled using a four lump method, for FCC riser in order to simulate and better understand the operation and investigate the effect of cluster formation on the performance of riser reactor. Simulation results reveal consistent patterns in flow behaviour, which allowed for further insights into the FCC hydrodynamics. This allowed for conducting a parametric study. The resulting findings were useful for optimal operation of industrial units. The model was validated against literature data and showed good agreement with an average correlation coefficient of $R^2 = 0.985$. The deviation between the model results and the pilot plant data reflect that the assumptions made in deriving the model equations were quite reasonable. A number of seven ordinary differential equations were used to describe the performance of FCC riser reactor. The sets are dependent on position. The differential equations were solved numerically by Dormand-Prince method, family of Runge-Kutta solutions method, using MATLAB environment.

The reaction kinetics was introduced using a four lump model along with catalyst deactivation that was based on coke deposition on the catalyst pellets. The kinetic model was coupled with hydrodynamic model through a material balance at each control volume along the axis in the upward direction of the riser. The resulting riser model predicts gas oil conversion and yields of gasoline, light gases and coke. Simulation result of the base case riser model match plant data sufficiently well with most of the deviation lies in between 1-13% due to assumptions developed and the complexities of the inlet of riser reactor.

Using the model developed the effect of main operating parameters, Inlet catalyst temperature and catalyst-to-oil ratio, on the reactor performance was studied. Since FCC reaction is an endothermic, riser model predictions point to higher conversion

rates at increased reactor temperature. However, the gasoline yield may not show a direct relationship to temperature. The Influence of the catalyst inlet temperature on conversion and gasoline yield while keeping all parameters invariant as base case parameters was determined. When catalyst inlet temperature was increased from 800K to 920K, there was significant rise in conversion. However, further increase in catalyst inlet temperature hardly resulted in increase in the predicted conversion. This was due to at same time increased coking at higher temperature. The gasoline yield might not show a direct relationship to temperature. This is because of the production of light gases and coke from gasoline, i.e. over cracking or secondary reaction, is also enhanced at elevated temperatures. The predicted gasoline yield exhibited a maximum with respect to catalyst inlet temperature. The gasoline yield at temperature of 860K was 55.2 % while it was 41.3% at the temperature of 920K. In fact, the yield of gasoline was highest at temperature of 860K. The difference in yield between 860k and 920K was 13.9% which was significant especially if intended for a commercial unit. This result shows that, the optimum gasoline yield is obtained at higher CTO ratio and lower temperature. So, the operating temperature requires careful consideration. The parameter study for FCC riser showed that higher catalyst-oil-ratio enhanced conversion rates. However, the riser encounters an upper limit of sustainable catalyst density due to choking issues. Besides it is better to keep in under consideration the high cost of catalyst before deciding for high CTO ratios. Back mixing in riser leads to a slower and dense solid phase with in reactor.

A case study was performed to investigate the effect of cluster formation on riser reactor performance. The existence of down ward flowing clusters induces strong solid back-mixing and non-uniform radial distributions of particle velocities and hold ups, which is undesirable for chemical reactions. However, the formation of clusters creates high solids hold-ups in the riser by inducing internal solids circulations, which are usually beneficial for increasing concentrations of solid catalysts or solid reactants. The formations of cluster increased the conversion. Nonetheless the higher the residence time due to cluster formation was produced higher quantity of coke. It was assumed that there is a cluster size which is 100 times the size of catalyst particle ($dc=100dp$) then it was obtained 74% conversion, this conversion corresponds to an

increase by 9 % compared to system without cluster formation. This is because of formation of cluster increase the residence time of the catalyst inside the riser.

The effect of cluster formation on gasoline production was also investigated and its effect on the production of gasoline at the inlet was higher but in the middle section of the riser the relation between the cluster formation and gasoline production were inverse relation.

5.2 Future Works

This study has been carried out to address the issue of cluster formation on riser performance using the model developed. Further study can therefore be performed by widening the scope:

- i. In this work to quantify cluster formation we use ratio of cluster size to single particle, so it is recommended to develop correlation with geometry of reactor and operating condition to determine cluster size. The determination of this correlation would improve the model accuracy.
- ii. It has been shown in this paper that the flow behaviour in the riser is near plug flow such that radial dispersion is negligible. In riser, this simplifying assumption is not applicable. Therefore, the riser model could be improved by also considering radial dispersion.
- iii. The models developed here are based on assumptions of steady state, which means that the effects of uncertainties in the parameters at transient condition are not addressed. The determination using transient state model would help to determine the amount accumulated in the riser.
- iv. A comprehensive review on the fundamental studies and industrial development at industrial-scale of riser reactors was made. It has been acknowledged that riser has favourable flow structures and plug flow reactor performance, which endowed the riser reactor unique advantages for the potential applications in the refinery technology so this approach can be extending further by including the effect of regenerator and separation vessel for riser reactor. Therefore, study on this phenomenon would result in improved understanding on FCC process.

Reference

- [1]. Bolkan, Y.G., *Modeling Circulating Fluidized Bed Riser and Downer Reactor and Their Application to Fluid Catalytic Cracking*, In *Chemical and Petroleum Engineering*. PhD Thesis, 2003, The University of Calgary: Calgary, Alberta. p. 316.
- [2]. Harding, R.H., A.W. Peters, and J.R.D. Nee, *New Developments in FCC Catalyst Technology*. Applied Catalysis A, General, 2001. **221**(1-2): p. 389-396.
- [3]. Gupta, A. and D. Subba Rao, *Model for the Performance of Fluid Catalytic Cracking (FCC) Riser Reactor: Effect of Feed Atomization*. Chemical Engineering Science, 2001. **56**(15): p. 4489-4503.
- [4]. Gupta, A. and D. Subba Rao, *Effect of Feed Atomization on FCC Performance: Simulation of Entire Unit*. Chemical Engineering Science, 2003. **58**(20): p. 4567-4579.
- [5]. Avidan, A.A., *FCC is Far From Being Mature Technology*. Oil & Gas Journal, 1992. **90**(10): p. 59-67.
- [6]. Wei, J. and J.C.W. Kuo, *Lumping Analysis in Monomolecular Reaction Systems. Analysis of the Exactly Lumpable System*. Industrial & Engineering Chemistry Fundamentals, 1969. **8**(1): p. 114-123.
- [7]. Williams, L.R., *Modeling and Optimization of a Two-Stage Regenerator Fluid Catalytic Cracking Unit*, In *Chemical Engineering*. PhD Thesis, 1998, Rice University: Houston, Texas. p. 133.
- [8]. Avidan, A.A., M. Edwards, and H. Owen, *Innovative Improvements Highlight FCC's Past and Future*. Oil and Gas Journal, 1990. **88**(2): p. 33-58.
- [9]. Bowman, B., *Advanced Numerical Simulation of Fluid Catalytic Cracking Riser Reactors*, In *Mechanical Engineering*. PhD Thesis, 2004, Purdue University. p. 204.
- [10]. Forzatti, P. and L. Lietti, *Catalyst Deactivation*. Catalysis Today, 1999. **52**(2-3): p. 165-181.
- [11]. Cerqueira, H.S., E.C. Biscaia Jr, and E.F. Souza-Aguiar, *Mathematical Modeling of Deactivation by Coke Formation in the Cracking of Gasoil*. Catalyst Deactivation, 1997. **111**: p. 303-310.
- [12]. K.A.Ali, H., *Dynamic Modeling and Control of a Riser-Type Fluid Catalytic Cracking Unit*, In *Chemical Engineering*. PhD Thesis, 1995, University of Saskatchewan: Saskatoon. p. 267.

- [13]. Elnashaie, S.S.E.H., & El-Hennawi, I. M, *Multiplicity of the Steady State in Fluidized Reactors. IV. Fluid Catalytic Cracker (FCC)*. Chemical Engineering Science, 1979. **34**: p. 1113.
- [14]. Weekman, V.W. and D.M. Nace, *Kinetics of Catalytic Cracking Selectivity in Fixed, Moving and Fluid Bed Reactors*. AIChE Journal, 1970. **16**(3): p. 397-404.
- [15]. Farag, K.Y., *Simulation of Fluid Catalytic Operation*. Math. Modeling, 1987. **8**: p. 311-316.
- [16]. Elshishini, S.S., & Elnashaie, S. S. E. H., *Digital Simulation of Industrial Fluid Catalytic Cracking Units: Bifurcation and its Implications*. Chemical Engineering Science, 1990. **45**: p. 553.
- [17]. Elnashaie, S. and S.S. Elshishini, *Modelling, Simulation, and Optimization of Industrial Fixed Bed Catalytic Reactors*. 1993: CRC Press.
- [18]. Lopez-Isunza, F., *Dynamic Modelling of an Industrial Fluid Catalytic Cracking Unit*. Computers and Chemical Engineering, 1992. **16**: p. S139–S148.
- [19]. Zheng, Y.Y., *Dynamic Modeling and Simulation of a Catalytic Cracking Unit*. Computers & Chemical Engineering, 1994. **18**: p. 39-44.
- [20]. Weekman Jr, V.W., *Kinetics and Dynamics of Catalytic Cracking Selectivity in Fixed-Bed Reactors*. Industrial & Engineering Chemistry Process Design and Development, 1969. **8**(3): p. 385-391.
- [21]. Lee, L.S., Yu-Wen Chen, Tsung-Nion Huang and Wen-Yen Pan, *Four-Lump Kinetic Model for Fluid Catalytic Cracking Process*. Can. J. Chem. Eng, 1989. **67**(4).
- [22]. Corella, J. and E. Francés, *Analysis of The Riser Reactor of a Fluid Catalytic Cracking Unit*. *Fluid Catalytic Cracking II: Concepts in Catalysis Design*, American Chemical Society, Washington, DC, 1991: p. 165–182.
- [23]. Theologos, K.N., A.I. Lygeros, and N.C. Markatos, *Feedstock Atomization Effects on FCC Riser Reactors Selectivity*. Chemical Engineering Science, 1999. **54**(22): p. 5617-5625.
- [24]. Sharma, A.K., Tuzla K., Matsen J., Chen J.C, *Parametric Effects of Particle Size and Gas Velocity on Cluster Characteristics in Fast Fluidized Beds*. Powder Technol, 2000. **111**(1): p. 114.
- [25]. Kikkinides, E.S., A.A Lappas, A. Nalbadian and I.A. Vasalos, *Correlation of Reactor Performance with Catalyst Structural Changes during Coke Formation in FCC Processes*. Chemical Engineering Science, 2002. **57**(6): p. 1011-1025.

- [26]. Pareek, V.K., Adesoji A. Adesina, Anwrap Srivastava and raj Sharam, *Modeling of a Non-Isothermal FCC Riser.* Chemical Engineering Journal, 2003. **92**(1-3): p. 101-109.
- [27]. Benyahia, S., G. Ortiz, and J.I.P. Paredes, *Numerical Analysis of a Reacting Gas/Solid Flow in the Riser Section of an Industrial Fluid Catalytic Cracking Unit.* International Journal of Chemical Reactor Engineering, 2002. **1**(1): p. 1024.
- [28]. León-Becerril, E., R. Maya-Yescas, and D. Salazar-Sotelo, *Effect of Modelling Pressure Gradient in the Simulation of Industrial FCC Risers.* Chemical Engineering Journal, 2004. **100**(1-3): p. 181-186.
- [29]. Nayak, S.V., S.L. Joshi, and V.V. Ranade, *Modeling of Vaporization and Cracking of Liquid Oil Injected in a Gas–Solid Riser.* Chemical Engineering Science, 2005. **60**(22): p. 6049-6066.
- [30]. Arandes, J.M. and H.I. De Lasa, *Simulation and Multiplicity of Steady States in Fluidized FCCUs.* Chemical Engineering Science, 1992. **47**(9-11): p. 2535-2540.
- [31]. Sertic-Bionda, K., Z. Gomezi, M. Fabulic and M. Muzic, *Study of Non-Isothermal Gas-Oil Catalytic Cracking Applying the Microactivity Test.* Petroleum Chemistry, 2008. **48**(1): p. 6-14.
- [32]. Fernandes, J.L., Janj. Verstraete, and Carla I.C Pinheiro, *Dynamic Modelling of an Industrial R2R FCC Unit.* Chemical Engineering Science, 2007. **62**(4): p. 1184-1198.
- [33]. Huilin Lu, Shuyan Wang, Yurong He, Jianmin Ding, Guodong Liu a, Zhenhua Haoa, *Numerical Simulation of Flow Behavior of Particles and Clusters in Riser using Two Granular Temperatures.* Powder Technology, 2008. **182**: p. 282–293.
- [34]. Manyele, S.V., J.H. Pärssinen, and J.X. Zhu, *Characterizing Particle Aggregates in a High-Density and High-Flux CFB Riser.* Chemical Engineering Journal, 2002. **88**(1-3): p. 151-161.
- [35]. Cabezas-Gómez, L., Da Silva Renato Cesar and Aparecida Navarro Helio, *Cluster Identification and Characterization in the Riser of a Circulating Fluidized Bed from Numerical Simulation Results.* Applied Mathematical Modelling, 2008. **32**(3): p. 327-340.
- [36]. Guenther, C. and R. Breault, *Wavelet Analysis to Characterize Cluster Dynamics in a Circulating Fluidized Bed.* Powder Technology, 2007. **173**(3): p. 163-173.
- [37]. Theologos, K.N. and N.C. Markatos, *Advanced Modeling of Fluid Catalytic Cracking Riser-Type Reactors.* AIChE Journal, 1993. **39**(6): p. 1007-1017.

- [38]. Jacob, S.M., Benjamin Gross, Sterling E. Voltz and Vern W. Weerman Jr., *A Lumping and Reaction Scheme for Catalytic Cracking*. AIChE Journal, 1976. **22**(4): p. 701-713.
- [39]. Takatsuka, T., S. Sato, Y. Morimoto and H. Hashimoto, *A Reaction Model for Fluidized-Bed Catalytic Cracking of Residual Oil*. Int Chem Eng, 1987. **27**(1): p. 107-116.
- [40]. Dave, N.C., G.J. Duffy, and P. Udaja, *A Four-Lump Kinetic Model for the Cracking/Coking of Recycled Heavy Oil*. Fuel, 1993. **72**(9): p. 1331-1334.
- [41]. Al-Khattaf, S. and H. De Lasa, *Activity and Selectivity of Fluidized Catalytic Cracking Catalysts in a Riser Simulator: The Role of Y-Zeolite Crystal Size*. Industrial and Energy Chemistry Research, 1999. **38**: p. 1350-1356.
- [42]. Kraemer, D., M. Larocca, and H.I. De Lasa, *Deactivation of Cracking Catalyst in Short Contact Time Reactors: Alternative models*. Canadian Journal of Chemical Engineering, 1991. **69**(1): p. 355-360.
- [43]. Liu, J., Grace J.R., Bi H., Morikawah, and Jingxu Zhu, *Gas Dispersion in Fast Fluidization and Dense Suspension Upflow*. Chemical Engineering Science, 1999. **54**(22): p. 5441-5449.
- [44]. Gidaspow, D., *Multiphase Flow and Fluidization: Continuum and Kinetic Theory Descriptions*. 1994: Academic Press.
- [45]. Wilhelm, R.H. and M. Kwauk, *Fluidization of Solid Particles*. Chem. Eng. Prog, 1948. **44**(3): p. 201-217.
- [46]. Kaye, B.H. and R.P. Boardman, *Cluster Formation in Dilute Suspensions*. Chem. Eng. Prog, 1962.
- [47]. Jayaweera, K., B.J. Mason, and G.W. Slack, *The Behaviour of Clusters of Spheres Falling in a Viscous Fluid Part 1. Experiment*. Journal of Fluid Mechanics Digital Archive, 2006. **20**(01): p. 121-128.
- [48]. Horio, M. and R. Clift, *A Note on Terminology: 'Clusters' and 'Agglomerates'*. Powder Technology, 1992. **70**: p. 196.
- [49]. Helland, E., H. Bournot, R. Occelli and L. Tadrist, *Drag Reduction and Cluster Formation in a Circulating Fluidised Bed*. Chemical Engineering Science, 2007. **62**(1-2): p. 148-158.
- [50]. Helland, E., R. Occelli, and L. Tadrist, *Numerical Study of Cluster Formation in a Gas-Particle Circulating Fluidized Bed*. Powder Technology, 2000. **110**(2): p. 210-221.

- [51]. Helland, E., R. Occelli, and L. Tadrist, *Computational Study of Fluctuating Motions and Cluster Structures in Gas–Particle Flows*. International Journal of Multiphase Flow, 2002. **28**(2): p. 199-223.
- [52]. Helland, E., R. Occelli, and L. Tadrist, *Numerical study of Cluster and Particle Rebound Effects in a Circulating Fluidised bed*. Chemical Engineering Science, 2005. **60**(1): p. 27-40.
- [53]. Horio, M. and H. Kuroki, *3-Dimensional Flow Visualization of Dilutely Dispersed Solids in Bubbling and Circulating Fluidized-Beds*. Chemical Engineering Science, 1994. **49**(15): p. 2413-2421.
- [54]. Yerushalmi, J., D.H. Turner, and A.M. Squires, *The Fast Fluidized Bed*. Industrial & Engineering Chemistry Process Design and Development, 1976. **15**(1): p. 47-53.
- [55]. Xu, G. and K. Kato, *Hydrodynamic Equivalent Diameter for Clusters in Heterogeneous Gas–Solid Flow*. Chemical Engineering Science, 1999. **54**(12): p. 1837-1847.
- [56]. Zhang, M.H., K.W. Chu, and F. Wei, *A CFD–DEM Study of the Cluster Behavior in Riser and Downer Reactors*. Powder Technology, 2008. **184**: p. 151-165.
- [57]. Agrawal, K., P. N. Loezos, S. Madhava, and S. Sankaran, *The Role of Meso-Scale Structures in Rapid Gas–Solid Flows*. Journal of Fluid Mechanics, 2001. **445**: p. 151-185.
- [58]. Mostoufi, N. and J. Chaouki, *Flow Structure of the Solids in Gas–Solid Fluidized Beds*. Chemical Engineering Science, 2004. **59**(20): p. 4217-4227.
- [59]. Shida, K. and T. Kawai, *Cluster Formation by Inelastically Colliding Particles in One-Dimensional Space*. Physica A, 1989. **162**(1).
- [60]. Tanaka, T., Yonemura, S., Kiribayashi, K., and Tsuji, Y., *Cluster Formation and Particle-Induced Instability in Gas–Solid Flows Predicted by the DSMC Method*. JSME International Journal. Series B, Fluids and Thermal Engineering, 1996. **39**(2): p. 239-245.
- [61]. McNamara, S. and W.R. Young, *Inelastic Collapse in Two Dimensions*. Physical Review E, 1994. **50**(1): p. 28-31.
- [62]. Issangya, A.S., E. American Institute of Chemical, and Meeting, *Flow Behavior in the Riser of a High-density Circulating Fluidized Bed*. American Institute of Chemical Engineers, 1996.
- [63]. Reichelt, L.F.S., *The MATLAB ODE Suite*. Society for Industrial and Applied Mathematics, 1997. **18**(1): p. 1-22.

- [64]. Han, I.S. and C.B. Chung, *Dynamic Modeling and Simulation of a Fluidized Catalytic Cracking Process. Part I: Process Modeling.* Chemical Engineering Science, 2001. **56**(5): p. 1951-1971.
- [65]. Han, I.S. and C.B. Chung, *Dynamic Modeling and Simulation of a Fluidized Catalytic Cracking Process. Part II: Property Estimation and Simulation.* Chemical Engineering Science, 2001. **56**(5): p. 1973-1990.
- [66]. In-Su Han, C.B.C., James B. Riggs, *Modeling of a Fluidized Catalytic Cracking Process.* Computers and Chemical Engineering, 2000. **24**: p. 1681 - 1687.
- [67]. Gupta, R.K., V. Kumar, and V.K. Srivastava, *A new Generic Approach for the Modeling of Fluid Catalytic Cracking (FCC) Riser Reactor.* Chemical Engineering Science, 2007. **62**(17): p. 4510-4528.
- [68]. Derouin, C., Nevicato, D., Forissier, M., Wild G., and Bernard, J., *Hydrodynamics of Riser Units and Their Impact on FCC Operation.* Industrial and Engineering Chemistry Research, 1997. **36**: p. 4504-4515.
- [69]. Ali, H.R., S. Corriou, J. P., *Modelling and Control of a Riser Type Fluid Catalytic Cracking (FCC) Unit.* Chemical Engineering R. and Design 1997. **75**(4): p. 401-412.
- [70]. Danner, R. P. and T. E. Daubert (1983). *Technical Data Book-Petroleum Refining,* The Dept.

Appendix - A

Development of the Riser Hydrodynamics Equations

This appendix provides the detailed derivations of the hydrodynamic model equation for riser section of reactor.

A.1 Solid volume fraction

From force balance on a cluster, we derived the catalyst void fraction.

$$\text{Net force on cluster} = \text{Drag force on cluster} - \text{Gravitational force}$$

$$m_c \frac{du_c}{dt} = C_D A_c \frac{1}{2} \rho_g (u_g - u_c)^2 - m_c g \quad (\text{A.1})$$

The mass and projected area of the cluster is:

$$m_c = \frac{\pi}{6} d_c^3 \rho_c \quad (\text{A.2})$$

$$A_c = \frac{\pi}{4} d_c^2 \quad (\text{A.3})$$

Substituting m_c and A_c in equation (A.1):

$$\frac{du_c}{dt} = \frac{3}{4} \left(\frac{C_D}{d_c} \right) \left(\frac{\rho_g}{\rho_c} \right) (u_g - u_c)^2 - g \quad (\text{A.4})$$

The velocity of cluster in a compartment is simply the volumetric flow of clusters divided by the fraction of cross sectional area available for clusters in the compartment.

$$u_c = \frac{F_c / \rho_c}{A \varepsilon_c} \quad (\text{A.5})$$

The time can be represented as ratio of distance and velocity:

$$dt = \frac{dz}{u_g} \quad (\text{A.6})$$

Actual gas velocity is:

$$u_g = \frac{u_0}{1 - \varepsilon_c} \quad (\text{A.7})$$

Using equation (A.4) – (A.7) we obtain:

$$\frac{-d\varepsilon_c}{dz} = \frac{A\rho_c}{F_c u_0} \varepsilon_c^2 (1 - \varepsilon_c) \left(\frac{3}{4} \left(\frac{C_D}{d_c} \right) \left(\frac{\rho_g}{\rho_c} \right) \left(\frac{u_0}{1 - \varepsilon_c} - \frac{F_c}{A\rho_c} \right)^2 - g \right) \quad (\text{A.8})$$

A.2 Momentum Balance

The pressure drop through the riser section of reactor is developed:

$$[\text{net force acting}] = [\text{rate of increase in momentum of contents}] \quad (\text{A.9})$$

Therefore,

$$[\text{pressure force}] - [\text{gas_wall friction force}] - [\text{solids_wall friction force}] - [\text{gravitational force}] = [\text{increase in momentum of the gas}] + [\text{increase in momentum of the solids}] \quad (\text{A.10})$$

$$\begin{aligned} -\Omega\delta P - F_{gw}\Omega\delta z - F_{cw}\Omega\delta z - (\Omega(1 - \varepsilon_g)\rho_p\delta z)g - (\Omega\varepsilon_g\rho_g\delta z)g \\ = \rho_g\Omega\varepsilon_g u_g \delta u_g + \rho_c\Omega(1 - \varepsilon_g)u_c \delta u_c \end{aligned} \quad (\text{A.11})$$

Take in to consideration momentum of solid particle:

$$-\Omega\delta P - F_{cw}\Omega\delta z - (\Omega(1 - \varepsilon_g)\rho_c\delta z)g = \rho_c\Omega(1 - \varepsilon_g)u_c \delta u_c \quad (\text{A.12})$$

Taking the limit at δz approaches zero, equation (A.12) becomes:

$$-\frac{dP}{dz} = \rho_c(1 - \varepsilon_g)g + \rho_c(1 - \varepsilon_g)u_c \frac{du_c}{dz} \quad (\text{A.13})$$

Appendix-B

Development of the Riser Kinetics Equation

This appendix provides the detailed derivations of the kinetic model of riser section of reactor equations using four-lump kinetic schemes.

The reaction rate equation for the four-lump model is as follows [38]:

$$-r_a = -\emptyset \rho_c \left(\frac{M_a}{\rho_g} \right) (K_{ab} + K_{ac} + K_{ad}) C_a^2 \quad (1.B)$$

$$-r_b = -\emptyset \rho_c \left[(K_{bd} + K_{bc}) C_b - \left(\frac{M_a}{\rho_g} \right) K_{ab} C_a^2 \right] \quad (2.B)$$

$$-r_c = \emptyset \rho_c \left(\left(\frac{M_a}{\rho_g} \right) K_{ac} C_a^2 + K_{bc} C_b \right) \quad (3.B)$$

$$-r_d = \emptyset \rho_c \left(\left(\frac{M_a}{\rho_g} \right) K_{ad} C_a^2 + K_{bd} C_b \right) \quad (4.B)$$

B.1 Gas Oil Balance:

Apply conservation principle on the gas oil concentration and the material balance equation is written as follows:

$$\Omega dz (1 - \varepsilon_g) \frac{dC_a}{dt} = f_a[j] - f_a[j+1] + \Omega dz (1 - \varepsilon_g) (-r_a) \quad (B.1)$$

Rearranging equation (B.1):

$$\frac{dC_a}{dt} = - \frac{Q}{\Omega(1 - \varepsilon_g)} \frac{\Delta C_a}{\Delta z} + (-r_a) \quad (B.2)$$

Taking the limit at dz approaches zero, equation (B.2) becomes:

$$\frac{dC_a}{dt} = -\frac{Q}{\Omega(1-\varepsilon_g)} \frac{\partial C_a}{\partial z} + (-r_a) \quad (\text{B.3})$$

Substitute for gas oil reaction term ($-r_a$) from equation (1.B) into (B.3)

$$\frac{dC_a}{dt} = -\frac{Q}{\Omega(1-\varepsilon_g)} \frac{\partial C_a}{\partial z} - \phi \left(\frac{M_a}{\rho_g} \right) (K_{ab} + K_{ac} + K_{ad}) C_a^2 \quad (\text{B.4})$$

By including the simplifying assumption of pseudo steady state ($\frac{dC_a}{dt} = 0$) equation (B.4) becomes:

$$\frac{Q}{\Omega(1-\varepsilon_g)} \frac{\partial C_a}{\partial z} + \phi \rho_c \left(\frac{M_a}{\rho_g} \right) (K_{ab} + K_{ac} + K_{ad}) C_a^2 = 0 \quad (\text{B.5})$$

By using superficial velocity u_0 equations (B.5) becomes:

$$\frac{u_0}{(1-\varepsilon_g)} \frac{\partial C_a}{\partial z} + \phi \rho_c \left(\frac{M_a}{\rho_g} \right) (K_{ab} + K_{ac} + K_{ad}) C_a^2 = 0 \quad (\text{B.6})$$

B.2 Gasoline Balance:

Applying conservation principle on the gasoline results in:

$$\Omega dz (1-\varepsilon_g) \frac{dC_b}{dt} = Q C_b[j] - Q C_b[j+1] + \Omega dz (1-\varepsilon_g) (-r_b) \quad (\text{B.7})$$

Rearranging equation (B.7):

$$\frac{dC_b}{dt} = -\frac{Q}{\Omega(1-\varepsilon_g)} \frac{\partial C_b}{\partial z} + (-r_b) \quad (\text{B.8})$$

Taking the limit at dz approaches zero, equation (B.8) becomes:

$$\frac{dC_b}{dt} = -\frac{Q}{\Omega(1-\varepsilon_g)} \frac{\partial C_b}{\partial z} + (-r_b) \quad (\text{B.9})$$

Substitute for gas oil reaction term ($-r_b$) from equation (2.B) into (B.9):

$$\frac{dC_b}{dt} = -\frac{Q}{\Omega(1-\varepsilon_g)} \frac{\partial C_b}{\partial z} - \emptyset[(K_{bd} + K_{bc})C_b - \left(\frac{M_a}{\rho_c}\right) K_{ab} C_a^2] \quad (\text{B.10})$$

By including the simplifying assumption of pseudo steady state ($\frac{dC_b}{dt} = 0$), equation (B.10) becomes:

$$\frac{Q}{\Omega(1-\varepsilon_g)} \frac{dC_b}{dz} + \emptyset \rho_c [(K_{bd} + K_{bc})C_b - \left(\frac{M_a}{\rho_g}\right) K_{ab} C_a^2] = 0 \quad (\text{B.11})$$

By using superficial velocity u_0 equations (B.11) becomes:

$$\frac{u_0}{(1-\varepsilon_g)} \frac{dC_b}{dz} + \emptyset \rho_c [(K_{bd} + K_{bc})C_b - \left(\frac{M_a}{\rho_g}\right) K_{ab} C_a^2] = 0 \quad (\text{B.12})$$

B.3 Light Gas Balance:

Applying conservation principle to the light gases concentration results in:

$$\Omega dz (1-\varepsilon_g) \frac{dC_c}{dt} = Q C_c[j] - Q C_c[j+1] + \Omega dz (1-\varepsilon_g) (-r_c) \quad (\text{B.13})$$

Rearranging equation (B.13):

$$\frac{dC_c}{dt} = -\frac{Q}{\Omega(1-\varepsilon_g)} \frac{\Delta C_c}{\Delta z} + (-r_c) \quad (\text{B.14})$$

Taking the limit at Δz approaches zero, equation (B.14) becomes:

$$\frac{dC_c}{dt} = -\frac{Q}{\Omega(1-\varepsilon_g)} \frac{\partial C_c}{\partial z} + (-r_c) \quad (\text{B.15})$$

Substitute for gas oil reaction term ($-r_c$) from equation (3.B) into (B.15):

$$\frac{dC_c}{dt} = -\frac{Q}{\Omega(1-\varepsilon_g)} \frac{\partial C_c}{\partial z} + \emptyset \rho_c \left(\left(\frac{M_a}{\rho_g} \right) K_{ac} C_a^2 + K_{bc} C_b \right) \quad (\text{B.16})$$

By including the simplifying assumption of pseudo steady state ($\frac{dC_c}{dt} = 0$), equation (B.16) becomes:

$$\frac{Q}{\Omega(1-\varepsilon_g)} \frac{dC_c}{dz} - \emptyset \rho_c \left(\left(\frac{M_a}{\rho_g} \right) K_{ac} C_a^2 + K_{bc} C_b \right) = 0 \quad (\text{B.17})$$

By using superficial velocity u_0 equations (B.17) becomes:

$$\frac{u_0}{(1-\varepsilon_g)} \frac{dC_c}{dz} - \emptyset \rho_c \left(\left(\frac{M_a}{\rho_g} \right) K_{ac} C_a^2 + K_{bc} C_b \right) = 0 \quad (\text{B.18})$$

B.4 Coke Balance:

Applying conservation principle to the coke concentration yields:

$$\Omega dz (1-\varepsilon_g) \frac{dQC_d}{dt} = QC_d[j] - QC_d[j+1] + \Omega dz (1-\varepsilon_g) (-r_d) \quad (\text{B.19})$$

Rearranging equation (B.19):

$$\frac{dC_d}{dt} = -\frac{Q}{\Omega(1-\varepsilon_g)} \frac{\partial C_d}{\partial z} + (-r_d) \quad (\text{B.20})$$

Taking the limit at dz approaches zero, equation (B.20) becomes:

$$\frac{dC_d}{dt} = -\frac{Q}{\Omega(1-\varepsilon_g)} \frac{\partial C_d}{\partial z} + (-r_d) \quad (\text{B.21})$$

Substitute for gas oil reaction term ($-r_d$) from equation (4.B) into (B.21):

$$\frac{dC_d}{dt} = -\frac{Q}{\Omega(1-\varepsilon_g)} \frac{\partial C_d}{\partial z} + \emptyset \rho_c \left(\left(\frac{M_a}{\rho_g} \right) K_{ad} C_a^2 + K_{bd} C_b \right) \quad (\text{B.22})$$

By including the simplifying assumption of pseudo steady state ($\frac{dC_d}{dt} = 0$), equation (B.22) becomes:

$$\frac{Q}{\Omega(1-\varepsilon_g)} \frac{dC_d}{dz} - \emptyset \rho_c \left(\left(\frac{M_a}{\rho_g} \right) K_{ad} C_a^2 + K_{bd} C_b \right) = 0 \quad (\text{B.23})$$

By using superficial velocity u_0 equations (B.23) becomes:

$$\frac{u_0}{(1-\varepsilon_g)} \frac{dC_d}{dz} - \emptyset \rho_c \left(\left(\frac{M_a}{\rho_g} \right) K_{ad} C_a^2 + K_{bd} C_b \right) = 0 \quad (\text{B.24})$$

B.5 Energy Balance

Energy balance equation is written as follows:

$$\Omega \Delta z \varepsilon_c \rho_c C p \frac{dT}{dt} = (F_c C p_c + F_g C p_g + F_s C p_s)(T - (T + \Delta T)) - \emptyset \Omega \Delta z \varepsilon_c M_a \left(\sum (\Delta H_i)(-r_i) \right) \quad (\text{B.25})$$

$$\sum (\Delta H_i)(-r_i) = \left(\rho_c \left(\frac{M_a}{\rho_g} \right) (H_{ab} K_{ab} + H_{ac} K_{ac} + H_{ad} K_{ad}) C_a^2 + C_b [H_{bc} K_{bd} + H_{bd} K_{bd}] \right) \quad (\text{B.26})$$

Rearranging equation (B.25):

$$\Omega(1-\varepsilon_g) \rho_c C p \frac{dT}{dt} = (F_c C p_c + F_g C p_g + F_s C p_s) \frac{\Delta T}{\Delta z} - \emptyset \Omega \varepsilon_c M_a \left(\sum (\Delta H_i)(-r_i) \right) \quad (\text{B.27})$$

Taking the limit when dz approaches to zero, equation (B.27) become:

$$\Omega(1-\varepsilon_g) \rho_c C p \frac{dT}{dt} = -(F_c C p_c + F_g C p_g + F_s C p_s) \frac{\partial T}{\partial z} - \emptyset \Omega \varepsilon_c M_a \left(\sum (\Delta H_i)(-r_i) \right) \quad (\text{B.28})$$

By including the simplifying assumption of the steady state ($\frac{dT}{dt} = 0$), equation (B.28) becomes:

$$(F_c C p_c + F_g C p_g + F_s C p_s) \frac{dT}{dz} = -\emptyset \Omega \varepsilon_c M_a \left(\sum (\Delta H_i)(-r_i) \right) \quad (\text{B.29})$$

Appendix -C

Determination of Some Physical Parameters

C.1 Gas oil Boiling Temperature

According to the plant data from literature [68], the following table shows the percent gas oil boiled and the corresponding temperature.

Table C.1: Percent Gas oil vaporized Vs Boiling Temperature [68]

% vaporized	Boiling temperature [K]
IBP(Initial boiling point)	532
10	631
30	678
50	714
70	751
90	802
FBP (Final boiling point)	825

The mean average boiling temperature of the gas oil feed is:

$$T_b = \frac{532 + 631 + 678 + 714 + 751 + 802 + 825}{7}$$

$$= 704.7 \text{ k}$$

Using the API technical data book [70], with feed API=21.8 and Watson characterization factor of 11.8 (data obtained from literature), the mean average boiling temperature of the gas oil feed is found to be 716.3K. So when we compare the boiling point of the gas oil feed of plant data from literature and from API technical data, the values have good agreement. So we can use either for our model parameter.

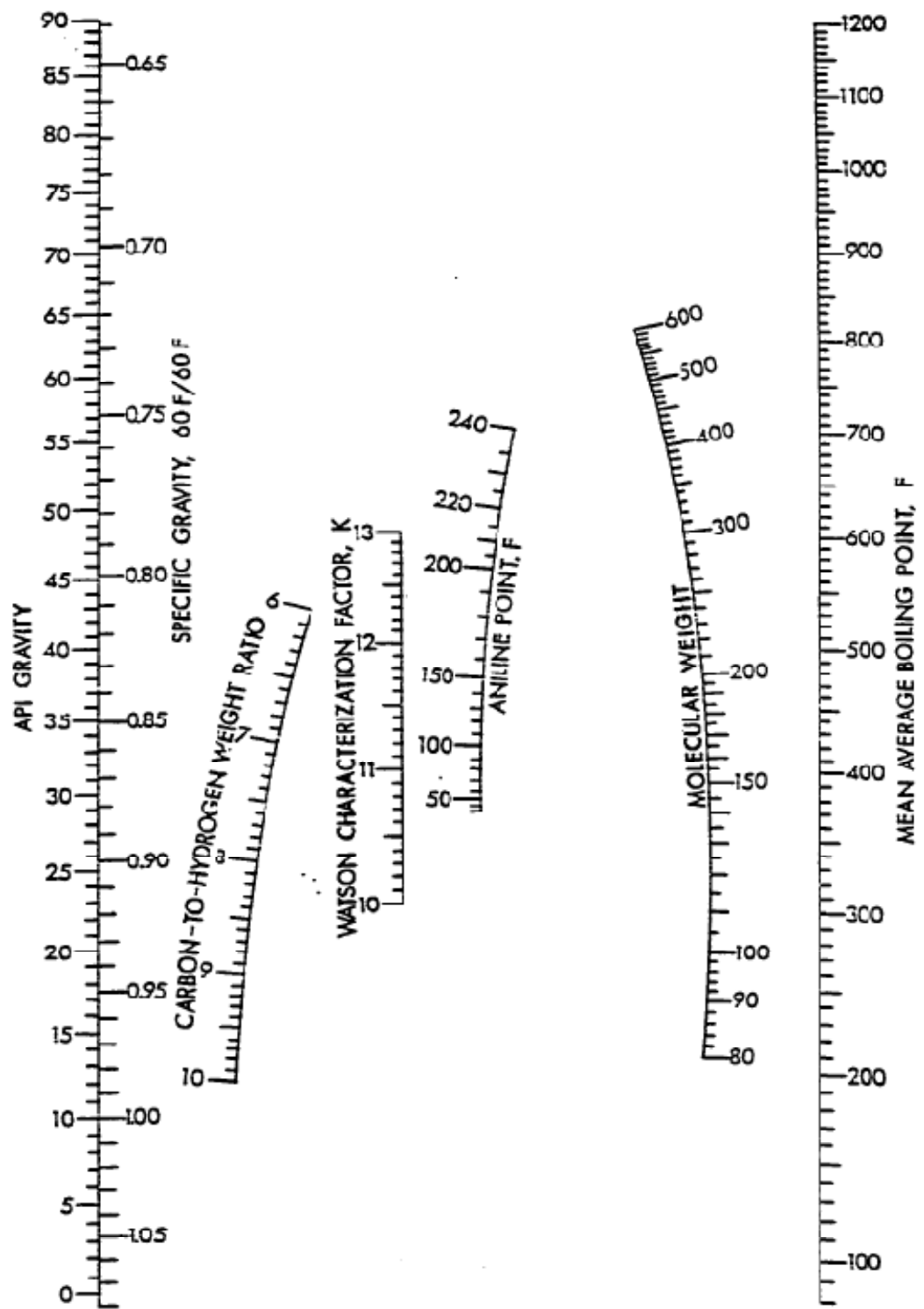


Figure C.1: Mean average boiling temperature of gas oil feed [70].

C.2 Feed liquid Heat Capacity

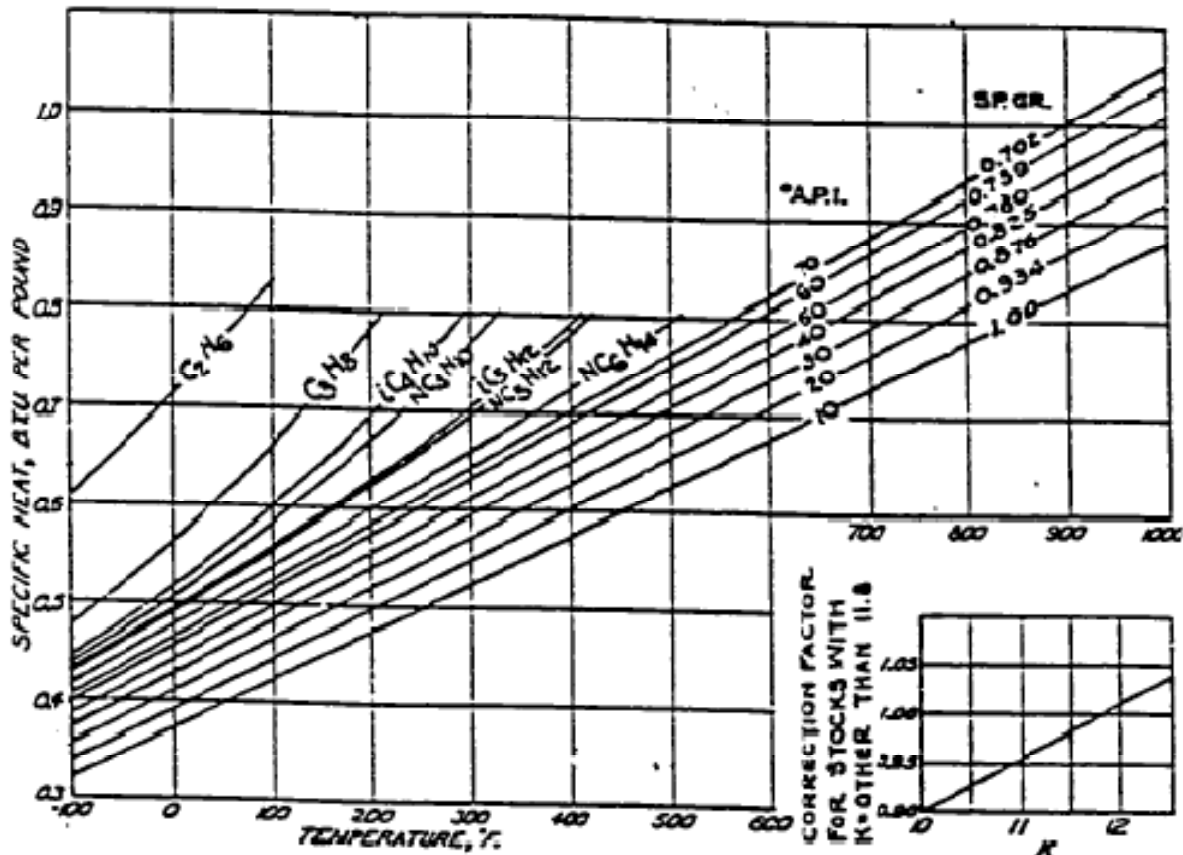


Figure C.2: Specific heat of liquid hydrocarbons [70].

Figure C.2 help us to determine the specific heat of liquid gas oil feed. To determine the specific heat capacity of the liquid feed gas oil hydrocarbon. From the above Figure C.2, at the feed inlet temperature 502k and with feed API of 21.8 the liquid heat capacity is found to be 2.1 KJ/ kg.

C.3 MATLAB Code

```

function [z,C]=riser_model(z,C0)
clear all; clc
display ('input parameter')
% Base case operating condition
Fg, Tf, CTO,Cpvf, Cplf, Tb,VHvap;
% Geometrical dimension
L, D;
A=pi*D^2;
% Catalyst property
dc, rhoc, Cpc, Tc;
Fc=CTO*Fg;
% Steam property
Fs, Ts, Cps;
% Constants
R, fg;
% Molecular weight of lumped model, [kg/kmol]
M=[350 100 40 400 18];
display ('initialization')
% Initial value
u0_0=8;
q_0=u0_0*A;

% Feed vaporiztion section, [K]
T0=(Fs*Cps*Ts+Fc*Cpc*Tc-Fg*Cplf*(Tb-Tf)-Fg*VHvap+Fg*Cpvf*Tb)/...
(Fc*Cpc+Fg*Cpvf+Fs*Cps);

```

```

% Initial value of C
c3=Fg/(M(1)*q_0);
c7=Fs/(M(5)*q_0);
c8=T0;

C=[0.55, 100000, c3, 0, 0, 0, c7, c8];
C(1,1)=0.55 ;
C(1,2)=300000;
C(1,3)=c3
C(1,4)=0;
C(1,5)=0;
C(1,6)=0;
C(1,7)=c7;
C(1,8)=T0;

uc_0=Fc/(A*rhoc*C(1,1));
ug_0=u0_0/(1-C(1,1));
c_total_0=C(1,3)+C(1,4)+C(1,5)+C(1,6)+C(1,7);
molar_flow_0=c_total_0*q_0;
% Molar volume used to indicate volumetric expansion
molarv_0=22.41*C(1,8)/273;
rhog_0=M(1)/molarv_0;

% Catalyst deactivation
COC_0=0.11e-3;
kd_0=1.1*10-5;
Ec=49000;
kd=kd_0*exp(-Ec/(R*T0));
pa_0=exp(-kd*COC_0);

```

```

% Pre-exponential constant
A0=[1457.50,127.59, 1.98, 256.18,6.29e-4,1.1*10-5];
% Activation energy
E=[57359, 52754,31820,65733,66570, 49000];
% Array of differential height of riser
dy=0.5;
n=[0:1:65];
z=dy.*n;
N=65;
display ('main loop solving the systems of differential equations')
K=zeros(65,6);
Output=zeros(65,8);

for i=1:N                                % Main loop

    % Kinetic constant loop
    if i==1
        for j=1:6
            K(i,j)=A0(j)*exp(-E(j)/(R*C(i,8)))
        end
        K;
        q0=q_0;
        rhog=rhog_0;
        ug=ug_0;
        uc=uc_0;
        u0=u0_0;
        pa=pa_0;
        Rec=(rhog*(1-C(i,1))*(ug-uc)*dc)/fg;
        C0=[C(i,1); C(i,2); C(i,3); C(i,4); C(i,5); C(i,6); C(i,7); C(i,8)];
    end
end

```

```

else
    for j=1:6
        K(i,j)=A0(j)*exp(-E(j)/(R*C(length(z),8)));
    end
    K;
    Rec=(rhog*(1-C(length(z),1))*(ug-uc)*dc)/fg ;
end
% Drag calcualtion
if Rec>=1000
    CD=0.44;
else 0<Rec<1000
    CD=(24/Rec)*(1+0.15*Rec^0.687);
end

% Call ode45 to solve the ODEs from z(i) up to z(i+1)
zspan=[z(i) z(i+1)];
options=odeset('reltol',10^-6,'abstol',10^-7);
[z,C]=Ode45( @model_equations, zspan, C0, options, K, CD, rhog, uc, u0, ug, pa);
[rhog, q, C3, C4, C5, C6, C7, uc, u0, ug, pa, tc]=volumetric_expansion(C,M, Fc, ...
    rhoc, A, q0, K, dy);

C0=[C(length(z),1); C(length(z),2); C3; C4; C5; C6; C7; C(length(z),8)];

% Collect the output result from each differential volume
for x=1:8
    Output(i,x)=C(length(C(:,x)),x);
end
Output;
[ x_go,y_gl,y_g,y_ck]=conversion(C,C3,C4,C5,C6);
end % End of the main loop

```

```

function dk_dz=model_equations(z,C,K,Cd,rhog,uc,u0,ug,pa)
% Heat of reaction, [kj/kg]
H=[195 670 745 530 690];
% The state passed to this routine in the C vector,
% Convert to natural notation
ec=C(1,:);
P=C(2,:);
Ca=C(3,:);
Cb=C(4,:);
Cc=C(5,:);
Cd=C(6,:);
Ce=C(7,:);
T=C(8,:);

% Ordinary differential equations for each differential volume:
dec_dz=-((A*rhoc)/(Fc*u0)*ec*ec*(1-ec)*(3/4*CD/dc*rhog/rhoc*...
(ug-uc)^2-g));
dP_dz=-(rhoc*(1-ec)*g+rhoc*(1-ec)*(uc/ug)*((3/4)*(CD/dc)* ...
(rhog/rhoc)*(ug-uc)^2-g/ug));
dCa_dz=-(1/u0*pa*(K(1)+K(2)+K(3))*Ca*Ca*M(1)/rhoc*ec*rhoc);
dCb_dz=(1/u0*pa*((K(4)+K(5))*Cb-(M(1)/rhoc)*K(1)*Ca*Ca)*ec*rhoc);
dCc_dz=(1/u0*pa*((M(1)/rhoc)*K(2)*Ca*Ca+K(4)*Cb)*ec*rhoc);
dCd_dz=(1/u0*pa*((M(1)/rhoc)*K(3)*Ca*Ca+K(4)*Cb)*ec*rhoc);
dCe_dz=0;
dT_dz=-(pa*A*ec*L*rhoc*M(1)/rhoc*((K(1)*H(1)+H(2)*K(2)+H(3)*K(3))*...
Ca*Ca+(H(4)*K(4)+H(5)*K(5))*Cb))/(Fc*Cpc+Fg*Cpg+Fs*Cps);
% The column vector of state derivative
dk_dz=[dec_dz; dP_dz; dCa_dz; dCb_dz; dCc_dz; dCd_dz; dCe_dz; dT_dz];
display ('subfunction for riser_model')

```

```

function [rhog,q,C3,C4,C5,C6,C7,uc,u0,ug,pa,tc]=...
    volumetric_expansion(C,M,Fc,rhoc,A,q0,dy,K)

% Molar volume used to indicate expansion
molarv=22.41*C(length(z),8)/273;
rhog=M(1)/molarv;
% volumetric expansion
c_total=C(length(z),3)+C(length(z),4)+C(length(z),5)+C(length(z),6)+
    C(length(z),7);
molar_flow=c_total*q0;
q=molar_flow*molarv;
tot_conc=molar_flow/q;
% concentration update due to volumetric expansion
C(length(z),3)=C(length(z),3)*(tot_conc/c_total);
C(length(z),4)=C(length(z),4)*(tot_conc/c_total);
C(length(z),5)=C(length(z),5)*(tot_conc/c_total);
C(length(z),6)=C(length(z),6)*(tot_conc/c_total);
C(length(z),7)=C(length(z),7)*(tot_conc/c_total);

C3=C(length(z),3);
C4=C(length(z),4);
C5=C(length(z),5);
C6=C(length(z),6);
C7=C(length(z),7);

% Velocity of catalyst
uc=Fc/(C(length(z),1)*rhoc*A);
% Volumetric flow update
u0=q/A;
% Gas velocity
ug=u0/(1-C(length(z),1));

```

```

% Catalyst deactivation
COC=(C(length(z),6)*M(4)*q)/Fc;
pa=exp(-K(6)*COC);
tc=0;
tc=tc +dy/uc;

function [ x_go,y_gl,y_g,y_ck]=conversion(C,C3,C4,C5,C6)
x_go=(C(1,3)-C3)/C(1,3);
y_gl=C4/C(1,3);
y_g=C5/C(1,3);
y_ck=C6/C(1,3);

% Ordinary differential equation solver/Dormand-prince method
function varargout = ode45(ode,tspan,y0,options,varargin)
solver_name = 'ode45';

% Stats
nsteps = 0;
nfailed = 0;
nfevals = 0;

% Output
FcnHandlesUsed = isa(ode,'function_handle');
output_sol = (FcnHandlesUsed && (nargout==1)); % sol = odeXX(...)
output_ty = (~output_sol && (nargout > 0)); % [t,y,...] = odeXX(...)
% There might be no output requested...
sol = []; f3d = [];

% Handle solver arguments
[neq, tspan, ntspan, next, t0, tfinal, tdir, y0, f0, odeArgs, odeFcn, ...
options, threshold, rtol, normcontrol, normy, hmax, htry,htspan, ...
dataType]=odearguments (FcnHandlesUsed, solver_name, ode, tspan, y0, ...
options,varargin);

```

```

nfevals = nfevals + 1;
outputFcn = odeget(options,'OutputFcn,[],'fast');
outputArgs = { };
if isempty(outputFcn)
    haveOutputFcn = false;
else
    haveOutputFcn = true;
    outputs = odeget(options,'OutputSel',1:neq,'fast');
    if isa(outputFcn,'function_handle')
        outputArgs = varargin;
    end
end
refine = max(1,odeget(options,'Refine',4,'fast'));
if refine>1
    outputAt = 'RefinedSteps';
    S = (1:refine-1) / refine;
end

% Handle the event function
[haveEventFcn,eventFcn,eventArgs,valt,teout,yeout,ieout] = ...
    odeevents(FcnHandlesUsed,odeFcn,t0,y0,options,varargin);
% Handle the mass matrix
[Mtype, Mfun, Margs, M] = odemass(FcnHandlesUsed,odeFcn,t0,y0,options,varargin);
% Non-negative solution components
idxNonNegative = odeget(options,'NonNegative',[],'fast');
t = t0;
y = y0;
% Allocate memory if we're generating output.
nout = 0;
tout = []; yout = [];

```

```

if nargout > 0
    chunk = min(max(100,50*refine), refine+floor((2^13)/neq));
    tout = zeros(1,chunk);
    yout = zeros(neq,chunk);

    nout = 1;
    tout(nout) = t;
    yout(:,nout) = y;
end

% Initialize method parameters.
pow = 1/5;
A = [1/5, 3/10, 4/5, 8/9, 1, 1];
B = [
    1/5      3/40     44/45   19372/6561   9017/3168   35/384
    0        9/40     -56/15  -25360/2187  -355/33      0
    0        0        32/9    64448/6561   46732/5247   500/1113
    0        0        0       -212/729    49/176      125/192
    0        0        0       0           0           -5103/18656
-2187/6784  0        0        0           0           11/84
    0        0        0       0           0           0 ];
E = [71/57600; 0; -71/16695; 71/1920; -17253/339200; 22/525; -1/40];
f = zeros(neq,7,dataType);
hmin = 16*eps(t);
if isempty(htry)

    % Compute an initial step size h using y'(t).
    absh = min(hmax, hspan);
    rh = norm(f0 ./ max(abs(y),threshold),inf) / (0.8 * rtol^pow);

```

```

if absh * rh > 1
    absh = 1 / rh;
end
absh = max(absh, hmin);
else
    absh = min(hmax, max(hmin, htry));
end
f(:,1) = f0;
% The main loop
done = false;
while ~done
    % By default, hmin is a small number such that t+ hmin is only slightly
    % different than t. It might be 0 if t is 0.
    hmin = 16*eps(t);
    absh = min(hmax, max(hmin, absh));    % couldn't limit absh until new hmin
    h = tdir * absh;

    % Stretch the step if within 10% of tfinal-t.
    if 1.1*absh >= abs(tfinal - t)
        h = tfinal - t;
        absh = abs(h);
        done = true;
    end

    % Loop for advancing one step.
    nofailed = true;                      % no failed attempts
    while true
        hA = h * A;
        hB = h * B;

```

```

f(:,2) = feval(odeFcn,t+hA(1),y+f*hB(:,1),odeArgs{:});
f(:,3) = feval(odeFcn,t+hA(2),y+f*hB(:,2),odeArgs{:});
f(:,4) = feval(odeFcn,t+hA(3),y+f*hB(:,3),odeArgs{:});
f(:,5) = feval(odeFcn,t+hA(4),y+f*hB(:,4),odeArgs{:});
f(:,6) = feval(odeFcn,t+hA(5),y+f*hB(:,5),odeArgs{:});

tnew = t + hA(6);
if done
    tnew = tfinal; % Hit end point exactly.
end
h = tnew - t; % Purify h.

ynew = y + f*hB(:,6);
f(:,7) = feval(odeFcn,tnew,ynew,odeArgs{:});
nfevals = nfevals + 6;

% Estimate the error.
NNrejectStep = false;
err = absh * norm((f * E) ./ max(max(abs(y),abs(ynew)),threshold),inf);
NNreset_f7 = false;
break;
% end
end
nsteps = nstems + 1;

if output_ty || haveOutputFcn
    % Computed points, with refinement
    if outputAt == 'RefinedSteps'
        tref = t + (tnew-t)*S;
        nout_new = refine;
        tout_new = [tref, tnew];
    end
end

```

```

yout_new = [ntrp45(tref,t,y,[],[],h,f,idxNonNegative), ynew];
end

if nout_new > 0
    if output_ty
        oldnout = nout;
        nout = nout + nout_new;
        idx = oldnout+1:nout;
        tout(idx) = tout_new;
        yout(:,idx) = yout_new;
    end
end
end      % output_ty || haveOutputFcn en

if done
    break
end

% If there were no failures compute a new h.

if nofailed
    % Note that absh may shrink by 0.8, and that err may be 0.
    temp = 1.25*(err/rtol)^pow;
    if temp > 0.2
        absh = absh / temp;
    else
        absh = 5.0*absh;
    end
end

```

```

% Advance the integration one step.

t = tnew;
y = ynew;
if normcontrol
    normy = normynew;
end
if NNreset_f7
    % Used f7 for unperturbed solution to interpolate.
    % Now reset f7 to move along constraint.
    f(:,7) = feval(odeFcn,tnew,ynew,odeArgs{:});
    nfevals = nfevals + 1;
end
f(:,1) = f(:,7); % Already have f(tnew,ynew)
end

solver_output = odefinalize(solver_name, sol,outputFcn, outputArgs, ...
    printstats, [nsteps, nfailed, nfevals],nout, tout,
    yout,..., haveEventFcn, teout, yeout,
    ieout,{f3d,idxNonNegative});
if nargout > 0
    varargout = solver_output;
end

function [neq, tspan, ntspan, next, t0, tfinal, tdir, y0, f0, ...
args, odeFcn,options, threshold, rtol, normcontrol, normy, hmax, htry, htspan, dataType ] = ...
odearguments(FcnHandlesUsed, solver, ode,..., ...
tspan, y0, options, extras)

if FcnHandlesUsed % function handles used
msg = ['When the first argument to ', solver,' is a function handle, '];
htspan = abs(tspan(2) - tspan(1));

```

```

tspan = tspan(:);
ntspan = length(tspan);
t0 = tspan(1);
next = 2;          % next entry in tspan
tfinal = tspan(end);
args = extras;           % use f(t,y,p1,p2...)
end

y0 = y0(:);
neq = length(y0);
tdir = sign(tfinal - t0);
f0 = feval(ode,t0,y0,args{:});    % ODE15I sets args{1} to yp0.
[m,n] = size(f0);
dataType = superiorfloat(t0,y0,f0);
% Get the error control options, and set defaults.
rtol = odeget(options,'RelTol',1e-3,'fast');
atol = odeget(options,'AbsTol',1e-6,'fast');
normcontrol = strcmp(odeget(options,'NormControl','off','fast'),'on');
atol = atol(:);
normy = [];
threshold = atol / rtol;
% By default, hmax is 1/10 of the interval.
hmax = min(abs(tfinal-t0), abs(odeget(options,'MaxStep',0.1*
(tfinal-t0),'fast'))));
htry = abs(odeget(options,'InitialStep',[],'fast'));
odeFcn = ode;

function solver_output = odefinalize(solver, sol,outfun, outargs, ...
printstats, statvect, nout, tout, yout, ...
haveeventfun, teout, yeout, ieout,interp_data)

```

```

fullstats = (length(statvect) > 3);
stats = struct('nsteps',statvect(1),'nfailed',statvect(2),...
    'nfevals',statvect(3));
statvect(4:6) = 0; % Backwards compatibility
solver_output = { };
if (nout > 0)
    if isempty(sol) % output [t,y,...]
        solver_output{1} = tout(1:nout).';
        solver_output{2} = yout(:,1:nout).';
        solver_output{end+1} = statvect(:); % Column vector
    end
end

function [yinterp,ypinterp] = ntrp45(tinterp,t,y,tnew,...  

                                         vnew,h,f,idxNonNegative)  

BI = [  

    1      -183/64     37/12      -145/128  

    0          0          0  

0    0      1500/371   -1000/159   1000/371  

    0      -125/32     125/12      -375/64  

    0      9477/3392   -729/106   25515/6784  

    0          -11/7          11/3  

-55/28  0      3/2      -4      5/2 ];
s = (tinterp - t)/h;
yinterp = y(:,ones(size(tinterp))) + f*(h*BI)*cumprod([s;s;s;s]);
ypinterp = [];

function [massType, massFcn, massArgs, massM, dMoptions] ...
=  

odemass(FcnHandlesUsed,ode,t0,y0,options,extras)
massType = 0;

```

```
massFcn = [];
massArgs = {};
massM = speye(length(y0));
dMOptions = []; % options for odenumjac computing d(M(t,y)*v)/dy
if FcnHandlesUsed % function handles used
    Moption = odeget(options,'Mass',[],'fast');
end

function [haveeventfun,eventFcn,eventArgs,eventValue,teout,yeout,ieout]
    =odeevents(FcnHandlesUsed,ode,t0,y0,options,extras)
haveeventfun = 0; % no Events function
eventArgs = [];
eventValue = [];
teout = [];
yeout = [];
ieout = [];
eventFcn = odeget(options,'Events',[],'fast');
```

C.4 Technical Paper

1. Mesfin Berhanu N., Shuhaimi Mahadzir, Performance of Riser section Fluid Catalytic Cracking Reactor: Effect of Cluster Formation. *The 2nd Thammasat University International Conference, Environmental and Energy Engineering, 2009.* Thammasat University, Thailand in Conjunction with Tokyo Institute of Technology, Japan. Paper ID: 001.
2. Mesfin Berhanu N., Shuhaimi Mahadzir, Model the Performance of Riser section Fluid Catalytic Cracking Reactor: Cluster Formation, *National Postgraduate Conference on Engineering, Science and Technology, 2009.* University Teknologi Petronas, Malaysia. Paper ID: 016.
3. Mesfin Berhanu N., Shuhaimi Mahadzir, Model the Performance of Riser section Fluid Catalytic Cracking Reactor: Cluster Formation, *Proceeding of the 3rd international Conference on chemical and Bioprocess Engineering in Conjunction with 23 rd symposium of Malaysian Chemical Engineers, 2009.* University Malaysia Sabah, Malaysia. Paper ID: 049.